

**Kasdi Merbah University - Ouargla -**

**Faculty of Hydrocarbons, Renewable Energies, Earth  
Sciences, and Universe**

**Department of Drilling and Mechanics of Oil Fields**



**Dissertation**

**Professional Master**

***Domain: Science and Technology***

***Field: Hydrocarbons***

***Specialty: Professional drilling***

**Submitted by:**

Salah Said Med AMEUR

Mohammed Abd El illah ABBOU

Amine DERGAOUI

**Title**

**Seismic While Drilling (SWD) Process Simulation Based on  
Stick-Slip Vibration Model in Algerian Petroleum Field**

Publicly defended

On: 18/06 /2023

Before the Jury

Dr. Abidi Saad Elfkeur	MCA	President	UKMO
Dr. Bouchema Kamel	MCB	Examiner	UKMO
Mr. Elhadi Atlili	AA	Supervisor	UKMO
Dr. Mohamed Zinelabidine Doghmane		Supervisor	Sonatrach Exploration Division

**Academic Year: 2022/2023**

## *Dedication*

First I dedicate this thesis to the memory of my parents, who passed away when I was very young. Although I never got the chance to know them, I have always felt their presence in my life through the stories and memories shared by loved ones. I am grateful for the foundation they laid for me, and for the resilience and strength they instilled in me. This thesis is a tribute to their memory and a reflection of the values they would have wanted me to uphold.

I dedicate this thesis to my beloved grandmother, my dear uncle, Moustapha, and my caring aunts, Fatima, Nasira, Nadia and Noria. They took on the responsibility of raising me when my parents were no longer able to do so. Their unwavering love, guidance, and support have been the driving force behind my academic success and personal growth. I am forever grateful for their sacrifices, encouragement, and belief in me. This thesis is a tribute to their selflessness and a testament to the profound impact they have had on my life.

To my loving brother, Anis. I would also like to extend my gratitude to my dear friends who have been my pillars of strength and support throughout my academic journey. Their encouragement, motivation, and camaraderie have made this journey not only bearable but also enjoyable. I am lucky to have such amazing friends in my life, and I dedicate this thesis to them as a token of my appreciation and affection

**Salah Said Med AMEUR**

## *Dedication*

I would like to express my deepest gratitude and dedicate this thesis to the following individuals who have been instrumental in my academic journey:

To my beloved mother and father, your unwavering love, support and encouragement have been my guiding light throughout this entire endeavor. Your sacrifices and belief in me have inspired me to pursue my dreams relentlessly. This accomplishment is as much yours as it is mine.

To my partners Ameer and Dergaoui, thank you for all your effort and sincerity. I was honored to work with you.

To my family, thank you for your endless support. Your words of encouragement have been constant source of motivation during challenging times. I am blessed to have such a loving and supportive family by my side.

Lastly, to all my friends, both near and far, thank you for your unwavering support and companionship.

**ABBOU Mohammed Abd El Illah**

## *Dedication*

I dedicate this thesis to:

My very dear mother, No matter what I do or say, I will never be able to thank you properly. Your affection covers me, your mercy guides me and your presence by my side has always been my strength to cope various obstacles.

My dear father, you have always been by my side to support and encourage me. I hope this work reflects my gratitude and thanks to you.

My family, my brothers, and those who shared all the emotional moments with me while doing this work. They have warmly supported and encouraged me throughout my journey.

My partners Abbou and Ameer, it was an honor to work with you, and I thank you for all your efforts that you exchanged with me, and your determination to work and persevere.

all my friends who have always encouraged me, and to whom I wish more success and progress.

**Dergaoui Amine**

## *Acknowledgements*

First and foremost, we would like to express our deepest gratitude to Allah for His unwavering guidance, blessings, and the strength He has bestowed upon us throughout this thesis. Without His divine support, this research would not have been possible.

We are deeply grateful to our supervisors, *Dr Mohamed Zinelabidine Doghmane, Dr Elhadi Atili, Dr Khelifa Cherif*, for their unwavering support, expertise, and encouragement. Their guidance and insightful feedback have been invaluable in shaping this research.

We would like to extend our heartfelt appreciation to the faculty members, for their profound knowledge and for sharing their expertise in oil field.

Our gratitude also goes to our families and friends for their endless love, encouragement, and understanding. Their unwavering support and belief in us have been a constant source of motivation throughout this journey.

We are grateful to the members of the jury, for their time, expertise, and valuable insights during the evaluation of this thesis. Their feedback and constructive criticism have greatly contributed to the improvement of our work.

Lastly, we would like to express our appreciation to any other individuals, not mentioned above, who have directly or indirectly contributed to this thesis. Your assistance, advice, and encouragement have played a significant role in its completion.

تستكشف هذه الأطروحة تطبيق الاهتزازات ذات الانزلاق العصي كمصدر زلزالي في طريقة الحفر الزلزالي أثناء الحفر في الجزائر. الهدف هو تقييم إمكانية استخدام اهتزازات الانزلاق العصي للتصوير تحت السطح في الوقت الفعلي ومحاكاة سلوك الموجات الزلزالية في هذه الطريقة. تدرس الدراسة خصائص الاهتزازات ذات الانزلاق العصي، ومدى ملاءمتها كمصدر زلزالي، والقيود المفروضة على المصادر الزلزالية التقليدية. من خلال جمع البيانات والمحاكاة، يوضح البحث أن الاهتزازات ذات الانزلاق العصي يمكن أن تعمل بشكل فعال كمصدر زلزالي في الزلزال أثناء الحفر، مما يساهم في تحسين التصوير تحت السطح وتقديم توصيات عملية لتحسين استخدامها في الجزائر.

#### الكلمات المفتاحية

اهتزازات انزلاق العصا، زلزالية أثناء الحفر، تصوير تحت السطح، محاكاة الموجات الزلزالية، الجزائر

#### Abstract

This thesis explores the application of stick-slip vibrations as a seismic source in the seismic while drilling method in Algeria. The objective is to assess the potential of utilizing stick-slip vibrations for real-time subsurface imaging and to simulate the behavior of seismic waves in this method. The study examines the characteristics of stick-slip vibrations, their suitability as a seismic source, and the limitations of conventional seismic sources. Through data collection and simulations, the research demonstrates that stick-slip vibrations can effectively serve as a seismic source in the seismic while drilling, contributing to improved subsurface imaging and offering practical recommendations for optimizing their utilization in Algeria.

**Keywords:** stick-slip vibrations, seismic while drilling, subsurface imaging, seismic wave simulation, Algeria.

#### Résumé

Ce mémoire explore l'application des vibrations stick-slip en tant que source sismique dans la méthode de sismique en cours de forage en Algérie. L'objectif est d'évaluer le potentiel de l'utilisation des vibrations stick-slip pour l'imagerie en temps réel du sous-sol et de simuler le comportement des ondes sismiques dans cette méthode. L'étude examine les caractéristiques des vibrations stick-slip, leur adéquation en tant que source sismique et les limites des sources sismiques conventionnelles. À travers la collecte de données et des simulations, la recherche démontre que les vibrations stick-slip peuvent efficacement servir de source sismique dans le sismique en cours de forage, contribuant à une amélioration de l'imagerie du sous-sol, et offre des recommandations pratiques pour optimiser leur utilisation en Algérie.

**Mots-clés :** vibrations stick-slip, sismique en cours de forage, imagerie du sous-sol, simulation des ondes sismiques, Algérie.

# Table of contents

<i>Dedication</i> .....	i
<i>Dedication</i> .....	ii
<i>Dedication</i> .....	iii
<i>Acknowledgements</i> .....	iv
Abstract.....	v
Table of contents .....	vi
List of tables.....	ix
List of Figures .....	x
List of Abbreviation.....	xiii
General Introduction .....	1

## Chapter I: Borehole Seismic and VSP

<b>I.1. Introduction</b> .....	4
<b>I.2. Conventional VSP</b> .....	4
<b>I.2.1. Equipment of VSP</b> .....	4
<b>I.2.2. Operating Principle</b> .....	5
<b>I.2.2.1. Types of VSP Surveys</b> .....	6
<b>I.2.2. Advantages and utility of the VSP</b> .....	15
<b>I.2.3. Limitations of the technique</b> .....	16
<b>I.3. Borehole Seismic Technique</b> .....	16
<b>I.3.1. History of the technique</b> .....	16
<b>I.3.2. Description of the technique</b> .....	17
<b>I.3.3. Advantages and utility of the approach</b> .....	20
<b>I.3.4. Drawbacks and Limitations</b> .....	20
<b>I.4. Conclusion</b> .....	21

## Chapter II: Seismic while drilling

<b>II.1. Introduction</b> .....	23
<b>II.2. History of the development of the method</b> .....	23
<b>II.3. Different methods of SWD technique</b> .....	24
<b>II.3.1. Surface seismic while drilling (SSWD)</b> .....	24
<b>II.3.1.1. Operating principle of the (SSWD) method</b> .....	25
<b>II.3.1.2. Description of the technique</b> .....	26
<b>II.3.1.3. Advantages of the technique</b> .....	26
<b>II.3.1.4. Limitation of the technique</b> .....	26
<b>II.3.1.5. The critical use of SSWD for drillers</b> .....	27
<b>II.3.2. The drill-bit SWD technique</b> .....	29
<b>II.3.2.1. Operating principle of the (drill-bit SWD)</b> .....	29

II.3.2.2.	Description of the technique.....	30
II.3.2.3.	Advantages and utility of the technique.....	30
II.3.2.4.	Limitations of the technique.....	31
II.3.3.	Vertical seismic profile while drilling (VSP-WD) .....	31
II.3.3.1.	Operating principle of the (VSP-WD) method.....	31
II.3.3.2.	Description of the technique(VSP-WD) .....	33
II.3.3.3.	Advantages and utility of the technique.....	35
II.3.3.4.	Limitations of the technique.....	36
II.3.4.	SWD using swept impulse hydraulic tool.....	36
II.3.4.1.	Operation principle of the technique.....	36
II.3.4.2.	Description of the technique.....	37
II.3.4.3.	Advantages of the method .....	39
II.3.4.4.	Drawbacks and Limitation of the technique.....	39
II.4.	Application around the world of SWD.....	39
II.5.	Conclusion .....	41

### Chapter III: Seismic while drilling using drill bit stick-slip vibrations

III.1.	Introduction.....	44
III.2.	Vibrations types in Drill bit.....	44
III.2.1	Axial or Longitudinal Vibrations (Bit Bounce).....	45
III.2.2.	Lateral or Transverse Vibrations (Whirling).....	45
III.2.3.	Torsional Vibrations (Stick-Slip).....	46
III.2.3.1	Mathematical Model .....	47
III.3.	Stick-Slip vibration as Sweep for SWD.....	51
III.4.	Operating Principle of the technique .....	51
III.5.	Advantages and Utilities .....	52
III.7.	Drawback and Limitations.....	53
III.8.	Why the SWD can be advantageous in Algerian Petroleum Industry? .....	53
III.9.	Conclusion .....	54

### Chapter IV: Simulation of SWD using Drill bit Stick-Slip Vibrations

IV.1.	Introduction.....	56
IV.2.	SeisLab Matlab toolbox .....	56
IV.2.1.	Initialization.....	56
IV.2.2.	Command-line help.....	57
IV.2.3.	Input arguments of functions.....	58
IV.2.4.	Test datasets.....	59
IV.3.	CREWES Matlab toolbox .....	59
IV.3.1.	THE V(Z) RAYTRACING FACILITY .....	61



<b>IV.4. GemPy toolbox</b> .....	73
<b>IV.4.1. Basics of geological modeling with GemPy</b> .....	73
<b>IV.5. Numerical example and simulation</b> .....	91
<b>IV.5.1. Simulation results</b> .....	92
<b>IV.5.2. Different rotation rotational speeds results</b> .....	93
<b>IV.6. Conclusion and recommendation</b> .....	95
<b>General conclusion</b> .....	97
<b>Bibliography</b> .....	99

## List of tables

Table I.1 General information about Zero Offset application.....	08
Table IV.1 Related example parameters.....	91

## List of Figures

### Chapter I: Borehole seismic and VSP

Figure I.1. Schematic of vertical seismic profile equipment.....	05
Figure I.2. Represent a simulation that we executed using MATLAB of upgoing and downgoing waves of conventional VSP.....	06
Figure I.3. Different types of reflections.....	06
Figure I.4. A checkshot VSP survey measuring the direct travel time.....	07
Figure I.5. a) A Zero-offset VSP survey measuring the two-way travel time above TD, b) A Zero-offset VSP survey measuring the two-way travel time below TD.....	08
Figure I.6. Source Geometry Sketch.....	09
Figure I.7. Geometry Information (X-Z).....	09
Figure I.8. Geometry Information (Y-Z).....	09
Figure I.9. Time Depth Plot.....	10
Figure I.10. Velocity Plot.....	10
Figure I.11. Digital processing of VSP data (One way time).....	11
Figure I.12. Digital processing of VSP data (zero time).....	12
Figure I.13. A VPS survey measuring the two-way travel time using Offset VSP .....	13
Figure I.14. One-way travel time using Walkabove technique.....	14
Figure I.15. A VPS survey measuring one-way travel time using Walk-away technique Modified from Arroyo et al.....	14
Figure I.16. Downhole technique (VSP).....	18

### Chapter II : Seismic While Drilling

Figure II.1. Illustrative image of (SSWD) in offshore.....	25
Figure II.2. Bottom intersection using SSWD.....	28
Figure II.3. Model of two different waves (shear and pressure) and there propagation in the ground.....	29
Figure II.4. The basic SWD setup and the cross-correlation concept between the pilot sensor and the Surface geophones.....	30
Figure II.5. VSP-WD procedures aspect.....	33
Figure II.6. Offshore airgun system.....	34
Figure II.7. Land airgun system.....	34

Figure II.8. High-pressure source to generate the airgun.....	35
Figure II.9. Seismic Navigation and Processing system.....	35
Figure II.10. Diagram of percussion drilling tool.....	37
Figure II.11. Internal pressure frequency time sample – impulse function times cycle frequency.....	38
Figure II.12. Hydraulic pulse tool with high-speed flow course housing and sweep mechanism.....	38
Figure II.13. The P-wave velocity model and the migrated images using SSWD, Note the imaged diffractions from interface intersections and the drill bit.....	41

### **Chapter III: Seismic while drilling using drill bit stick-slip vibrations**

Figure III.1: Three types of drill string vibrations: a) axial, b) torsional, c) lateral.....	44
Figure III.2: BHA whirl: forward whirl and backward whirl .....	46
Figure III.3. Measured vibration using BlackBox in Well-1.....	47
Figure III.4. Three elements proxy model of rotary drilling system.....	48
Figure III.3. Acquisition geometry of SWD using stick-slip vibrations technique.....	52

### **Chapter IV: Simulation of SWD using Drill bit Stick-Slip Vibrations**

Figure IV.1 Filtered Gaussian noise; created by s_plot (s_data).....	59
Figure IV.2. A ray is traced across a set of horizontal layers.....	62
Figure IV.3 The two-point problem of tracing a fan of rays down to a reflector and back up to receivers through N layers (left) is equivalent to tracing the rays directly through a stack of 2N layers (right).....	63
Figure IV.4. A simple layered medium is shown as characterized by its P-wave velocity curve (right) and its S-wave velocity curve (left). Note the 200 m water layer at the top.....	65
Figure IV.5. This sequence of Matlab code uses the velocity model of Figure IV.4 to trace P-P rays and create Figure IV.6.....	65
Figure IV.6. Running the code of figure IV.5 creates this figure using the velocity model of figure IV.4. In the top frame are the actual raypaths as plotted by traceray_pp in line 3. In the bottom frame, the traveltimes are plotted versus offset.....	66
Figure IV.7. This sequence of Matlab code uses the velocity model of Figure IV.4 to trace P-S rays and create Figure IV.8.....	66
Figure IV.8. Running the code of Figure IV.7 creates this figure using the velocity model of Figure IV.4. In the top frame are the actual raypaths as plotted by traceray_ps in line 3. In the bottom frame, the traveltimes are plotted versus offset.....	67

Figure IV.9. This code models a P-P reflection for offset VSP geometry.....	68
Figure IV.10. A P-P reflection for an offset VSP recording is shown. The raypaths (top) and traveltimes (bottom) were computed by the code in Figure IV.9.....	68
Figure IV.11. This code models a P-S reflection for an offset VSP.....	69
Figure IV.12. A P-S reflection for an offset VSP is shown. This was created by the code in Figure IV.11...	69
Figure IV.13. This code example illustrates the use of <code>tracray_pp</code> to create a complicated multiple that remains a P-wave at every bounce.....	70
Figure IV.14. The raypath of a complicated multiple is shown (top) that remains a P-wave at every bounce.....	71
Figure IV.15. This code creates a multimode similar to that of Figure IV.14 except that the raycode requests a P-S conversion at 1300 m, an S-P conversion at 3000 m, and another P-S conversion at 1500 m (on the up leg).....	71
Figure IV.16. The raypath for a complicated P-S multimode is shown (top) as produced by the code snippet in Figure IV.15.....	72
Figure IV.17. Torque and angular velocity of top drive and drill bit with torsional vibration.....	92
Figure IV.18. Angular velocity at 1 rad/s.....	93
Figure IV.19. Angular velocity at 5 rad/s.....	94
Figure IV.20. Angular velocity at 50 rad/s.....	94
Figure IV.21. Angular velocity of the drill bit at different WOBs.....	95

## List of Abbreviation

**VSP:** Vertical Seismic Profiling

**TD:** Total Depth

**SSWD:** Surface Seismic While Drilling

**SWD:** Seismic While Drilling

**IFP:** French Institute of Petroleum

**VSP-WD:** Vertical Seismic Profiling While Drilling

**BHA:** Bottom Hole Assembly

**PDC:** Polycrystalline Diamond Compact

**HZ:** Hertz, a unit of frequency measurement

**SEC:** Second, a unit of time measurement

**P wave:** Primary waves

**S wave:** Secondary waves

**MWD:** Measurement While Drilling

**PSDM:** Pre-Stack Depth Migration

**WOP:** Weight on Bit

**SEG-Y:** Standard Exchange format for Geophysical data

**SAC:** Seismic Analysis Code

**LAS:** Log ASCII Standard

**ASCII:** American Standard Code for Information Interchange

**RGB:** Red Green Blue

**CDP:** Common Depth Point

**CREWES:** Consortium for Research in Elastic Wave Exploration Seismology

**OBC:** Ocean Bottom Cable

# General Introduction

---

## **General Introduction**

In the ever-evolving field of oil exploration, seismic techniques play a crucial role in extracting vital information about subsurface geological structures. Over the years, various seismic methods have been employed to enhance the accuracy and efficiency of data acquisition. Among these methods, vertical seismic profiling (VSP), borehole seismic, and seismic while drilling (SWD) have emerged as valuable tools for acquiring real-time data during drilling operations. However, in order to optimize drilling processes, it is essential to evaluate and compare these techniques, particularly in the context of the Algerian petroleum field.

This thesis aims to investigate the SWD process simulation based on the stick-slip vibration model and its applicability in the Algerian petroleum field. We will delve into the multifaceted aspects of seismic techniques, seeking to uncover the strengths and limitations of each method. Through a comparative analysis, we aim to highlight the advantages of the proposed SWD approach, shedding light on its potential to revolutionize drilling operations in this region.

As the industry continues to face challenges related to wellbore stability, drilling efficiency, and real-time reservoir characterization, the significance of innovative drilling techniques cannot be overstated. By integrating the stick-slip vibration model into the SWD process, we explore the potential to mitigate drilling-related issues while simultaneously improving data acquisition capabilities.

Furthermore, this thesis endeavors to address the specific requirements and geological characteristics of the Algerian petroleum field. Algeria, with its diverse reservoirs and challenging drilling conditions, presents a unique environment where the efficacy of seismic techniques must be evaluated thoroughly. By focusing on this geographical context, we aim to provide valuable insights and recommendations for the application of SWD in Algerian oil fields.

Through a comprehensive literature review, numerical simulations, and analysis of field data, we aim to offer a holistic understanding of the stick-slip vibration model and its impact on SWD in the Algerian petroleum field. By considering both technical and operational perspectives, we strive to contribute to the ongoing efforts in optimizing drilling processes and decision-making within the industry.

Finally, this thesis endeavors to bridge the gap between theoretical understanding and practical implementation of SWD in the Algerian petroleum field. We seek to provide a comprehensive analysis of seismic techniques, with a particular emphasis on the stick-slip vibration model. The findings and recommendations of this research will not only benefit operators and drilling engineers in the Algerian petroleum industry but also contribute to the broader knowledge base in the field of seismic while drilling.



# Chapter I

## Borehole seismic and VSP

---

## I.1. Introduction

Borehole seismic surveys are versatile downhole measurement techniques used in the oil field that offer significant benefits by linking time-based surface seismic images with depth-based well logs. These surveys improve 3D subsalt imaging, stimulation monitoring, and high-pressure and high-temperature acquisition. Additionally, vertical seismic profiling (VSP) is a powerful tool that can acquire travel times, wave amplitudes, and reflection coefficient data, providing a more detailed seismic view of the subsurface in the vicinity of the borehole than conventional surface seismic data [1][2]. In this chapter, we will provide more detailed information about borehole seismic and its techniques, specifically the conventional VSP technique.

## I.2. Conventional VSP

The VSP has numerous applications in the oil industry. Primarily, VSP data have been used to aid surface seismic interpretation by providing time-to-depth values and a zero-phase, mostly multiple-free reflectivity trace. VSP has also provided insight into the nature of seismic wave propagation in the earth and estimated rock properties such as interval velocities and attenuation near the borehole. It is a geophysical exploration technique that involves acquiring downhole measurements of acoustic signals originating from surface seismic sources using a borehole seismic tool. Seismic waves are typically generated by controlled explosions, vibroseis trucks, or air guns and travel from the source into the earth's interior. However, in Algerian petroleum fields, vibroseis trucks are the most commonly used source of seismic signals. When reflections occur at layer interfaces, acoustic impedance contrast is detected due to differences in velocities and densities between layers.

### I.2.1. Equipment of VSP

A Vertical Seismic Profile (VSP) survey requires several pieces of equipment, including:

**Seismic source:** A seismic source is used to generate seismic waves, such as an explosive charge, a weight drop, or a vibrator (Figure I.1).

**Seismic sensors:** Seismic sensors, such as geophones or hydrophones, are placed in the borehole and on the surface to record the seismic waves. Geophones typically have a frequency range of 2-20 Hz and a sensitivity of 10-100 V/m/s. Hydrophones have a frequency range of 0.5-20 kHz and a sensitivity of 1-100  $\mu$ V/Pa (Figure I.1).

**Data acquisition system:** A data acquisition system is used to record the seismic signals from the sensors. The system includes a cable to connect the sensors to the recording unit (seismograph), a

recording unit to digitize and store the signals, and a power source to supply power to the recording unit and sensors.

**Downhole tools:** Downhole tools are used to deploy the seismic sensors in the borehole. These tools may include a wireline, a slickline, or a coiled tubing unit.

**Data processing software:** Data processing software is used to process the recorded seismic data and create a subsurface velocity model. The software may include tools for filtering, gain recovery, and velocity analysis.

It is important to note that the specific equipment used for a VSP survey will depend on the survey objectives, the subsurface conditions, and the available budget. The cost of a VSP survey can range from tens of thousands to several million dollars, depending on the complexity of the survey [5].

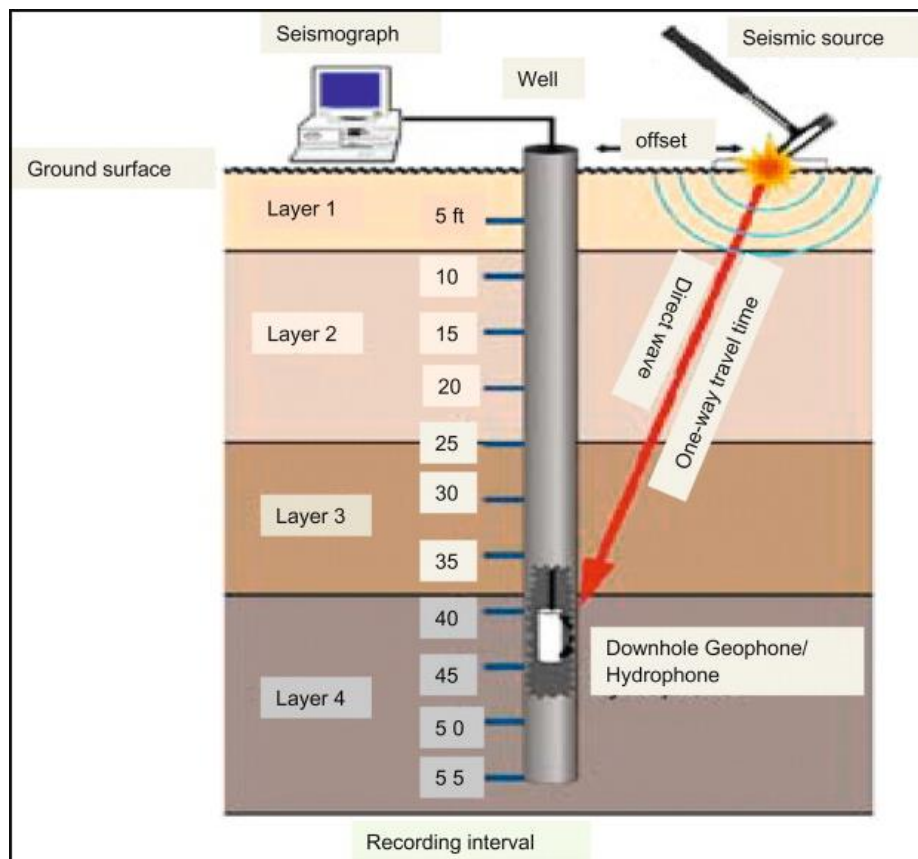


Figure I.1. Schematic of vertical seismic profile equipment [7]

### I.2.2. Operating Principle

An array of geophones in the borehole used for a VSP survey records both upgoing waves that are reflected from layers beneath the receivers and downgoing waves that come straight from the source. Figure Processing separates waves that propagate upward and downward. The initial downgoing wave arrivals (Figure I.2)

The waves are used to calibrate a continuous velocity log. Similar to how reflection seismic data is analyzed, waves that are propagating upward are also processed. A VSP survey makes it possible to relate surface seismic data recorded in time to wellbore data recorded in depth. It can also be used to differentiate primary from secondary events (multiples) and to determine the depths of layers where reflections are generated (Figure I.3) [3] [4].

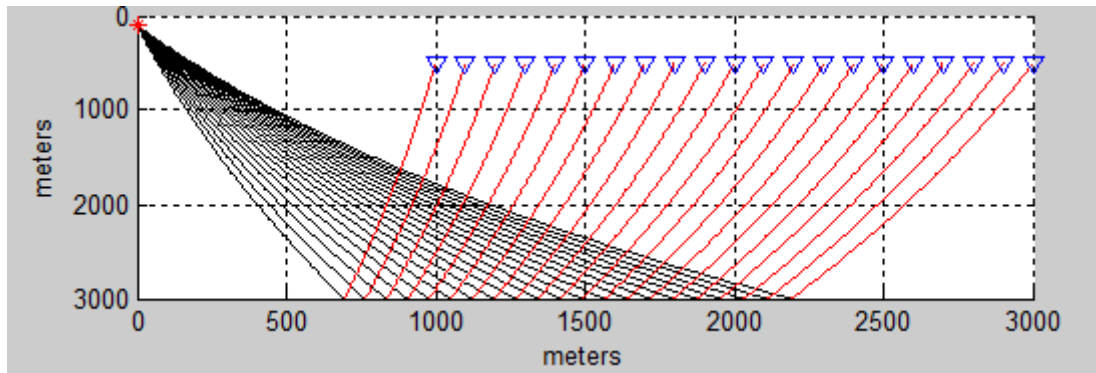


Figure I.2. Represent a simulation that we executed using MATLAB of upgoing and downgoing waves of conventional VSP.

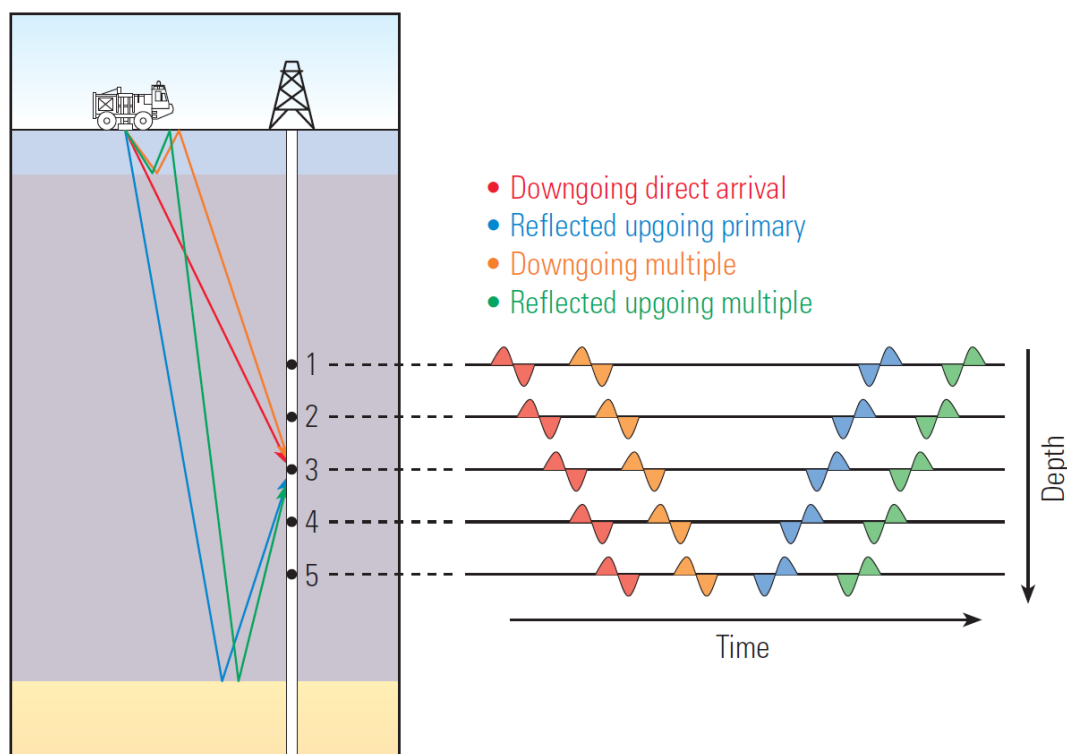


Figure I.3. Different types of reflections [1]

### I.2.2.1. Types of VSP Surveys

The source and receiver geometries distinguish many different variants of the VSP technique.

### a. Check-shot VSP

The check shot is the most common type of VSP survey. It is known as a low-cost velocity survey and has been used since 1940 [5]. This method doesn't use reflection to estimate the direct travel time from the source to the receiver. It provides a measurement of seismic velocity near the well and relates seismic time to well depth. To acquire data, an immobile seismic source is used, and a receiver measures the direct travel time indication from the surface to a specific reflector [5] (Figure I.4). In Algeria, this method is widely used due to its ease of implementation and low cost compared to other methods.

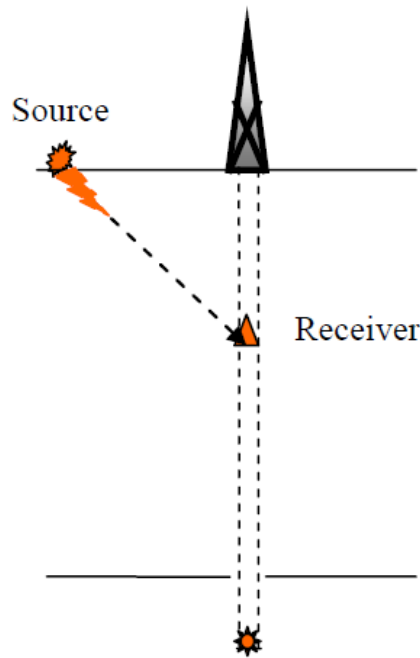


**Figure I.4:** A checkshot VSP survey measuring the direct travel time. [5].

### b. Zero Offset VSP

The conventional vertical seismic profile (also called standard VSP) has been used since 1950. In this method, the vibration source is positioned directly above the receivers, typically very close to the wellbore, and the reflected seismic signal is captured, delivering a seismic image below the total depth of the well [5] (Figure I.5).

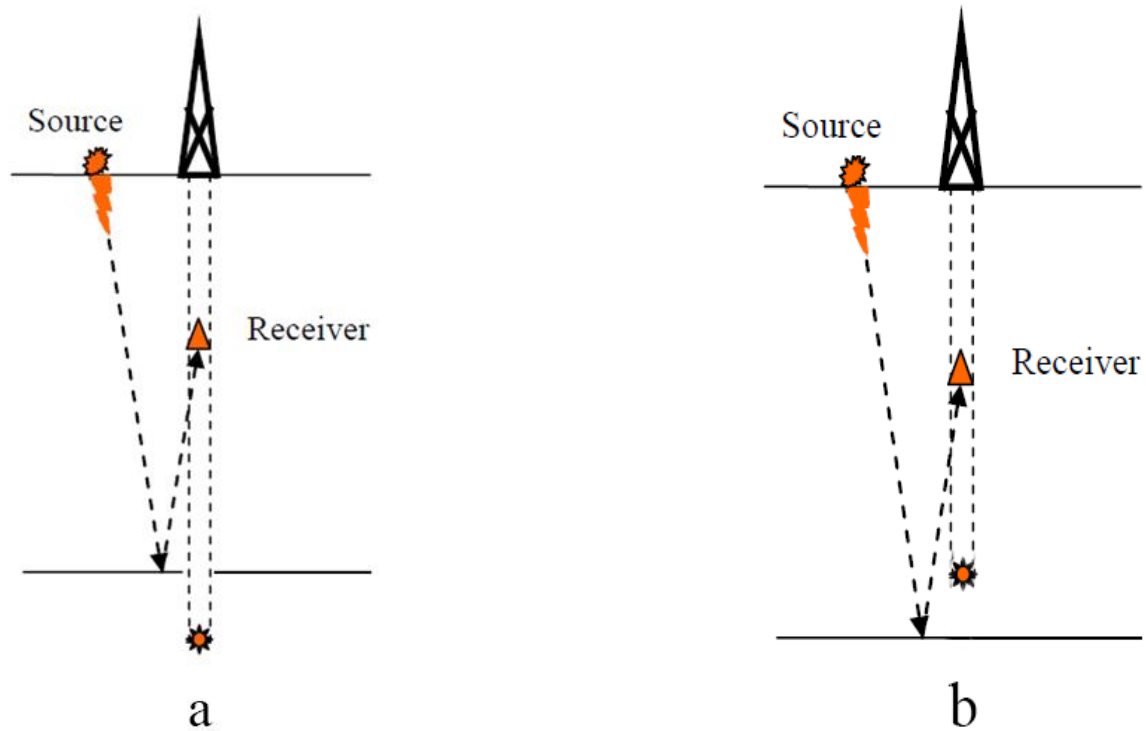


**Figure I.5.** a) A Zero-offset VSP survey measuring the two-way travel time above TD, b) A Zero-offset VSP survey measuring the two-way travel time below TD [5]

### Example of Zero Offset VSP

This example is taken of well-1 located in Algerian hydrocarbons field

**Table I.1** General information about Zero Offset application

Survey Type	Zero Offset VSP
Surface Recording Length	14000.0 ms
Surface Sampling Rate	2.0 ms
Downhole Recording Length	18000.0 ms
Downhole Sampling Rate	2.0 ms
Top of Survey	29.5 m
Bottom of Survey	3000.0 m
Number of Shots	68
Number of Downhole Traces	688
Number of Downhole Traces used for Processing	659

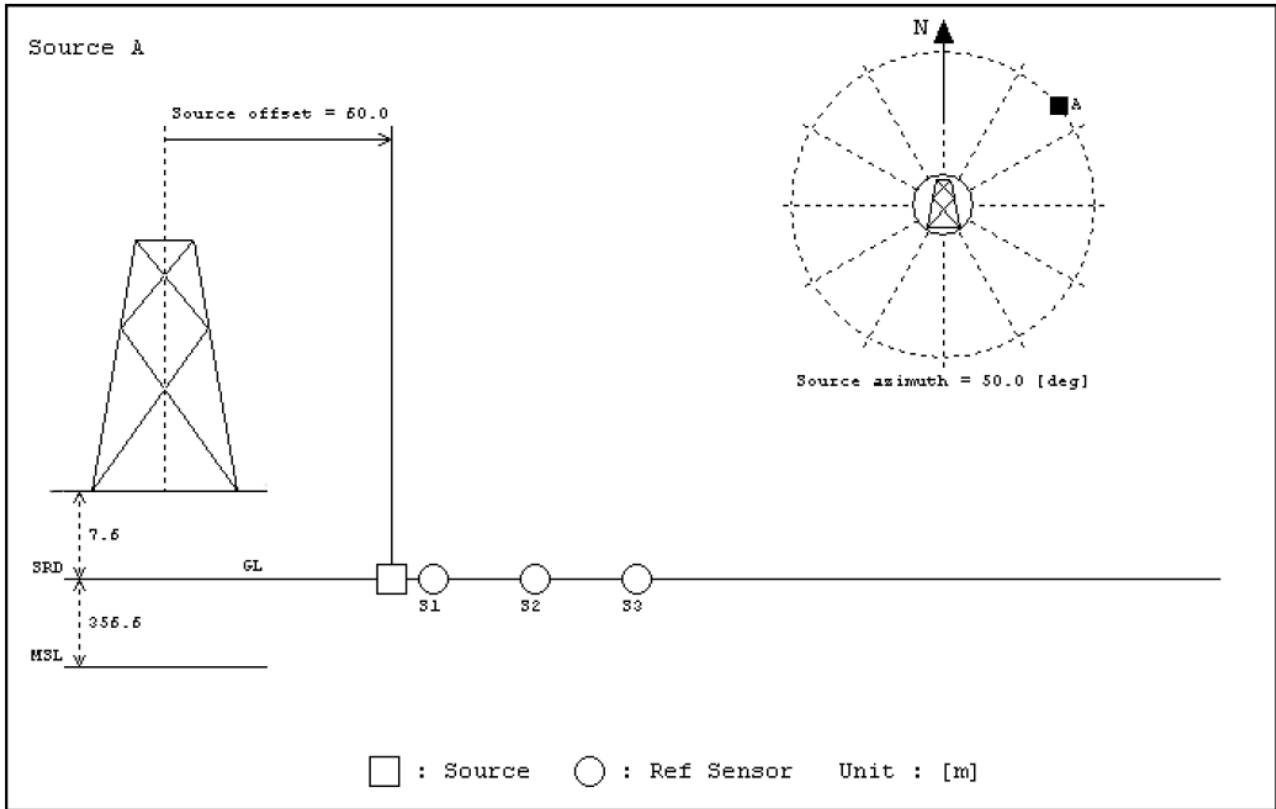


Figure I.6. Source Geometry Sketch

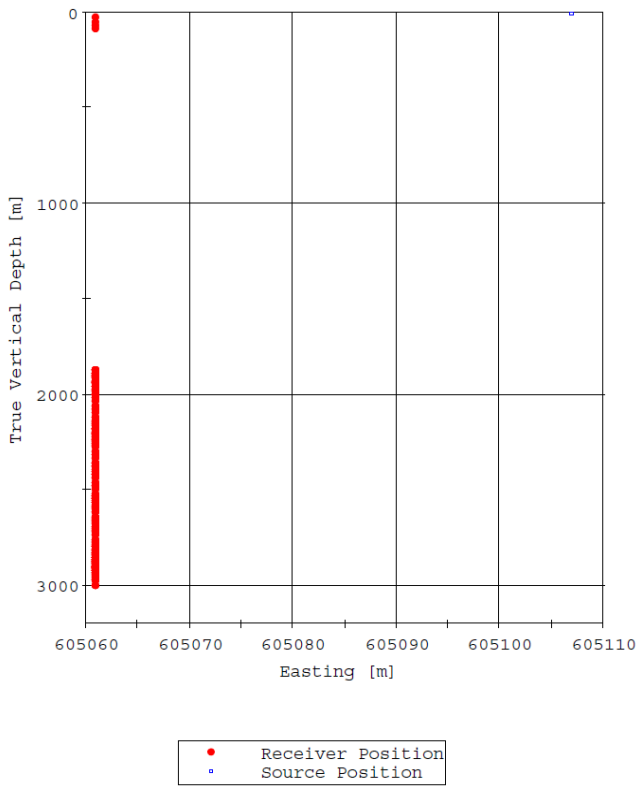


Figure I.7. Geometry Information (X-Z)

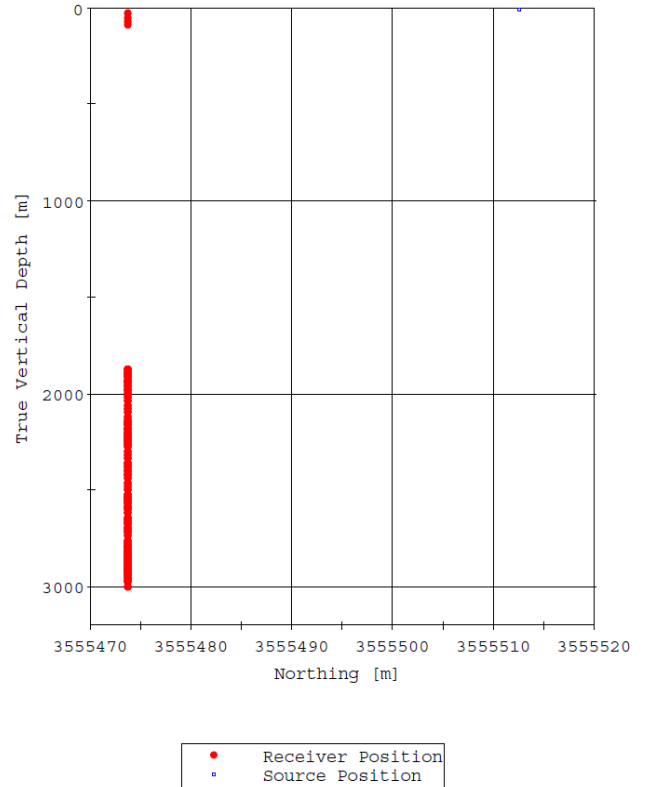


Figure I.8. Geometry Information (Y-Z)

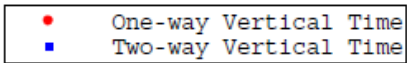
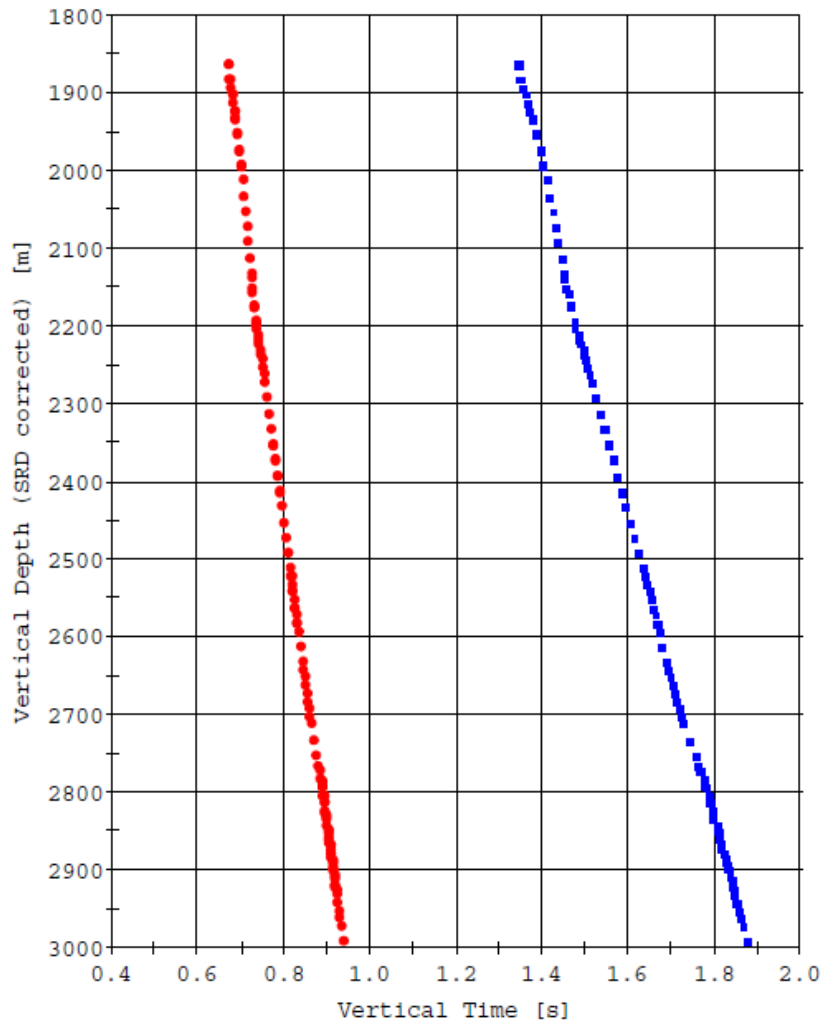


Figure I.9. Time Depth Plot

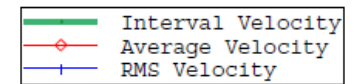
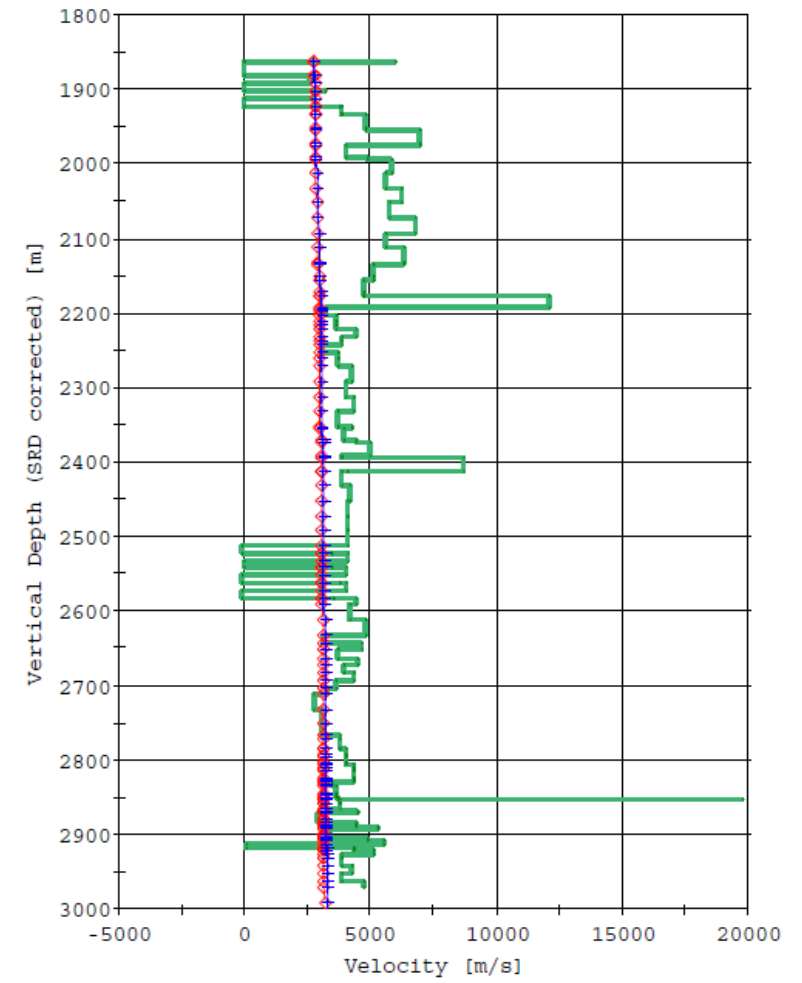


Figure I.10. Velocity Plot



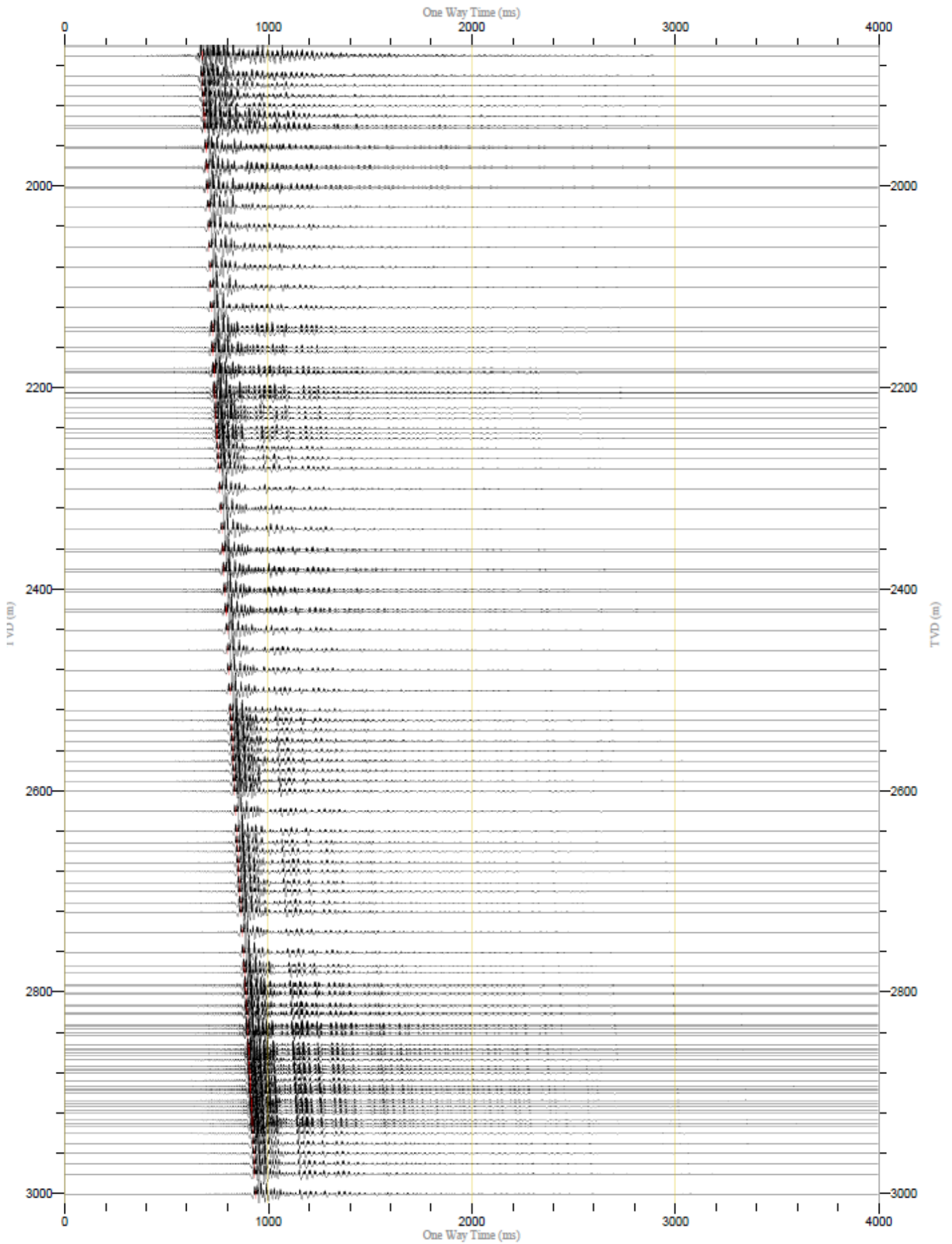


Figure I.11. Digital processing of VSP data (One way time)

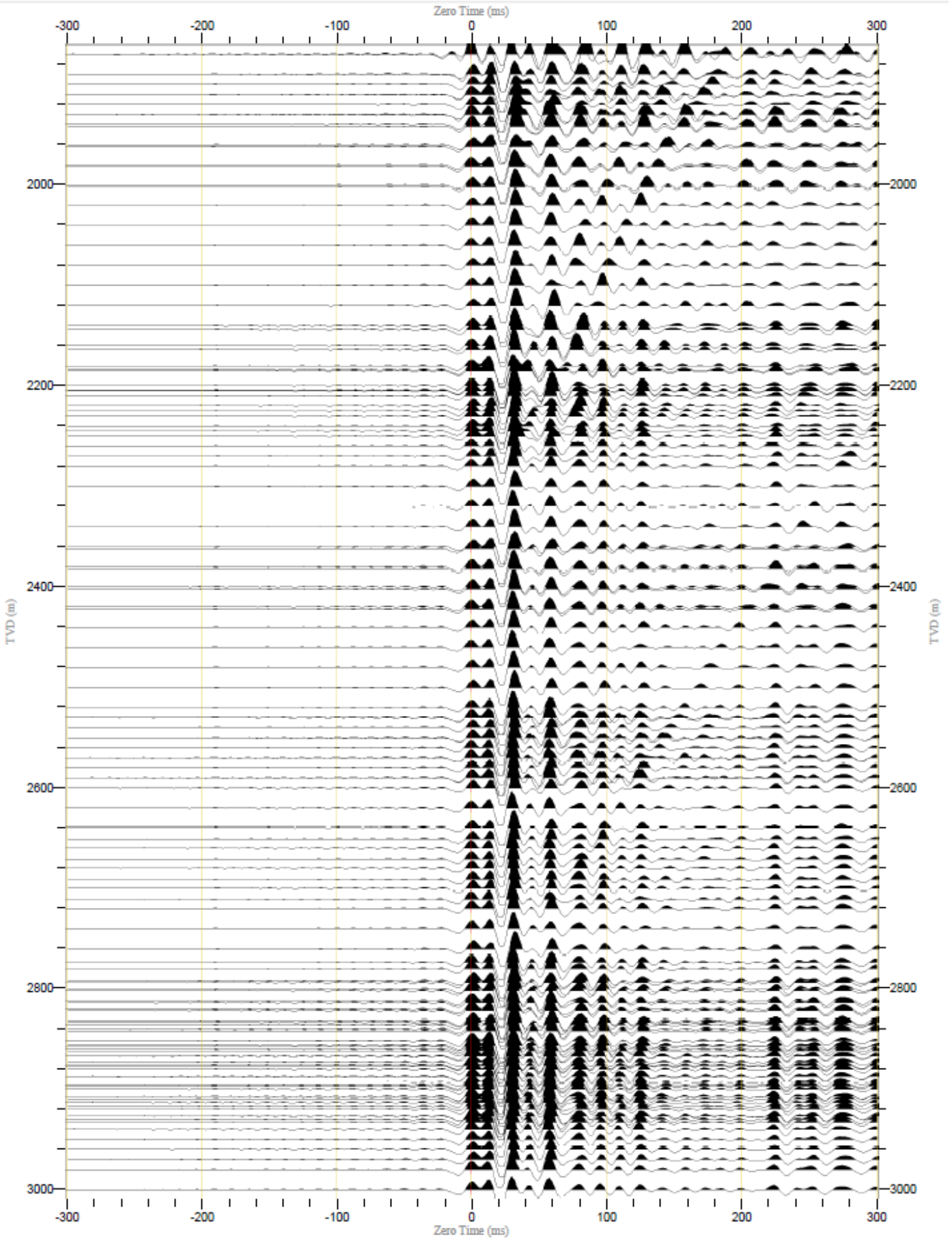
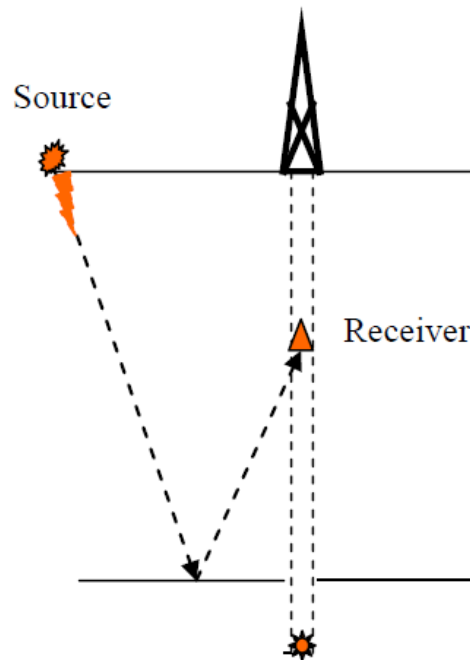


Figure I.12. Digital processing of VSP data (zero time)

### c. Offset VSP

The offset VSP is achieved by positioning a single source far from the well. Reflections coming from reflectors that are farther from the wellbore are picked up by the downhole geophones, allowing imaging to some distance away from the wellbore [5] (Figure I.13). The far offset VSP refers to the distance between the source and the wellbore.



**Figure I.13.** A VPS survey measuring the two-way travel time using Offset VSP [5]

### d. Walk-Above VSP

This technique is used to accommodate the geometry of a deviated well. Each receiver is in a different lateral position with the source directly above the receiver for all cases. Such data provide a high-resolution seismic image of the subsurface below the trajectory of the well [5] (Figure I.14). In Algeria, this method has not been widely used due to factors such as the complexity of the method, limited availability of the necessary equipment, or the method's high cost compared to other VSP methods.

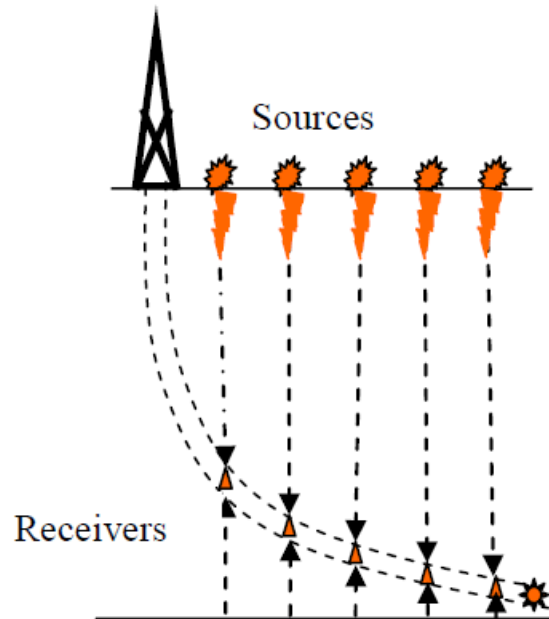


Figure I.14. One-way travel time using Walkabove technique [5]

#### e. Walk-Away VSP

A seismic walk-away is a series of offset VSPs in which a receiver array of five to seven geophones is used. Surface source locations are placed along a line from the well, and hundreds of sources are activated in sequence [5] (Figure I.15). Following data processing, a subsurface image with greater resolution than a surface seismic survey is produced.

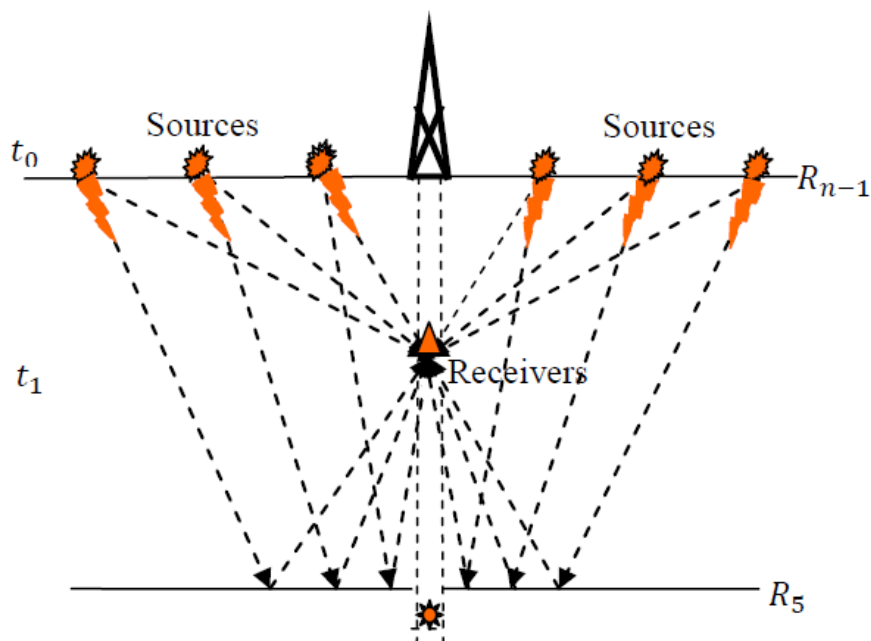


Figure I.15. A VSP survey measuring one-way travel time using Walk-away technique Modified from Arroyo et al [5]

## Comparison between different techniques of VSP

**Check-shot VSP:** This is a type of VSP survey in which a seismic source is generated by a vibroseis truck or other source, and the resulting seismic waves are recorded at a number of shallow boreholes located at various distances from the source. The data collected is then used to calibrate seismic data gathered from other sources.

**Offset VSP:** This type of VSP survey is used to gather information about subsurface rock formations and fluid reservoirs by recording seismic waves generated by a surface source and recorded at various depths downhole. The "offset" refers to the distance between the source and the recording location.

**Walk-Above VSP:** This type of VSP survey is similar to the Offset VSP, but instead of using a fixed surface source, the source is made to walk along a line above the recording locations. This allows for the acquisition of VSP data over a larger area and at a higher spatial resolution than with a fixed source.

Each of these VSP techniques has its own advantages and disadvantages, and the choice of which to use depends on the specific goals of the survey, the geology of the area being studied, and other factors.

### I.2.2. Advantages and utility of the VSP

#### a. Benefits of the VSP

- Provides greater vertical and lateral or spatial resolution than surface seismic.
- Inserting seismic sensor deep into oil and gas wells allows the recording of much higher frequencies as compared to placing sensors at the earth's surface.
- Borehole seismic signals tend to have higher frequencies compared to surface seismic signals, which provides an increase in subsurface resolution.
- The down-going and up-going wave-fields show the variation with depth of acoustic properties such as impedance and viscous damping. The relationship between acoustic impedance ( $Z$ ) and velocity ( $V$ ) of a material is given by the equation:

$$Z = \rho * V$$

Where  $\rho$  is the density of the material

- The VSP generate a seismogram provides a clearer reflection profile than that obtained from the sonic logs, that due to the different amount of data provided by two method since the sonic log gives an image just near the borehole unlike VSP which gives a wider image.
- High resolution images for reservoir boundaries, salt flank imaging, and fault identification in complex areas.

- The direct down-going wave-field can be used to determine velocities which provide insight on rock properties.

#### **b. Application of VSP**

- Predicting depths of seismic reflectors.
- Predicting rock conditions ahead of the drill-bit - defining reservoir boundaries.
- Locating faults near well bore.
- Describing reservoirs via seismic tomography.
- Predicting high-pressure zones ahead of the bit.
- Detecting mud-made fractures.

#### **I.2.3. Limitations of the technique**

- Have high costs and some operational risk (The cost of drilling equipment is directly related to the number of offset sources at the surface, which increases dramatically. Risks are due to having the drill string out of the well for one or more days).
- VSP surveys have limited lateral resolution due to the geometry of the sources and receivers, which are typically located along a single vertical wellbore. This can make it difficult to resolve lateral variations in subsurface structures or properties.
- Complex subsurface structures, such as intersecting faults, can cause multiple reflections and refractions, making it challenging to accurately interpret the VSP data.
- VSP data processing is complex and requires specialized software and expertise. The processing steps must be carefully designed to remove noise and enhance the signal, and mistakes in processing can lead to incorrect or misleading results.

### **I.3. Borehole Seismic Technique**

There are many uses for borehole seismic methods, including the characterization of oil and gas reservoirs, the monitoring of CO<sub>2</sub> storage, the evaluation of geothermal areas, the planning of subsurface waste disposal, the management of groundwater, the characterization of mining sites, and the evaluation of petroleum sites. Accurate interpretation of downhole data requires a thorough understanding of the properties of the source's radiated energy in a borehole and its coupling to the formation.

#### **I.3.1. History of the technique**

The history of borehole seismic can be traced back to the early 20th century, when the first experiments with downhole seismography were conducted.

In the 1940s and 1950s, the development of downhole seismography was driven by the need to explore for oil and gas reserves. During this time, seismic waves were generated at the surface and their arrival times were recorded at downhole receivers to determine the subsurface velocity structure [9].

In the 1960s and 1970s, borehole seismology became more sophisticated with the introduction of advanced technologies such as multi-component sensors and cross-hole seismics. These techniques allowed for the imaging of the subsurface in three dimensions and provided more detailed information about subsurface geology and geophysical properties.

In the 1980s and 1990s, borehole seismology continued to evolve with the introduction of high-resolution downhole seismometers and new data processing techniques. During this time, borehole seismology became an important tool for environmental and engineering applications, such as the study of soil and rock mechanics and the assessment of underground storage reservoirs [10].

Today, borehole seismology is a well-established field that is widely used in the oil and gas industry, geothermal exploration, and other subsurface imaging applications. Advances in technology have made it possible to acquire high-quality seismic data in a variety of subsurface environments, and new data processing and imaging techniques have improved our understanding of the subsurface [11]. In Algeria, it was introduced for the first time in the 1970s or 1980s, as the technology was becoming more widely adopted in the oil and gas industry led by SONATRACH.

### **I.3.2. Description of the technique**

Borehole seismic surveys can be carried out in several different ways:

#### **a. Downhole technique (VSP)**

When making downhole measurements, the seismic source is positioned on the surface while the geophones are placed in a borehole. The travel times of the seismic waves between the source and the different depths of geophones provide information on the seismic velocities and thus on the hardness and type of rock (Figure I.16).



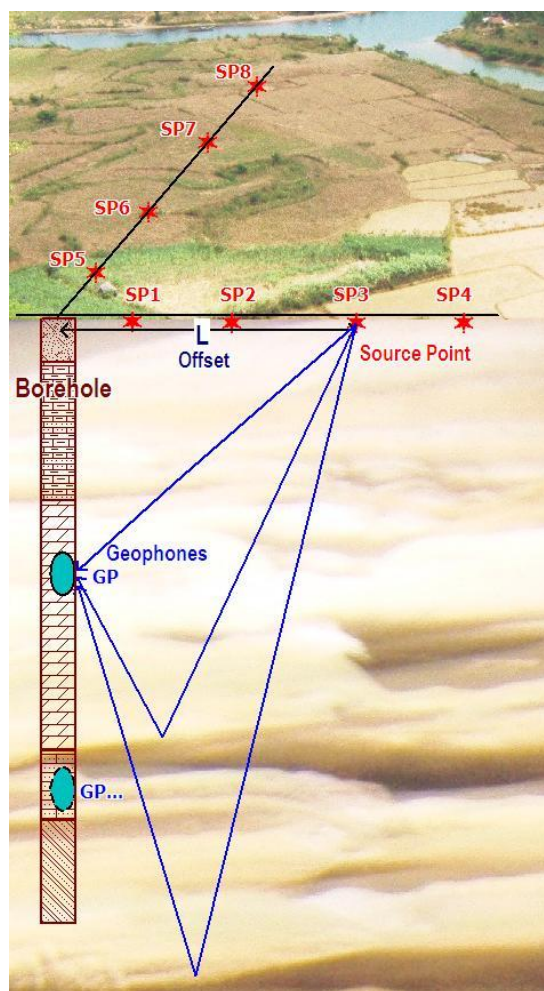


**Figure I.16.** Downhole technique (VSP) [8]

The following are some of the equations that are commonly used in the processing and interpretation of VSP data:

### **Time-Depth Conversion**

The time-depth conversion equation is used to convert the travel time of seismic waves from the surface to depth in the subsurface. The equation is based on the velocity of the seismic waves through the subsurface, which can be determined from the VSP data.

The equation for time-depth conversion is given by:

$$\text{Depth} = \text{velocity} * (\text{travel time}) / 2$$

Where:



Velocity is the velocity of the seismic waves in the subsurface, typically measured in meters per second (m/s)

Travel time is the time it takes for the seismic waves to travel from the surface to a certain depth in the subsurface, typically measured in seconds (s)

Depth is the depth in the subsurface, typically measured in meters (m)

### **Reflection coefficient**

The reflection coefficient is usually defined in terms of the voltage wave and is given by the following equation:

$$R = \frac{I_2 - I_1}{I_2 + I_1} \quad (1)$$

Where:

R: reflection coefficient (%)

$I_1$  : Impedance of the first layer, typically measured in ohms ( $\Omega$ )

$I_2$  : Impedance of the second layer, typically measured in ohms ( $\Omega$ )

#### **b. Uphole technique (check-shot)**

To get more accurate velocity values, small explosive charges are placed at defined depths in a borehole and the travel time of the waves is measured by the geophones on the surface.

#### **c. Cross-hole technique**

A technique for measuring a signal sent from a source located in a borehole, to a receiver array placed in a neighboring well.

The cross-hole and downhole seismic methods are widely used in engineering as a reliable means of in situ determination of the variation of elastic moduli with depth. The cross-hole method is more expensive to conduct in the field than the downhole method, but it is also easier to analyze the seismic results. However, if a soft layer is sandwiched between two hard layers, it is often difficult to identify the first arrival of the direct shear wave in cross-hole records.

### I.3.3. Advantages and utility of the approach

#### a. Benefits of Borehole Seismic

- Unique combination of large depth and high resolution
- Focus on deep targets
- Direct lateral view on steeply dipping targets
- Increased resolution due to target proximity
- Avoid resolution loss in near-surface weathering
- Minimize instrumental deployment on surface
- Reduces the overall cost of the seismic survey

#### b. Application of Borehole Seismic

- Calculation of elastic moduli and dynamic rock properties.
- Detection of faults, shear zones and voids.
- Diagnosis of problem areas in 2-D or 3-D.
- Pre and post-grouting surveys.
- Quality control tool for structural repairs.
- Quantitative evaluation of material by seismic velocity analysis.
- Seismic shear-wave and compressional wave velocity soundings.
- Determination of rock quality through the estimation of the dynamic coefficients of the materials.
- Detection of faults and shear zones in bedrock.

### I.3.4. Drawbacks and Limitations

Borehole Seismic and Vertical Seismic Profile (VSP) methods have several drawbacks and limitations, including:

**Cost:** Both methods are more expensive compared to surface seismic methods. The cost of drilling a borehole, installing geophones, and recording data can be significant.

**Complexity:** Borehole seismic and VSP methods require specialized equipment, and the data interpretation can be challenging especially for second arrivals (multiple)

**Limited depth:** Both methods are limited in terms of the maximum depth that can be explored, which is usually a few kilometers.

Poor resolution in some areas: Poor quality data can result from factors such as low frequency of the seismic source, presence of borehole fluid, or poor geophone placement.

Limited data coverage: Borehole seismic and VSP methods provide limited data coverage, with only one borehole in a single location. Surface seismic methods, on the other hand, can provide data coverage over large areas.

Limited temporal resolution: Both methods have limited temporal resolution, meaning that they may not be able to capture rapid changes in subsurface conditions.

#### **I.4. Conclusion**

VSP data acquisition is extremely demanding in terms of equipment type and quality, technical skills, engineering and geophysical specialized knowledge, survey objectives, and so on. As a result, it is relatively common for VSP data acquisition to be prone to errors and inaccuracies. Identifying the most common errors and malpractices in VSP surveys took several years of research into numerous case studies.

Borehole seismic surveys are important for the understanding of the orientation and types of fractures determining solution for mine optimization and faults controlling mineralization.

Seismic methods offer a very high resolution vs. the volume covered.

The cost of borehole seismic is extremely acceptable, compared with surface deployments. Seismic method, and among these, borehole technique, were identified as the best tool to potentially characterize alteration and structurally compromised zones.

Borehole and surface 3D seismic investigation combine presently their benefits to produce site models with increased levels of detail and reliability.

However, new technologies are being developed in order to improve the reservoir monitoring not just after drilling but in real time while drilling, among these technologies we proposed the surface seismic while drilling SSWD, which will be discussed in more details in the next chapter.

# Chapter II

## Seismic While Drilling

---

## **II.1. Introduction**

Seismic while drilling (SWD) is a technology that can provide subsurface velocity information, which in theory can reduce the uncertainties in determining depth velocity. SWD has been around for over 20 years, but its usage has been constrained by sensing and operational limitations. In this chapter, we will provide a more in-depth understanding of the different types of SWD technologies available.

Seismic while drilling is an innovative technique used to gather geological information about subsurface rock formations during the drilling process. It combines the traditional seismic surveying method with modern drilling technology to produce a more comprehensive understanding of the subsurface. This information is crucial for various applications, including reservoir evaluation and drilling planning. By using seismic while drilling, drilling engineers can make informed decisions, reduce risks, and optimize drilling operations.

There are two main types of SWD: active and passive. In active SWD, an energy source, such as a hydraulic vibrator or an explosive charge, is used to generate seismic waves. In passive SWD, the seismic waves are generated naturally by the drilling process itself. Both types of SWD can provide valuable information about the subsurface, such as the identification of subsurface faults and the thickness and character of subsurface formations. In this chapter, we will provide a more detailed explanation of the different varieties of SWD techniques and their applications, based on research from various sources [12, 13]

## **II.2. History of the development of the method**

SWD is a valuable and interesting geophysical technique, which has undergone extensive research, testing, and improvement throughout its history.

The first method of SWD was surface seismic while drilling (SSWD), which was widely used in the international oil field industry due to its basic principle of functioning. However, its limitations and potential risks led to the invention of the next technique.

In the past 30 years (since 1991), the drill-bit SWD has been in use by the oil field industry, utilizing the vibration energy generated by the tri-cone bit to provide vital real-time data and look-ahead information during the drilling process. Before this, there were very limited technical interactions between geophysicists and drillers, but that has changed since the fully developed SWD (1990-2000), and credit for its development belongs to IFP (French Institute of Petroleum) and its partners [14, 18].

Another emerging technique that has been mainly used by Schlumberger since 2000 is the vertical seismic profiling while drilling (VSP-WD), which involves capturing and recording the signal emitted by a surface seismic source on hydrophone sensors integrated inside the downhole borehole assembly (BHA).

The most recently introduced technique is the swept impulse hydraulic tool, which is capable of generating a seismic signal at the bit location while drilling. This tool overcomes the limitations of drill-bit seismic technology, particularly in soft formations, and allows for seismic operations while still drilling with the polycrystalline diamond compact (PDC) bit. The high-intensity compression wave signal is used for high-resolution (broadband) seismic profiling and look-ahead imaging while drilling [17, 18].

### **II.3. Different methods of SWD technique**

There are several methods of seismic while drilling (SWD) including:

- Surface seismic while drilling (SSWD).
- The drill-bit SWD technique.
- Vertical seismic profile while drilling (VSP-WD).
- SWD using swept impulse hydraulic tool.

#### **II.3.1. Surface seismic while drilling (SSWD)**

Surface seismic while drilling is used for general subsurface mapping, locating oil and gas accumulations, and keeping track of reservoir changes brought on by oil and gas production. While gathering surface seismic data, the z-axis (depth below the surface) is determined by the two-way travel times of the sound waves. The x- and y-axes' horizontal distances are expressed in meters.

The depth (Z-axis) in drilling operations is measured in meters. It is necessary to know the velocity of the underground rocks in order to convert between the two domains (depth conversion). Drilling prognosis is frequently uncertain because of inconsistent velocity information.

Surface seismic data has a lower resolution and the frequency content of the signal decreases with burial depth. The typical normal resolution is one quarter of a wavelength, which is 10 meters for a seismic wavelength of 40 meters with a typical center frequency of 50 Hz and a velocity of 2000 meters/sec [26]. Seismic is also used in the borehole. The principle was investigated as early as 1930 [26]. Today, several techniques exist with different applications and limitations. A typical system consists of a source to create a seismic signal and receivers to record these signals. All borehole seismic techniques utilize a setup where one component (source or receiver) is located on the surface, and the other in the borehole. Hence the “one-way travel time” of the waves is recorded, in contrast to surface

seismic where it is the waves that have traveled both ways that are utilized. Borehole seismic is used extensively worldwide today.

### II.3.1.1. Operating principle of the (SSWD) method

Seismic imaging techniques may occasionally allow the detection of vertically aligned objects whose diameter is greater than the seismic wavelength. A novel technique that makes use of this reality and, more specifically, the seismic diffraction response from the borehole, is surface seismic while drilling (SSWD). Utilizing surface seismic data, a technique is applied to visualize well routes (Figure II.1). The advantage of this approach is that the well is imaged within the context of the seismic image, which means that the well trajectory is imaged using the same imaging techniques as the seismic image, removing any ambiguities in projecting the well onto the seismic image. In other words, the SSWD approach provides more details of the well.

Furthermore, surface seismic while drilling (SSWD) is based on using seismic data acquired at the surface to image the well path. The method uses conventional seismic equipment (receivers and sources) together with specialized setup, procedure and processing to accurately display the well on the seismic image (Figure II.1). The method is based on the principle that the wellbore represents a reflective and diffractive object for the seismic waves, and therefore is not dependent on the presence of steel in the wells (Figure II.1) [14].

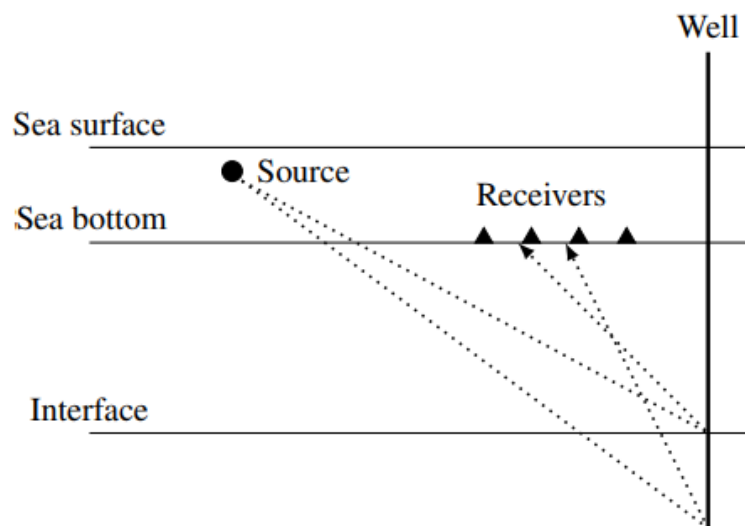


Figure II.1. Illustrative image of (SSWD) in offshore

### II.3.1.2. Description of the technique

When the drill bit penetrates the subsurface formations, it causes changes in the subsurface. With high-resolution seismic data, these changes can be detected, allowing for the accurate tracking of the well path while it's being drilled..

Before drilling, a reference seismic image of the subsurface is obtained. This could be the initial seismic data collected before drilling or a simulated dataset from an earth model. The seismic survey is repeated as the bit drills deeper into the earth, using fixed seismic sensors and sources installed on the surface or offshore equipment for offshore locations.

The newly obtained seismic data is then subtracted from the reference seismic image, resulting in only the changes in the subsurface being visible. Seismic simulations have shown that this method can accurately track the true well path as its being drilled (*Johansen & Sangesland, 2013*)[26]. If successfully utilized, this technology can revolutionize several aspects of drilling technology.

### II.3.1.3. Advantages of the technique

- This technique uses geophysical principles seismic, no tools or steel are required in the well.
- It does not depend upon interrupting the drilling operation.
- Favorable property of the SSWD method is that the well path is imaged directly into the seismic image. As a result, the well path's location in relation to its geological surroundings is depicted.
- Any other wells in the region are imaged using SSWD.
- The well path's mapping into the seismic image is done without big uncertainty.

### II.3.1.4. Limitation of the technique

- SSWD requires specialized equipment, and the data interpretation can be challenging.
- It is more expensive compared to traditional surface seismic methods, due to the need for specialized equipment and expertise.
- The use of seismic sources and recording equipment can have a significant impact on the environment, including noise pollution and disruption of wildlife habitats.
- It is limited in terms of the maximum depth that can be explored, which is usually a few kilometers.
- SSWD can interfere with drilling operations, potentially leading to delays and increased costs.
- Poor quality data can result from factors such as low frequency of the seismic source, presence of borehole fluid, or poor geophone placement.



### **II.3.1.5. The critical use of SSWD for drillers**

Johansen et al. (2013) proposed the use of repeated surface seismic while drilling (SSWD) to measure the relative distance between two wells in real-time while the relief well is being drilled. Modern relief wells bear little resemblance to the first relief wells drilled in the early 20th century, as they directly intersect the original well at a depth of several miles and usually less than a foot in diameter. Traditional depth and positioning instruments are prone to horizontal errors of up to 100 meters, which do not provide the required accuracy for direct access to the intersection between two wells. To overcome this limitation, special registration tools have been developed using steel tubes in blown wells. This is achieved by acquiring reference seismic data before drilling commences and continuously repeating the seismic survey as the bit propagates down into the earth. Subtracting the reference seismic data from the newly acquired seismic data yields only the changes in the subsurface, allowing the true well path to be determined. This method has the potential to facilitate a direct intersection, regardless of the presence of steel in the blowing wellbore [20].

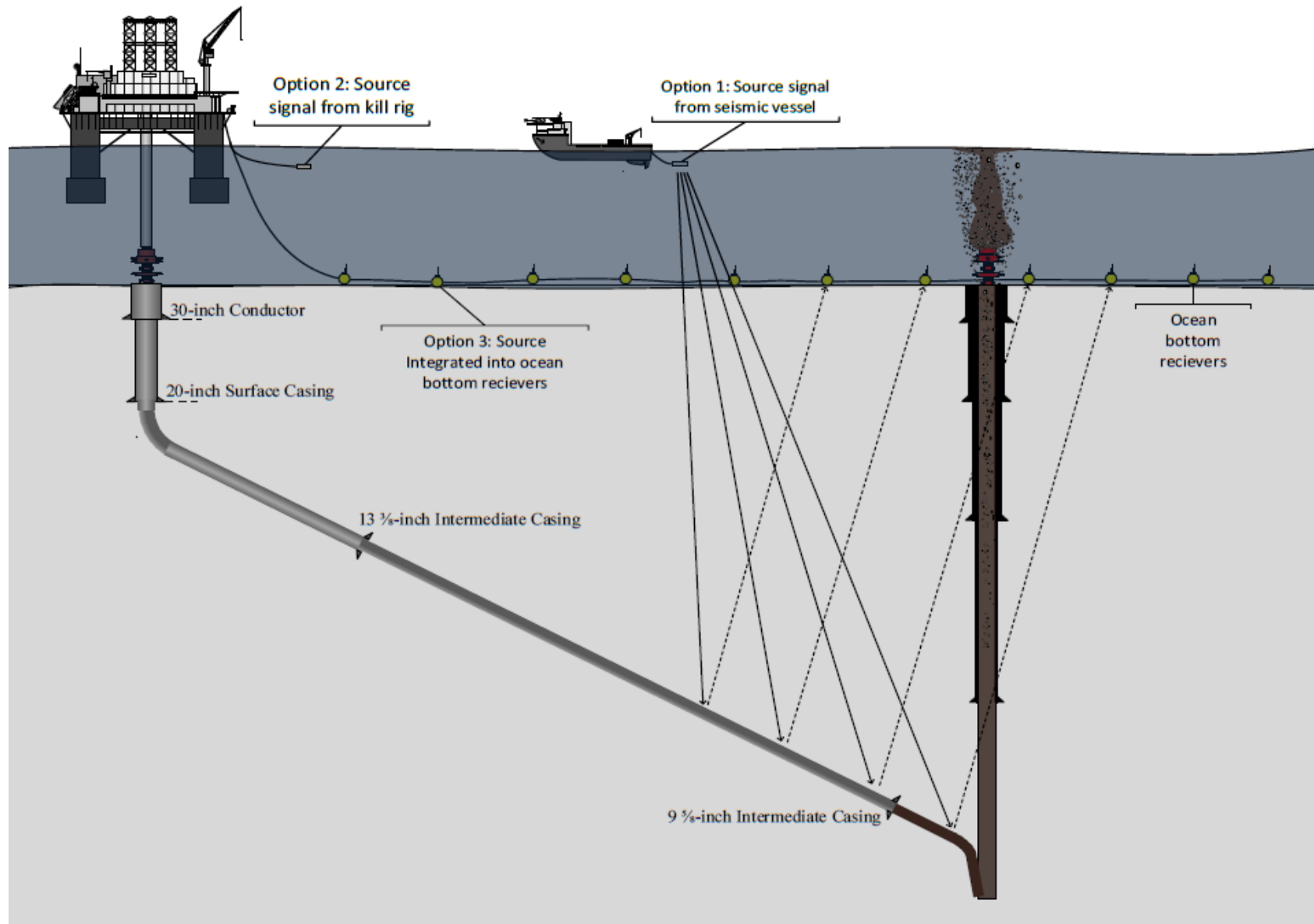


Figure II.2. Bottom intersection using SSWD [26]

### II.3.2. The drill-bit SWD technique

The drill-bit SWD method provides real-time data by using the drill-bit as a source of vibrations due to its impact on the rock formation during drilling. The waves propagate through the subsurface and get recorded and traced by surface geophones, which provide real-time information about the subsoil [14].

#### II.3.2.1. Operating principle of the (drill-bit SWD)

The operating principle of this SWD method involves in **generating** seismic waves by the bit-formation interaction and **recording** the reflected waves to provide subsurface data.

Additionally, seismic waves generated by the drill bit are both compressional waves known as primary waves (P) and shear waves also known as secondary waves (S). The primary waves are the first ones to arrive at the geophone. They have the capability to move through solids, liquids, or gases. Unlike them, the S waves, which are the second to arrive during the bit vibration, are much slower than the P waves and can travel only through solids (Figure II.3) [15].

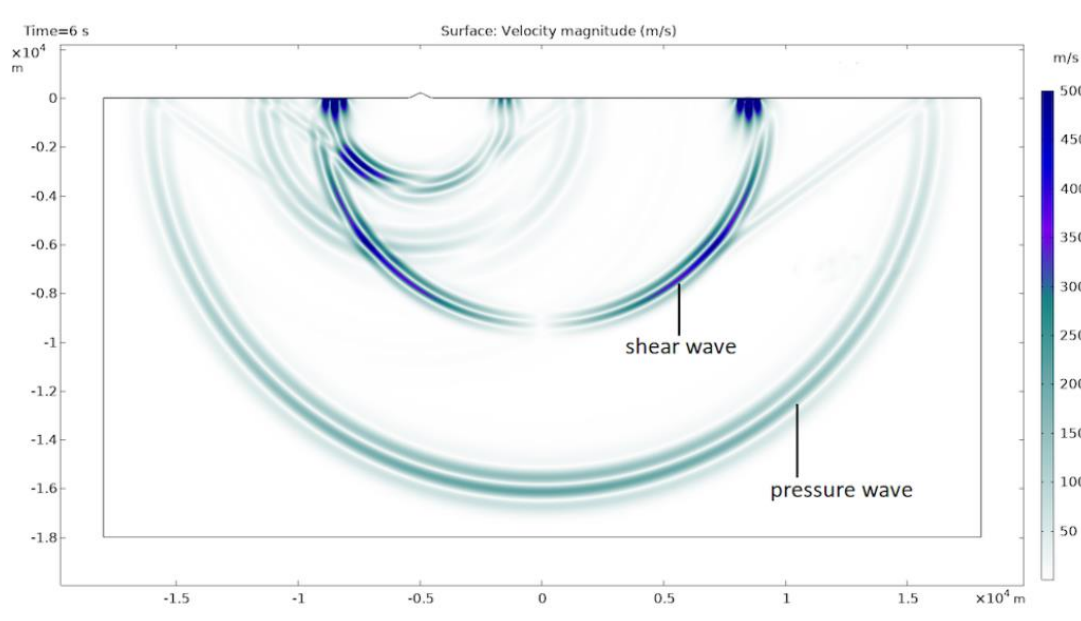


**Figure II.3.** Model of two different waves (shear and pressure) and there propagation in the ground [16]

The application of drill-bit seismic during drilling is a development of the traditional seismic technique, which makes use of signals with zero start timings and established signatures (as we mentioned previously in the first chapter). The while-drilling technology requires preprocessing of the acquired time-incoherent raw-field data (referring to the conventional seismic surveys) to obtain impulsive shaped seismograms with

known zero times. This is accomplished using very long recording intervals, that is, using several tens of minutes of passive listening for each depth point [15].

### II.3.2.2. Description of the technique

Drill-bit SWD is a geophysical technique that can be distinguished by its setup, which consists of the drill bit as the source of vibrations (the impact of the bit on the rock formation), and the waves generated by the drill bit are captured by receiver elements deployed on the surface. A geophone, known as a pilot sensor, is mounted at the top of the drill string to record the source signature, as shown in Figure II.4. Using the response of the pilot sensor as a pilot signal, analogous to a vibrator sweep signal, a seismogram can be obtained by cross-correlation with the response of each receiver element.

SWD, a method with geometry like reverse-VSP, can be used to gather formation boundary and velocity information both above and below the drill-bit. The location of the drill-bit in the seismic section can be known while drilling by converting the velocity information from drilling depth to two-way travel time. The location of the drill bit and information about the formation boundary are then combined to forecast and prevent drilling problems [14].

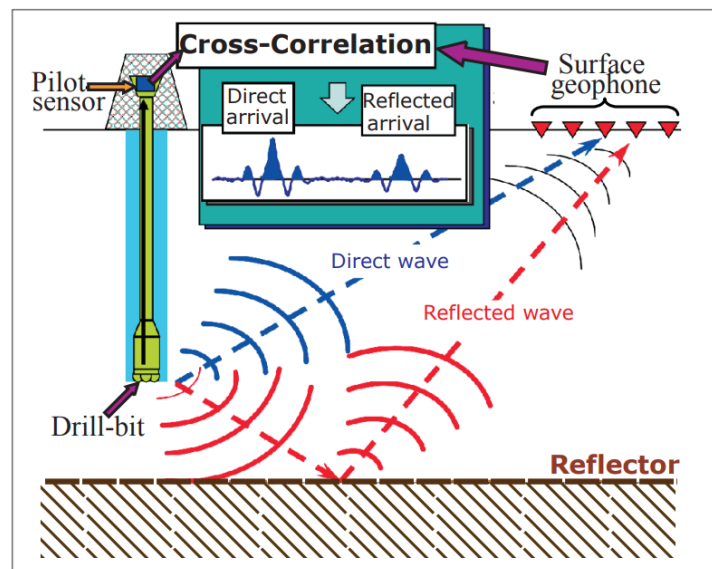


Figure II.4. The basic SWD setup and the cross-correlation concept between the pilot sensor and the Surface geophones [14]

### II.3.2.3. Advantages and utility of the technique

- Provides real-time subsurface information that can be used to adjust drilling parameters, improve drilling accuracy, and reduce the risk of geological surprises.

- Helps to identify subsurface geological features, such as faults, reservoirs, and hydrocarbon-bearing formations, which can improve understanding of the subsurface and reduce exploration risk
- Can help to identify areas of weak or unstable rock formations, which can be avoided to improve wellbore stability and reduce the risk of a well collapse
- Can be used to optimize well placement, helping to maximize reservoir contact, reduce drilling costs, and improve the efficiency of hydrocarbon recovery
- Can reduce exploration risk by providing real-time information about subsurface geology and reducing the risk of drilling into areas with undesirable geology.

#### II.3.2.4. Limitations of the technique

- This technology is unreliable in either soft rocks or very deep (> about 18,000ft) and horizontal wells [25]
- It cannot be used in highly deviated holes as the drill bit signature measured at surface is attenuated too much by high hole angle
- It can only work reliably when drilling with roller cone Bit. It cannot be used with polycrystalline diamond compact (PDC) bits
- In which the drilling operation is realized, that comes with sudden unpredictable variations that can affect the quality of the seismic data
- Strict timing: the acquisition cannot be repeated at the same depth level once it has been drilled, and any contingent failure of the acquisition system can lead to irreparable loss of data

#### II.3.3. Vertical seismic profile while drilling (VSP-WD)

As mentioned in the history of the SWD technique, the VSP-WD method is mainly used by Schlumberger. This method is a transfer of wireline borehole seismic to drilling operations by using the same surface source and downhole hydrophones as the conventional VSP. The real difference is that there is no cable connection between the tool and the surface.

##### II.3.3.1. Operating principle of the (VSP-WD) method

This technique employs downhole sensors integrated in the borehole assembly (BHA), which receive seismic signals from a seismic source deployed on a source vessel (boat or rig). The source is emitted while

making the drill string connection (tripping-time) or during drilling pauses, when mud circulation is stopped and drill pipes are stationary so that drilling noises do not interfere with the data processing.

The VSP-WD technique employs a downhole sensor integrated into the borehole assembly (BHA) which receives seismic signals from a seismic source deployed on a source vessel, such as a boat or rig. The source is emitted during drilling pauses or while making drill string connections (tripping-time) when the mud circulation is stopped and the drill pipes are stationary to prevent drilling noise from interfering with data processing. Seismic signals are received by the VSP-WD tool in a closely synchronized acquisition process by a conventional source, such as an airgun on offshore rigs, or vibroseis or dynamite (explosive) on land. The tool can collect both the direct and reflected seismic signals. The downhole tool contains sensitive receivers, processors, and memory. The signals are processed downhole to determine crucial first break-time, or check shot time, and this information is then transferred up-hole in real-time by a mud pulse telemetry system. Current mud pulse telemetry systems do not have the required data rates to send full-waveform data up-hole. However, the VSP-WD tool can store raw full-waveform data in the downhole memory storage which can be retrieved later during tripping of the bit.

The tool needs to be configured before it is run in the borehole with the BHA to prepare it for data processing. The source can be turned on during tripping while the tool is at the appropriate depth. Seismic signals are collected by the tool's memory for later processing. These waves can be recorded directly from the source as one-way travel time or reflected by the formation known as two-way travel time. The entire procedural aspect of the tool is shown in Figure II.5.

The sensor prepares the data for transmission up-hole when mud-pulse telemetry (which will be detailed later in this paragraph) starts. In order to locate the bit on the surface using seismic imaging, the time-depth relationship in real-time is applied through MWD. Only the most crucial data is transmitted up-hole, while the rest is retained in downhole memory.

**A brief description of mud-pulse telemetry technology:** This binary coding transmission method is used with liquids and is called mud pulse telemetry. This is achieved using a valve that modifies the drilling mud pressure inside the drill string and translates the recordings from the sensors positioned on the drill head into pressure pulses, which act as signals. The drilling mud is used to transmit these pulsations to the surface. The pressure pulses are measured on the surface by a pressure transmitter and converted into an electrical signal, which is transmitted to a computer in digital form. For more details, please see [Annex] [17, 21, 23].

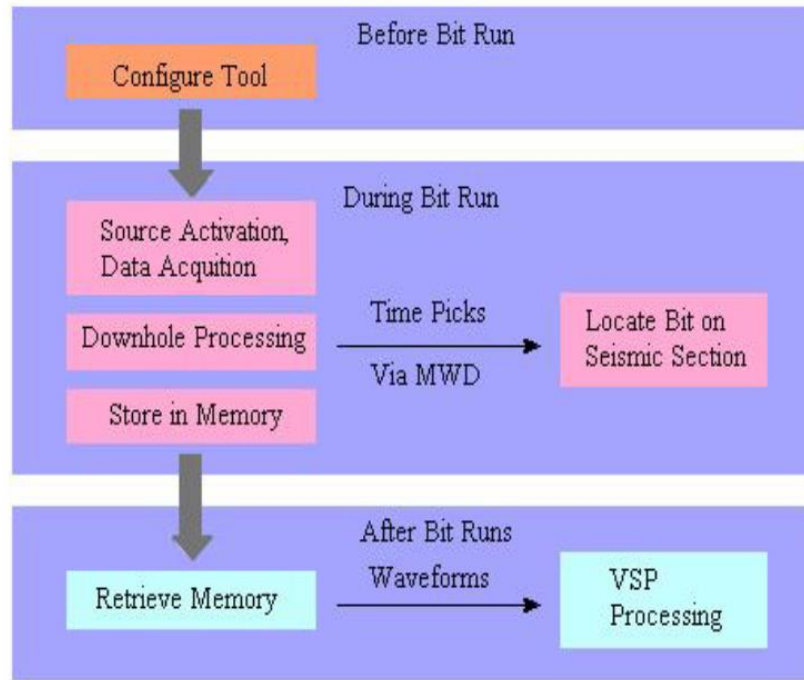


Figure II.5.VSP-WD procedures aspect [17]

### II.3.3.2. Description of the technique(VSP-WD)

Synchronized clocks serve as the foundation of the VSP-WD technology. The key technical achievement was the creation of a downhole clock with millisecond precision measurement capabilities that was also strong enough to withstand the downhole environment (high pressure and temperature).

The tool measures seismic energy from a surface source using hydrophones and geophones. analyses waveforms below the surface to calculate the first break time, and transmit this information up-hole through mud-pulse telemetry. Various components make up **the necessary surface equipment**, depending on the application. To process VSP images, waveform data can be retrieved from the tool memory and delivered to a processing center. The geometry of the well and the location of the source both play a significant role in the process. For this application, vertical wells with zero offset sources perform best. **The following tools are necessary** for any application:

- **An airgun system** (Figure II.6), (Figure II.7).
- **A surface computer to provide timing information and process the data.**
- **A source of high pressure (approx. 3000psi) of air** (Figure II.8).
- **A navigational system.** (Figure II.9).
- **A processing software.**



- A **tap tester**, is used to test synchronization of the clocks and entire system operation during a shallow hole test just prior to running in hole.

At the surface, the engineer decides whether to fire the airguns or not. If the driller is making a connection and the downhole tool is stationary, the engineer enables the automatic gun firing software. This software fires the airguns exactly 15 seconds apart at the start of this window.

When the seismic signal is analyzed by the downhole tool, an algorithm determines whether or not there will be a first break. If a shot is considered to be good, it is put into a buffer to isolate it.

While each shot is stored in memory for further processing, real-time measurement requires at least three consecutive shots to arrive at the tool with the same wave-shape and offset in time. This prevents the tool from activating in response to rig noise. If at least three shots are observed, the tool begins stacking the waveforms and continues to do so with each shot.

Once the pumps resume, the tool calculates the first break-time from the stacked waveform, passes this to the MWD telemetry, and sends it up-hole immediately after the survey [17, 21, 22, 24].

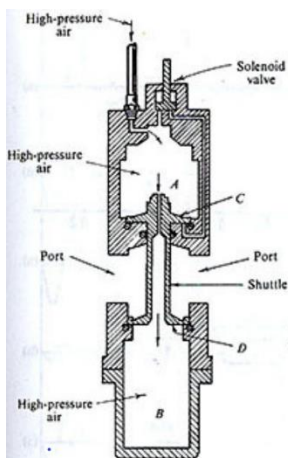


Figure II.6. Offshore airgun system [17]

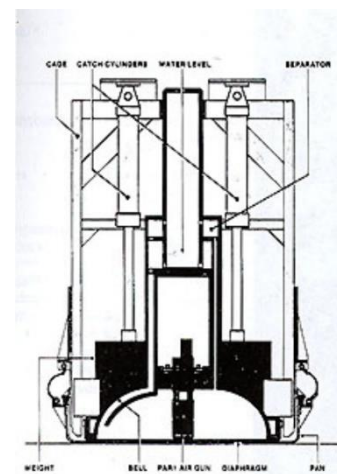
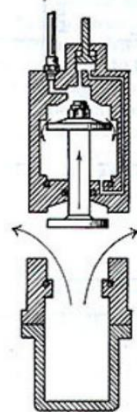


Figure II.7. Land airgun system [17]





Figure II.8. High-pressure source to generate the airgun [17]

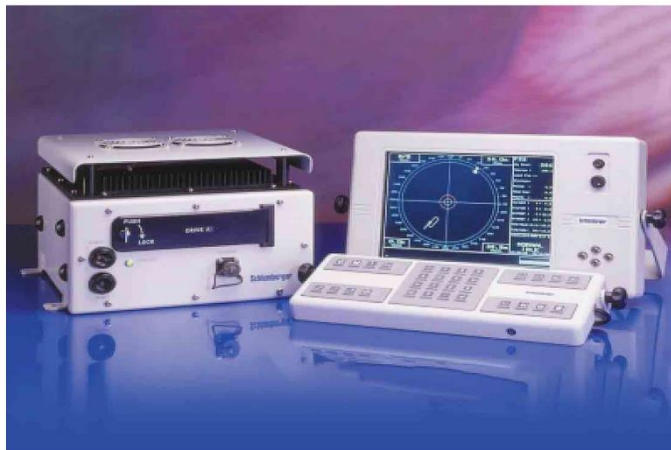


Figure II.9. Seismic Navigation and Processing system [24]

### II.3.3.3. Advantages and utility of the technique

- In the horizontal part of the wells, it seems like the only method to record VSP- type data, since the drillers are extremely reluctant to re-enter the borehole with the drillstring pushing a wireline VSP tool, for reasons of borehole wall instability and security.
- It places the bit on the seismic map or section. Since the seismic is now corrected down to the bit position, the driller can be aware of their present position and what lies ahead. An important result of correcting the seismic down to the bit position is that the seismic uncertainty ahead of the bit is reduced. It can reduce uncertainty from an unbelievable 700m to 10m. [17, 21].

- While coring operations well can be drilled very close to the interface where the core is needed. This eliminates a large amount of unnecessary hole that needs to be drilled, thus avoiding reduced or missed core data and saving time as well as money.
- Large saving can be realized using VSP-WD service. It saved the cost of running intermediate wireline VSP, which was not a preferred option when the drilling was proceeding approximately at 400m/day, the cost of 12 hrs of rig time would have been \$42,000.27 [17, 21].
- The unconformities that are seen in the look ahead VSP and ‘NOT’ seen in the surface seismic.

#### **II.3.3.4. Limitations of the technique**

- It is claimed that it provides look-ahead imaging, however the range and accuracy of this capability is still not accurately known
- Mud Pulse telemetry of processed velocity is planned but not presently commercial.
- The biggest limitation of VSP-WD services is to ensure a good mechanical coupling of the VSP seismic sensor with the borehole and high precision required on downhole clock.

#### **II.3.4. SWD using swept impulse hydraulic tool**

Deep drilling operations face a serious obstacle in the form of slow penetration rates in highly pressured formations. High mud weight, hard rock, and high borehole pressure severely decrease the drilling penetration rate while long drill strings restrict the amount of hydraulic power that can be applied to the bit. To address this issue, a device is used to produce strong suction pulses at the drill bit, which can boost the overbalanced drilling rates.

##### **II.3.4.1. Operation principle of the technique**

Conventional rotary drilling is a mature method and has played a primary role in drilling technology for more than one hundred years. However, its rate of penetration is generally low, especially when drilling hard rock formations. The use of hydraulic pulse drilling technology was created primarily to address challenges associated with deep drilling in excessively pressured rocks and help overcome the limitations of conventional drilling methods.

The hydraulic pulse valve that makes up the sweeping impulse source has a mechanism that adjusts the gap between impulses, as demonstrated in Figure II.10.

Sweeping the cycle rate allows for seismic profiling and reflection imaging of formations ahead of the bit.

The energy of the mud circulation is converted into percussive power by a mud turbine that is mounted directly above the drill. The application of a percussion mechanism with a hydraulic power unit, which is independent of the drilling mud, powers the hydraulic hammer. The impacts caused by the hydraulic-accelerated hammer can be used as an energy source for both drilling and seismic wave generation. As the hammer is deployed just above the drill bit, emission losses of both impact power and seismic energy are minimal [14, 17, 26].

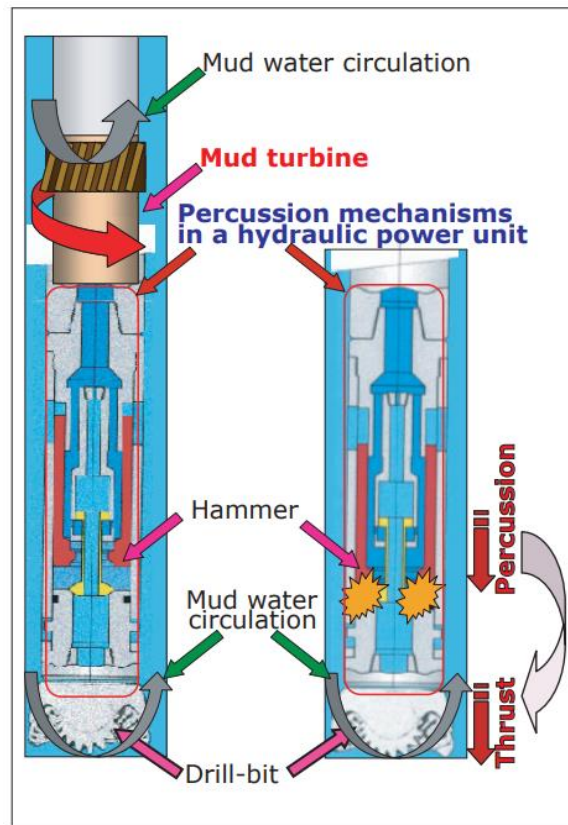


Figure II.10. Diagram of percussion drilling tool [14]

#### II.3.4.2. Description of the technique

Several experiments with the hydraulic pulse tool have shown that signals can travel well to the surface from a depth of 2700' and beyond [27]. A mechanism has been developed to sweep the cycle rate of the tool through almost an octave (an octave is the logarithmic ratio of two frequencies) as shown in Figure II.9.

The impulse cycle duration runs for approximately 4 seconds, and the cycle rate varies from 11 to 19 Hz [6]. The suction pulse is omni-directional, allowing applications in vertical or deviated wellbores. When drilling, the tool produces a powerful shear wave, but when the bit is off-bottom, there is no S-wave propagation. This ability allows for profiling of both P- and S-wave velocity with direct application to gas detection. The presence of even small amounts of free gas at the bit will immediately eliminate the seismic signal, providing early warning of a gas kick.

A hydraulic pulse valve is included in the swept impulse source, and it has a mechanism that varies the duration between two pulses. Sweeping the cycle rate while drilling enables seismic profiling and high-resolution look-ahead imagery [14]. To create a vertical seismic signal, the signal picked up by the geophones is cross-correlated with a pressure pilot signal located at the top of the drill-string. Real-time processing is done with a software correlator.

Since the tool is capable of stopping all of the mudflow, a series of bypass ports may be incorporated to ensure circulation in the event that the valve fails in the closed position (Figure II.12).

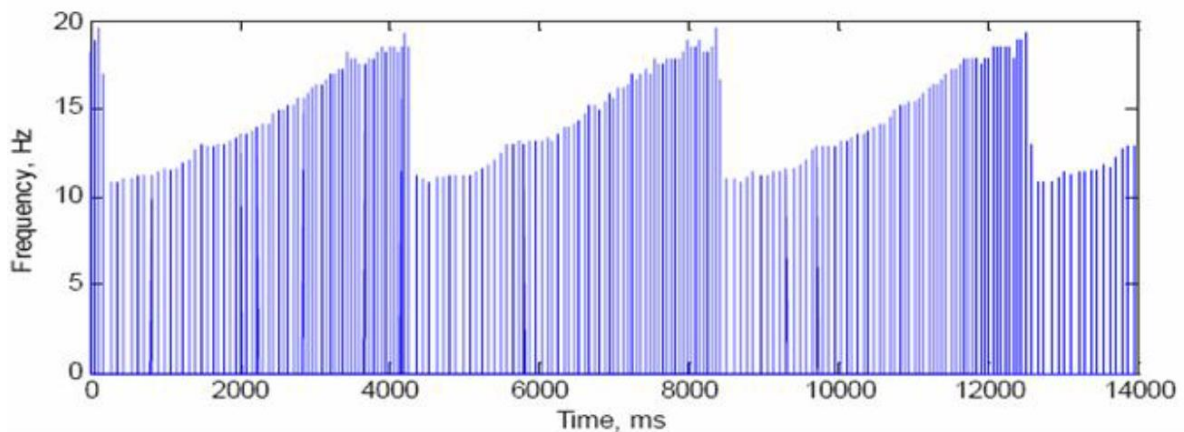


**Figure II.11.** Internal pressure frequency time sample – impulse function times cycle frequency [27]

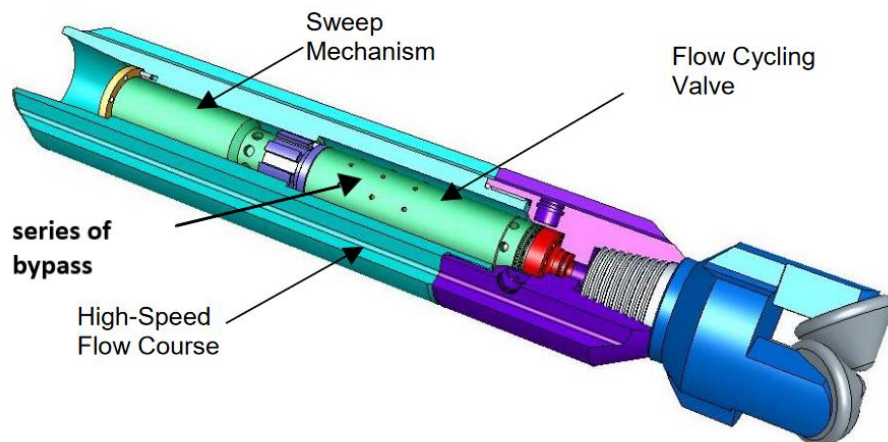


**Figure II.12.** Hydraulic pulse tool with high-speed flow course housing and sweep mechanism [27]

### II.3.4.3. Advantages of the method

- The swept impulse seismic source generates broadband, high-intensity shear and compression waves that can be used for seismic profiling and look-ahead imaging while drilling.
- The combined compression and shear wave data can be used to predict pore pressure ahead of the bit.
- The tool can be used with no interruption of conventional drilling operations, with any bit type in any well geometry.
- The primary advantage of swept impulse seismic tool over VSP-WD services is the ability to generate and display a VSP corridor stack in real-time while drilling
- Provide formation velocities within 5% of a conventional wireline VSP service.
- Real time prediction – defined as less than 10 hours.

### II.3.4.4. Drawbacks and Limitation of the technique

- SWD using swept impulse tool requires specialized maintenance and understanding, it is more expensive than the other methods in this aspect
- Risk and danger, the impulse tool uses strong sheer waves that can damage the bottom hole and the mistake while using it is very punishable
- IF the bypass system fail, that will lead to reservoir damage

## II.4. Application around the world of SWD

The SSWD method has been successfully applied to image vertical well bores (Evensen et al., 2014; Moser et al., 2016a) and even an already drilled relief well using streamer field data (Moser et al., 2016b). To demonstrate the utility of SSWD during relief well drilling, the authors utilized a synthetic model based on outcrop data from the Kvalhovden area in East-Spitsbergen, Norway (Johansen et al., 2007). The model simulates a reservoir in one of the rotated fault blocks with a vertical production well (Figure II.13a). The pre-stack depth migrated (PSDM) image is shown in Figure II.13b. Now, let's assume that due to some unforeseen circumstances, the production well experiences a blowout and needs to be stopped. The procedure for doing this involves drilling a relief well that intersects the blowing well at the bottom (as shown by the dotted line in Figure II.13a) [13].

The authors then simulate four seismic surveys at different stages of the relief well drilling. Receivers with a spatial spacing of 10 m are placed at the sea surface, and 401 shots with a shot distance of 5 m are

used in each survey. The seismic data at each stage is generated using ray-Born modeling. For each stage, the SSWD method is employed to image the relief well.

In the first stage, the well is drilled down to a depth of approximately 425 m and positioned at 720 m. In the SSWD image (Figure II.13c), both the relief and production wells are clearly visible, and diffraction responses from the wells are visible at the interfaces in the geological structure. This image, in combination with the PSDM image (Figure II.13b), can be used to identify in which geological unit the drill bit is located. In each of the next stages, the relief well is drilled about 50 m until it intersects the blowing well (Figure II.13f). The SSWD images from each of the stages are given in Figures II.13d-13f. Note that they used time-lapse data to image only the newly drilled section of the relief well in the figures. They observe that the newly drilled sections are clearly visible in the images by their intersection with geological interfaces and the drill bit itself [13].



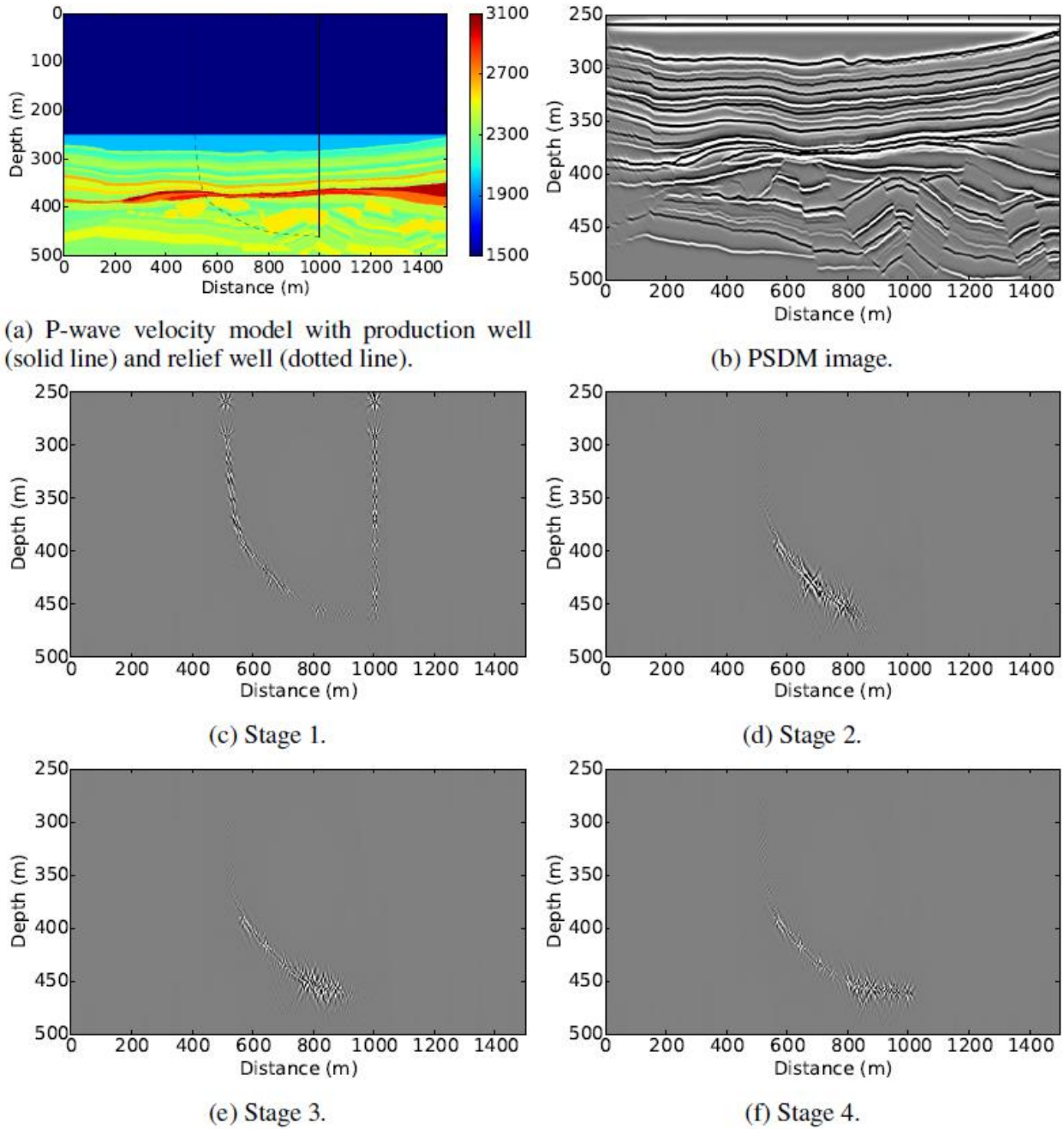


Figure II.13. The P-wave velocity model and the migrated images using SSWD, Note the imaged diffractions from interface intersections and the drill bit [13]

## II.5. Conclusion

In this chapter, we have seen different types of SWD that have been developed and used throughout the petroleum industry. Even though these techniques face different challenges due to geological specifications from one region to another, their outcomes can be very useful in improving exploration and production performance. The most recent and advanced technique is based on using the stick-slip as a seismic source.

This technique can be very interesting in Algerian petroleum, and therefore, it will be discussed and explored in more detail in the next chapter.



# Chapter III

## Seismic while drilling using drill bit stick-slip vibrations

---

### III.1. Introduction

Seismic-While-Drilling (SWD) is a geophysical technology used for exploring Earth's subsoil during drilling for oil and gas, as well as for geothermal purposes [28]. The drill-bit SWD application is an improvement of the conventional seismic method, which uses signals with known signatures and zero start times. The while-drilling technology requires preprocessing of the acquired time-incoherent raw field data to obtain impulsive-shaped seismograms with known zero times. This is accomplished by using long recording intervals, with several tens of minutes of passive listening for each depth point. In this chapter, we introduce a technique that uses the stick-slip vibrations produced by drill-bit impacts on the formation during drilling as a downhole seismic energy source for acquiring inverse VSP surveys (the source and receiver positions of conventional VSP are reversed). The technique is called Seismic-While-Drilling using Drill-Bit Stick-Slip Vibration or Drill-Bit VSP.

### III.2. Vibrations types in Drill bit

The vibration of the drill string occurs when the frequency of the applied force matches the natural vibration frequency of the drill string. Rotation of the drill string at its natural resonant frequency results in excessive and rapid wear of the drill string and can result in fatigue failure. Three types of vibrations that occur during drilling are axial, torsional, and lateral (Figure III.1). The destructive nature of each type is different [29].

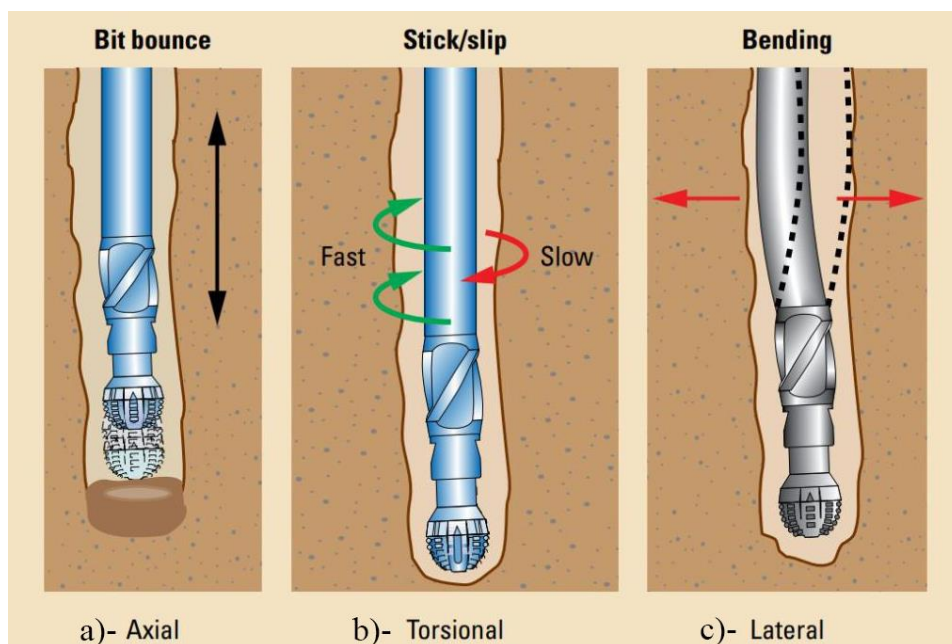


Figure III.1: Three types of drill string vibrations: a) axial, b) torsional, c) lateral [29]

### **III.2.1. Axial or Longitudinal Vibrations (Bit Bounce)**

Bit-bounce is a phenomenon caused by axial vibrations that result from fluctuations in the weight on bit (WOB) when the bit lifts off the bottom and then impacts the bottom hole again. Drilling hard and abrasive formations can also cause bit bounce. This problem is usually encountered in vertical wells that use tricone bits, and severe issues have been recorded with this type of bit. For example, reducing the penetration rate may result in the failure of the bit and bottom hole assembly (BHA) components. These vibrations can even affect surface equipment at shallow depths, resulting in top drive bounce. In such circumstances, this phenomenon is relatively easy to detect. It also affects the drilling mud by causing pressure fluctuations. Axial oscillations are damped in deep wells, preventing them from rising to the surface. These vibrations are classified as secondary vibrations for PDC bits.

### **III.2.2. Lateral or Transverse Vibrations (Whirling)**

When the BHA rotates eccentrically along the well axis, lateral vibrations result. The drill string's axis of rotation deviates because of inertia forces that try to make it unstable. This is the most destructive type of vibration and can create large shocks as the BHA impacts the wellbore wall. This type of vibration causes a phenomenon known as "whirling," which may appear on a drill bit or a BHA (Figure III.2). According to oil and gas companies, the major issues caused by this phenomenon are: hole widening due to irregular bit rotation, reduction in drill pipe service life due to cyclic variations in vibrations, instantaneous drill string rupture (appearance of micro-cracks that increase as the phenomenon occurs), and severe contacts with borehole walls. According to the direction in which it occurs, the whirling phenomenon can be divided into three main types: the first type is 'forward whirl', in which the precession of the drill string turns in the same direction as the bit rotation; the second type is 'backward whirl', which means that the precession takes place in the opposite direction of rotation. Besides, in the third type, the precession has a random direction [30].

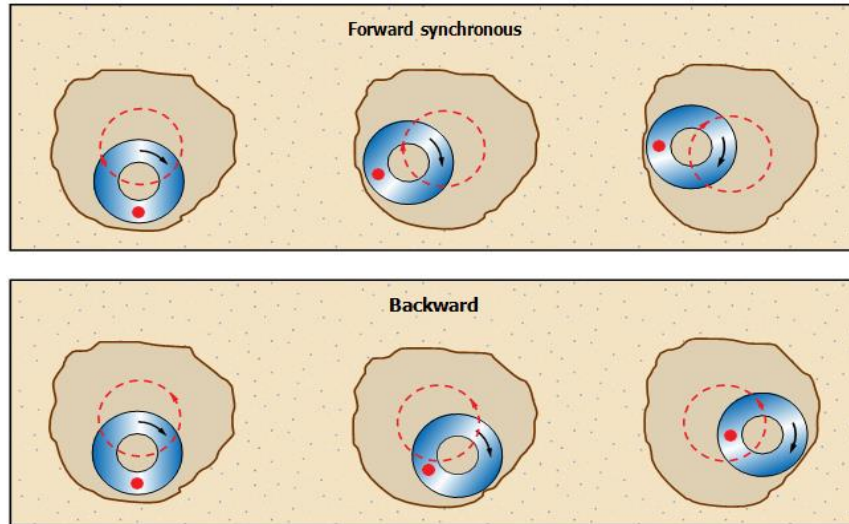


Figure III.2: BHA whirl: forward and backward whirl

### III.2.3. Torsional Vibrations (Stick-Slip)

Torsional vibrations are the most dangerous type of vibrations that can occur during drilling. The phenomenon that causes these vibrations to occur is called 'stick-slip'. Stick-slip happens when the drill bit is in non-linear frictional contact with the formation, causing the bit to alternate between two phases: an adhesion phase and a sliding phase. As a result, the velocity undergoes intense variations, and the severity of this phenomenon can lead to a complete halt of the drilling process. Rotational speed variations are considered a strong indicator of stick-slip [30].

In seismic while drilling (SWD) we consider the Stick-Slip as the main source and we don't take into account the rest of the previously mentioned types of vibration, because Stick-Slip is the origin of the vibration and the other follow from it. Stick-slip is not the only type of vibration considered in seismic while drilling (SWD). While stick-slip is the most significant type of vibration, lateral and axial vibrations can also affect the quality of seismic data obtained through SWD.

Recordings from the MWD (measurement while drilling) of Well-1, located in an Algerian hydrocarbon field, indicate that the rotational speeds at the bit are irregular. Specifically, the curve representing this speed contains peaks and valleys (Figure III.3). The speed corresponding to a peak is six times the value of the speed measured at the surface. Also, the speed corresponding to the stuck phase can reach zero, indicating that the bit is completely blocked, unlike the surface where nothing is indicated. The duration of the stuck phase varies from 1 to 5 seconds. While the bit is stuck at the bottom of the borehole, the top drive system continues to rotate at a constant velocity, causing the drill string to twist. This torsion makes the pipes store elastic energy; however, beyond a certain quantity, the torque

applied to the bit becomes greater than the resisting torque (static torque), which consequently releases the bit, and the cycle is repeated again [30].

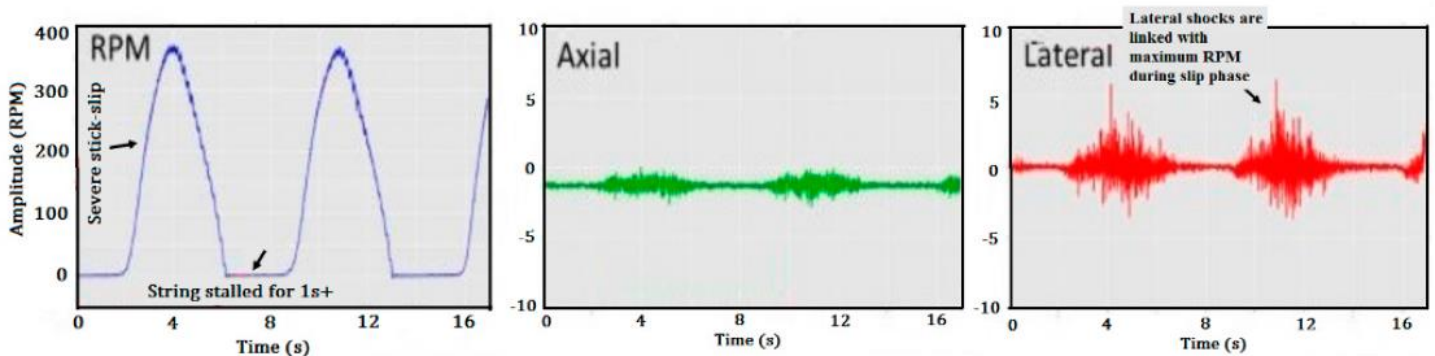


Figure III.3. Measured vibration using BlackBox in Well-1 [30]

### III.2.3.1 Mathematical Model

This part will focus on studying the different vibrations that affect an operating drillstring. Many researchers have demonstrated that torsional vibrations are the most dangerous; their severe appearance can lead to the stick-slip phenomenon. Several methods can be used to properly assimilate this phenomenon, including the mass-spring-damper model. The drillstring, in this model, is considered as a torsional pendulum shown in Figure III.4. The drill pipes represent the torsional spring with the torsional stiffness  $k$ , the BHA is represented by a mass  $M$ , the moment of inertia  $I$  represents the inertia of the BHA and that of the drill pipes. The viscous friction between the drillstring and the drilling fluid behave as a damper with a damping coefficient  $C$  [30].

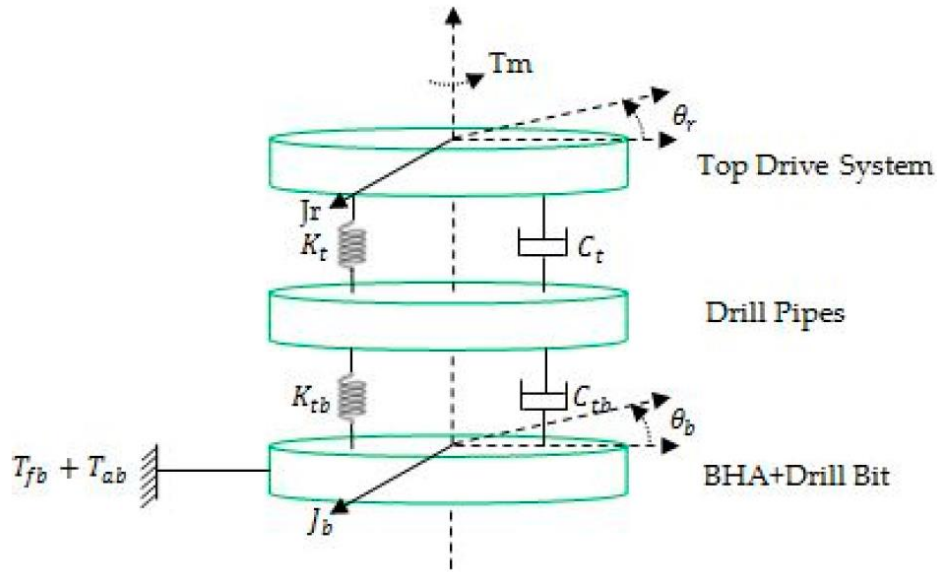


Figure III.4. Three elements proxy model of rotary drilling system [30]

Assuming that the system rotates with a constant velocity  $\Omega_0$  applied by the top drive, and that  $\Phi$  represents the angular position of the bit, the equation of motion according to the principle of dynamics (the sum of the moments of the external forces is equal to the derivative of the angular momentum) is given in (1).

$$I\ddot{\Phi} + C\dot{\Phi} + K(\Phi - \Omega_0 t) = T_b \quad (1)$$

$T_b$  : is the torque generated by the frictional forces along the drillstring and is a function of the rotational velocity of the bit [31]. Equation (1), referred to as the classical equation, represents a lumped system of one degree of freedom. This model contains three parameters: the moment of inertia  $I$ , the damping coefficient  $C$ , and the torsional stiffness  $k$  for two elements: the spring representing the drill pipes and the disk of mass  $M$  representing the BHA. This model is the basic model considered for rotary drilling systems. However, several assumptions can be added to it, such as considering each drill pipe as a disk of mass  $M$  and inertia  $I$  instead of considering them as a single spring.

$J_r$  is the inertia of the top drive;  $J_p$  is the inertia of the drill pipes,  $J_b$  is the inertia of the BHA (including drill bit),  $k_t$  is the torsional stiffness of the spring between the top drive and drill pipes,  $k_{tb}$  is the torsional stiffness of the spring between drill pipes and the BHA,  $C_t$  is the viscous damping along drill pipes,  $C_{tb}$  is the viscous damping along the BHA,  $T_{ab}$  is the viscous damping torque at the bit, and  $T_{fb}$  is the friction torque at the bit [31].

Studying the drillstring's dynamic behavior while it is operating is the goal of the model introduced in this section. This model integrates the bit-rock interaction with the mechanical response of the drillstring to torsional vibrations. The top rotating system, drill pipes, and BHA are the three primary components of the drillstring. Each element is represented by a disk of mass ( $m$ ) and inertia ( $J$ ), the disks are connected to each other by springs with a torsional stiffness ( $k_t$ ) and a viscous damping coefficient ( $C_t$ ). The drillstring is shown in Figure III.4 as a torsion pendulum that is propelled by the top drive.

The interaction of the drilling mud with the drillstring can be simplified in the form of viscous damping  $C_t$  and  $C_{tb}$  along the drill pipes and the BHA, respectively. It is assumed that the top drive rotates with an initial velocity  $\theta_r$  and provides a torque  $T_m$  (with neglecting the damping and frictional torques at the top drive). According to the fundamental principle of the rotational dynamics [30]

$$\frac{d\vec{L}}{dt} = \vec{M} \quad (2)$$

Where

L: angular momentum

M: dynamic moment of external forces

$$\vec{L} = J \frac{d\theta}{dt} \vec{e} \quad (3)$$

$\vec{e}$  is unit vector. Substituting (3) in (2), Equation (4) is obtained.

$$J\ddot{\theta} = M \quad (4)$$

Taking into account the viscous forces and the rigidity of elements, the equation of motion becomes

$$J_i \ddot{\theta}_i = M - C_{i+1} (\dot{\theta}_i - \dot{\theta}_{i+1}) - k_{i+1} (\theta_i - \theta_{i+1}) + C_i (\dot{\theta}_{i-1} - \dot{\theta}_i) + k_i (\theta_{i-1} - \theta_i) \quad (5)$$

C is viscous damping, k is torsional stiffness, i is current element, i + 1 is next element. By applying Equation (5), equations of motion for three elements are given in (6)

$$\begin{cases} J_r \ddot{\theta}_r + C_t (\dot{\theta}_r - \dot{\theta}_p) + k_t (\theta_r - \theta_p) = T_m \\ J_p \ddot{\theta}_p - C_t (\dot{\theta}_r - \dot{\theta}_p) - k_t (\theta_r - \theta_p) + C_{tb} (\dot{\theta}_p - \dot{\theta}_b) + k_{tb} (\theta_p - \theta_b) = 0 \\ J_b \ddot{\theta}_b - C_{tb} (\dot{\theta}_p - \dot{\theta}_b) - k_b (\theta_p - \theta_b) = -T_b(\dot{\theta}_b) \end{cases} \quad (6)$$

Where

$T_b(\dot{\theta}_b) = T_{ab}(\dot{\theta}_b) + T_{fb}(\dot{\theta}_b)$  is the torque on the bit

$T_{ab} \approx c_b * \dot{\theta}_b$  approximates the influence of the drilling mud on the bit

$T_{fb}(\dot{\theta}_b)$  is the non-linear friction torque due to bit-rock contact interaction, it is given in (7)

$$T_{fb}(\dot{\theta}_b) = \text{WOB} * R_b * \mu_b(\dot{\theta}_b) * \text{sign}(\dot{\theta}_b) \quad (7)$$

Where

WOB is the weight on the bit

$R_b$  is the bit radius

$\text{sign}(\dot{\theta}_b)$  represents the rotational direction

$\mu_b(\dot{\theta}_b)$  is the bit dry friction, which follows the Karnopp friction model and it is given in (8).

$$\mu_b(\dot{\theta}_b) = \mu_{cb} + (\mu_{sb} - \mu_{cb}) e^{-\frac{\gamma_b}{v_f} |\dot{\theta}_b|} \quad (8)$$

Where

$\mu_{sb}$  is the static friction coefficient

$\mu_{cb}$  is the Coulomb friction coefficient

$\gamma_b$  and  $v_f$  are constants verifying the following assumptions:  $0 < \gamma_b < 1$  and  $v_f > 0$  to simplify calculation, it is assumed that  $\lambda = \frac{\gamma_b}{v_f}$

The sign function is defined in (9).



$$\text{sign}(\dot{\theta}_b) = \frac{\dot{\theta}_b}{|\dot{\theta}_b|} \text{ if } \dot{\theta}_b \neq 0, \text{sign}(\dot{\theta}_b) \in [-1, 1] \text{ if } \dot{\theta}_b = 0 \quad (9)$$

### III.3. Stick-Slip vibration as Sweep for SWD

Seismic-while-drilling (SWD) is a technique used in the exploration and production of oil and gas resources. It involves the use of a drill bit that generates low-frequency stick-slip vibrations as it rotates and penetrates the formation. These vibrations create seismic waves that propagate through the rock and are recorded by sensors located in the surface. The seismic data can then be used to obtain information about the subsurface geology and to guide the drilling process in real-time.

### III.4. Operating Principle of the technique

The signal paths exploited to process stick-slip vibrations for inverse VSP are shown in Figure III.5. The vibrations propagate into the earth and up the drillstring. At the very bottom of the drillstring, a pilot sensor is positioned to pick up waves that are moving upward. To pick up the seismic waves moving through the earth, receivers are placed on the surface or at the bottom of the borehole. For crosswell imaging, a downhole receiver can also be inserted into a nearby borehole. Each receiver signal has a cross-correlation with the signal picked up by the pilot sensor. This stage is comparable to the Vibroseis approach, in which a sweep signal and a geophone signal are cross-correlated.

The cross-correlation function provides a reference frame in which the arrival times of drill-bit energy can be measured. Assuming  $R(t)$  is the signal recorded by the pilot sensor at the top of the drillstring and  $G(t)$  is the signal recorded by the receiver, an unnormalized estimate of the cross-correlation function in discrete time is given by:

$$\text{cc}(\tau) = \sum_{n=1}^N R(nt)G(nt + \tau) \quad (10)$$

Where

$\tau$ : Time shift between the signals  $R$  and  $G$

$n$ : Number of recording samples

$N$ : Total recording length (in samples)

$t$ : sampling interval

The cross-correlation function is then normalized to produce a value between 0 and 1, indicating the degree of similarity between the two signals. The lag at which the maximum correlation occurs provides an

estimate of the time delay between the two signals. This time delay can be used to determine the distance between the drill bit and the receiver and to create an image of the subsurface structure.

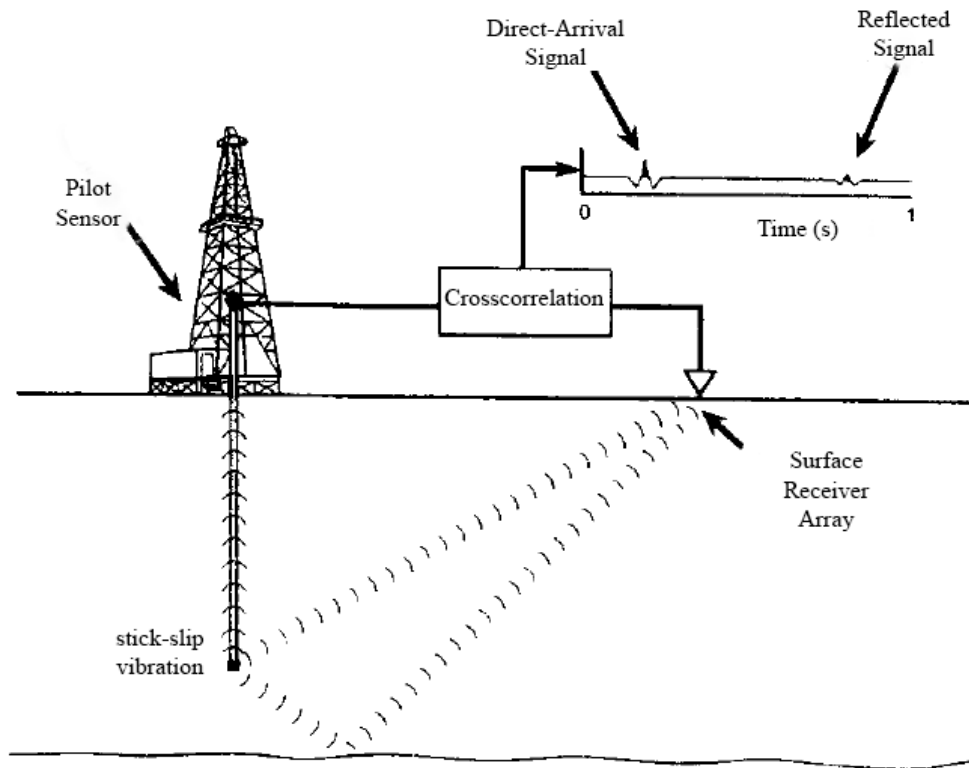


Figure III.3. Acquisition geometry of SWD using stick-slip vibrations technique

### III.5. Advantages and Utilities

#### Advantages

Advantages of using SWD with stick-slip vibrations include:

- The stick-slip vibrations can provide real-time information about the drilling conditions, helping to optimize drilling parameters and avoid stuck pipe incidents.
- The stick-slip signals can provide information about the subsurface formation, including rock type, stress state, and fluid content, which can help drillers and geologists to make more informed decisions
- The real-time information provided by SWD with stick-slip vibration can help to identify potential drilling hazards, such as overpressure zones or fractures, before they cause problems
- The stick-slip vibrations surveys are acquired without any downhole instrumentation, which means there is no interruption to drilling, no lost rig time

### Utilities

- The information obtained from SWD can be used to guide well placement, ensuring that the well is drilled in the optimal location
- The stick-slip signals can help to optimize reservoir characterization and improve hydrocarbon production
- The stick-slip vibrations can provide information about the mechanical properties of the subsurface formation, which can help to optimize wellbore stability and avoid collapse or failure

### **III.7. Drawback and Limitations**

- The method involves a combination of drilling and seismic techniques, which can be complex and challenging to implement
- The technique requires sensitive equipment to detect stick-slip vibrations, and any interference or malfunction of the equipment can impact the accuracy of the results
- The cost of equipment and data processing can be high, making the technique less economically viable for some applications
- The process can be time-consuming, as it requires collecting and processing large amounts of data during drilling operations
- The technique can generate noise and vibration, which can have negative impacts on the environment and nearby communities

### **III.8. Why the SWD can be advantageous in Algerian Petroleum Industry?**

The Algerian formation is renowned for its extreme hardness, which frequently causes stick-slip vibrations during drilling operations. However, instead of being a hindrance, these vibrations can be harnessed for seismic while drilling applications. In fact, it is common in Algerian fields to encounter standard errors that prevent the drilling process from reaching the intended target point. By utilizing the stick-slip vibrations, we can avoid such errors and ensure more accurate wellbore placement.

Moreover, the use of seismic while drilling technology in the Algerian formation can provide valuable insights into the subsurface geology. By analyzing the seismic waves generated by the stick-slip vibrations, we can obtain a clearer picture of the geological formations surrounding the wellbore, which can be useful for reservoir characterization and management. Furthermore, this real-time information can help optimize drilling parameters, such as weight on bit and rotary speed, to ensure maximum drilling

efficiency while minimizing the risk of drilling-related incidents, such as stuck pipe or borehole instability.

### **III.9. Conclusion**

In this chapter, we have discussed how we can use the stick-slip vibration, which is a common problem in drilling operations, as a reliable seismic source. We have explained the operating principle of this technique and highlighted its advantages over conventional seismic surveys. However, we have also pointed out the potential limitations and challenges that may arise with this new method.

In the next chapter, we will explore the application of this technique in the Algerian oil field through simulations of both conventional VSP and SWD using stick-slip vibration. These simulations will provide us with a better understanding of the potential benefits and limitations of using stick-slip vibration for seismic surveys in the Algerian formation. By analyzing the simulation results, we can make informed decisions about the feasibility and effectiveness of this technique in this specific geological setting.

# Chapter IV

## Simulation of SWD using Drill bit Stick-Slip Vibrations

---

## IV.1. Introduction

As we know, simulating an idea is crucial to understanding its potential in reality. This is particularly important when it comes to complex processes such as seismic data analysis. In this chapter, we will discuss how we can use MATLAB and Python functions to simulate seismic data and well log curves. These functions will allow us to input, output, and manipulate seismic data, enabling us to analyze it in depth. Additionally, we will also cover functions that manipulate tables and pseudo-wells, which are commonly used in the industry for data analysis. By the end of this chapter, we will have a solid understanding of how these tools can be used to improve our understanding of seismic data and its potential applications [32].

## IV.2. SeisLab Matlab toolbox

SeisLab is a toolbox for MATLAB that is designed to facilitate seismic data processing and analysis. The toolbox contains a number of functions and tools that can be used to read, write, manipulate, and visualize seismic data in various formats [33].

Some of the main features of SeisLab include:

- Support for various seismic data formats, including SEG-Y, SAC, and SEGY.
- Basic seismic data processing functions, such as filtering, gain adjustment, and time shifting.
- Advanced seismic data processing functions, such as deconvolution, spectral analysis, and wavelet analysis.
- Visualization tools, including functions for creating time series plots, spectrograms, and seismograms.
- Support for seismic data inversion and imaging

### IV.2.1. Initialization

In order to function properly, SeisLab needs certain parameters. These parameters are set by function presets which calls two other functions, *systemDefaults4Seislab* and *userDefaults4Seislab*. The latter sets parameters that a user is likely to customize (such as the directories where data files, such as SEG-Y files or LAS files with well data, are located). Function *systemDefaults4Seislab*, on the other hand, sets those parameters that do not depend on a user's environment. In any case, every parameter defined in *systemDefaults4Seislab* can be changed in *userDefaults4Seislab*. Since these parameters are used in many functions, a session using SeisLab functions should be preceded by *presets*

The following three statements represent a simple example of a SeisLab session.

```
presets           % Initialize parameters
seismic=s_data;  % Create a synthetic seismic dataset
s_wplot (seismic) % Plot the seismic dataset
```

### IV.2.2. Command-line help

Matlab's standard help tools, *help* and *lookfor* are, of course, available for SeisLab functions as well. In addition, the following functions are intended to locate quickly functions that perform specific tasks for a particular type of data structure [33].

- *l\_tools* List functions that deal with well logs.
- *s\_tools* List functions that deal with seismic data.
- *pw\_tools* List functions that deal with pseudo-well structures.
- *t\_tools* List functions that deal with tables.

Without argument each of these functions displays all the functions available for the specific type of dataset, together with a one-line explanation of their purpose. In order to restrict the output a search term can be added. Thus

```
>> s_tools plot
s_2d_spliced_synthetic      Plot synthetic spliced into seismic line
s_3d_header_plot           Make contour plot of one header as function of...
s_3d_spliced_synthetic     Plot synthetic spliced into inline and cross-line...
s_compare                  Plot one seismic data set on top of another for...
s_cplot                    Plot seismic data in form of color-coded pixels...
s_header_plot              Plot header values of a seismic data set
s_ispectrum                Interactively pick windows on seismic plot and...
s_plot                     "Quick-look" plot of seismic data (color if more ...
s_spectrum                 Plot amplitude and/or phase spectra of one or...
s_spick1                   Interactively pick time/trace pairs from a plot...
s_spicks                   Interactively pick time/trace pairs from a plot...
```

<i>s_volume_browser</i>	<i>Interactive display/plot of a 3D seismic data set...</i>
<i>s_wedge_model</i>	<i>Compute/plot synthetic from wedge model and...</i>
<i>s_wplot</i>	<i>Plot seismic data in wiggle-trace format</i>

Displays only functions that are related to plotting of seismic data sets; ellipses (...) indicate truncated lines [33].

### IV.2.3. Input arguments of functions

The majority of SeisLab functions have required and optional input arguments. Required arguments precede optional arguments and are “positional”; they are in a specific position (e.g. first, second, etc.) in the list of arguments. The order of subsequent optional input arguments, if any, is arbitrary. They consist of a keyword followed by one or more values — all encapsulated in a cell array. Keywords are strings. The following SeisLab function call, which plots the seismic dataset seismic in wiggle-trace format, illustrates this.

```
s_wplot (seismic, {'trough fill', [0.6 0.6 0.6]}, {'annotation', 'cdp'})
```

The first input argument, seismic, i.e. the name of the seismic dataset to plot, is required. The other two input arguments — enclosed by curly brackets — are optional.

The first string within a set of curly brackets is the name of a parameter (also called “keyword”) and the subsequent numbers and/or variables define its value(s). In the example above, *'trough\_fill'* is a keyword specifying what color should be used to fill the troughs of the seismic wiggles; hence, *{'trough fill', [0.6 0.6 0.6]}* specifies that the troughs of the seismic wiggles, which — by default — are not filled with any color, should be gray (the three-component vector *[0.6 0.6 0.6]* is the RGB representation of a lighter shade of gray). The other optional argument, *{'annotation', 'cdp'}*, specifies that the traces should be annotated by CDP number; the default annotation is trace number [33].

Keywords can be abbreviated / shortened as long as the abbreviation is unique, i.e. as long as there is no other keyword for which it is also an abbreviation. For example, if there are two keywords that start with “line”, say, *linestyle* and *linewidth*, they could be abbreviated to *linest* and *linewi*, respectively, or even to *lines* and *linew*. However, dropping one more character from either keyword would make the abbreviations non-unique. Keyword abbreviations can be disallowed by setting field *'keyword expansion'* of global variable *S4M* to *false* [33].



## IV.2.4. Test datasets

For testing and demonstration purposes it is frequently desirable to have quick access to test data. Hence, there are functions that create a variety of test datasets. It is a common feature of these functions that they have no input arguments and only one output argument: the dataset. They generally follow a naming convention of the form *x\_data* and *x\_datann* where *x* stands for the letters *l*, *pw*, *s*, *t*; and *nn* is a one-digit or two-digit number, or — as in the case below — a digit and a letter [33].

### Test datasets for seismic data

- *s\_data* creates a seismic dataset consisting of 12 traces, 1000 ms long, of filtered random noise as shown in Figure IV.1. It has one header: CDP.
- *s\_data3d* creates a 3-D seismic dataset; the only difference between a 2-D dataset and a 3-D dataset is that the latter must have headers with location information — preferably inline numbers and cross-line numbers. Consequently, the dataset output by *s\_data3d* has two headers: *iline\_no* and *xline\_no*.

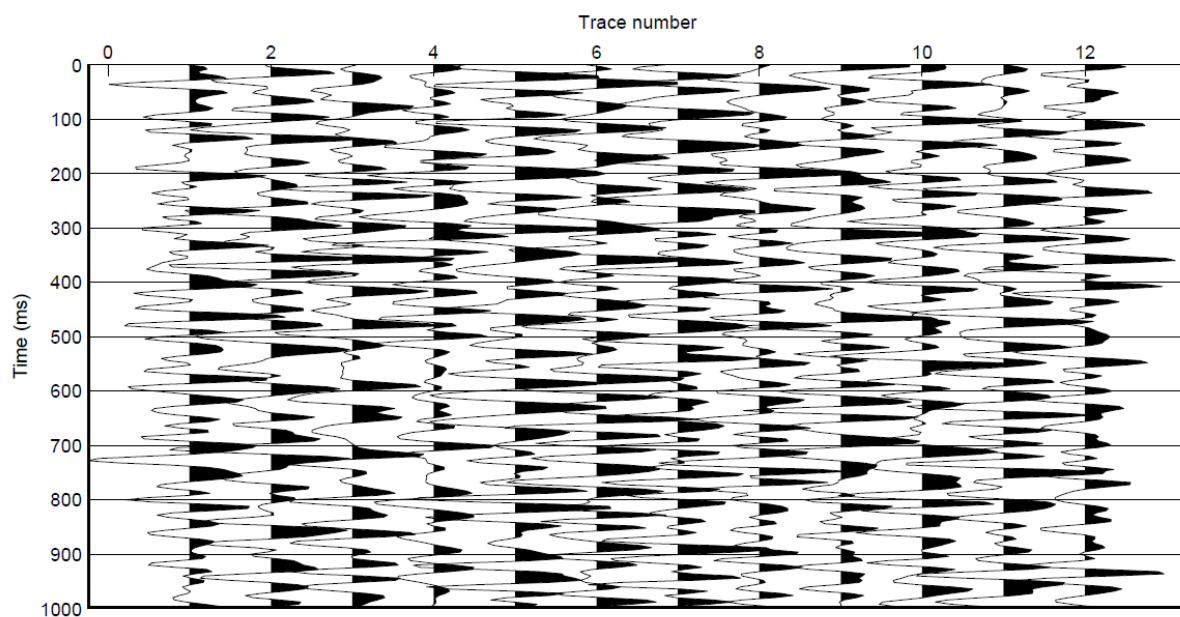


Figure IV.1 Filtered Gaussian noise; created by *s\_plot (s\_data)*

## IV.3. CREWES Matlab toolbox

The CREWES Matlab toolbox is a collection of software tools developed by the Consortium for Research in Elastic Wave Exploration Seismology (CREWES) at the University of Calgary in Canada. The toolbox provides a set of functions and scripts for processing and analyzing seismic data, with a

focus on exploration seismology. The toolbox includes a range of tools for seismic data processing, such as seismic signal processing, velocity analysis, wavelet analysis, and seismic imaging. It also includes modules for synthetic seismogram generation, well log analysis, and seismic data visualization.

Matlab has been used to develop a number of new seismic modeling tools. Raytracing for  $v(z)$ , raytracing for  $v(x, z)$ , full waveform modeling by diffraction summation, and acoustic finite difference modeling are among them. The first and last of these have previously existed but have been significantly upgraded. The  $v(x, z)$  raytracer and diffraction summation modeling is both novels [34].

The  $v(z)$  raytracing facility is a fast, flexible raytracer that determines traveltimes in isotropic, horizontally layered media. It can shoot fans of rays or perform twopoint raytracing. (Two-point raytracing means that a ray is traced through specific beginning and ending points. Ray shooting means that the starting point and take-off angle of the ray are prescribed but its ending point is not.) Functions are provided for automatic determination of traveltimes of primary reflections in shot-record geometry for P-P, S-S, P-S, and S-P modes. With slightly more effort, an arbitrary multimode can be traced and other geometries (such as VSP) can be modeled.

The  $v(x, z)$  raytracer can shoot rays through an arbitrarily variable velocity field (in 2D) and thereby determine traveltimes. It works by solving the differential equation of rays on a spatial grid. Rays are stepped at constant-time increments across the grid using a fourth-order Runge-Kutta solver (Press et al., 1992) [34]. Tools are provided for normal incidence modeling and migration.

Full-waveform, zero-offset modeling is provided with the event facility. This produces high-resolution synthetics by superimposing zero-offset diffraction responses. Diffraction hyperbolae can be superimposed along an arbitrary track in  $(x, z)$  and simple geometric correction factors are included. This is useful for studying the performance of migration algorithms and for documenting the response of simple geologic structures.

Finally, the acoustic finite difference facility, described in Youzwishen and Margrave (1999) has been updated and improved [34]. Numerous bugs have been repaired, performance improved, and function interfaces have been streamlined. This is a very flexible facility that can model acoustic wave propagation in heterogeneous, isotropic media. Sources and receivers can be placed in arbitrary locations so that source records, VSPs, and cross-well geometries are all easily handled. Also, an exploding reflector function is provided for quick simulation of stacked seismic sections.

### IV.3.1. THE V(Z) RAYTRACING FACILITY

#### Technical description

Raytracing in constant velocity and linear gradient media can be done with analytic expressions (e.g. Slotnick 1959) [1]. For a ray identified by its ray parameter (horizontal slowness)  $p$ , the expression for travelttime from depth  $z_1$  to depth  $z_2$  is

$$t(p) = \int_{z_1}^{z_2} \frac{1}{v(z)\sqrt{1-p^2v^2(z)}} dz \quad (1)$$

and the horizontal distance travelled is

$$x(p) = \int_{z_1}^{z_2} \frac{pv(z)}{\sqrt{1-p^2v^2(z)}} dz \quad (2)$$

A computer implementation of these equations can be done by approximating  $v(z)$  by a set of  $N$  discrete layers  $v_k$ ,  $k=1,2,..,N$ . For a ray that travels from the top of layer 1 to the bottom of layer  $N$  (layer number increases with  $z$ ), the travelttime expression becomes

$$t(p) = \sum_{k=1}^N \frac{\Delta Z_k}{v_k \sqrt{1-p^2v_k^2}} \quad (3)$$

and the distance equation transforms to

$$x(p) = \sum_{k=1}^N \frac{pv_k \Delta Z_k}{\sqrt{1-p^2v_k^2}} \quad (4)$$

These expressions can be vectorized and implemented very efficiently in Matlab. This is done in the function *shootray* (italics will be used to denote Matlab function names). The quantity  $pv_k$  is easily shown to be  $\sin \theta_k$  where  $\theta_k$  is the angle the ray makes with the vertical in the  $k^{th}$  layer (Figure IV.2). For a single  $p$  value, let **sn** denote a column vector of  $\sin \theta_k$ , **cs** a similar vector of  $\cos \theta_k$ , and **dz** a similar vector of layer thicknesses. Then equation (4) is implemented with the single line of Matlab code as: **x=sum ((sn.\*dz)./cs)**. This expression uses the array multiplication and division operators (**.\*** and **./**) that perform element-by-element operations on matrices. The **sum** operator does the obvious summation. The same single line of code can trace  $M$  rays simultaneously if **sn**, **cs**, and **dz** are extended to matrices with one ray per column. Then, the resulting  $x$  is a row vector with one entry per ray. This operation is

extremely fast and, for traveltimes, equation (3) can be implemented with similar efficiency. These ideas are implemented in *shootray* and form the basic computation module for  $v(z)$  raytracing [34].

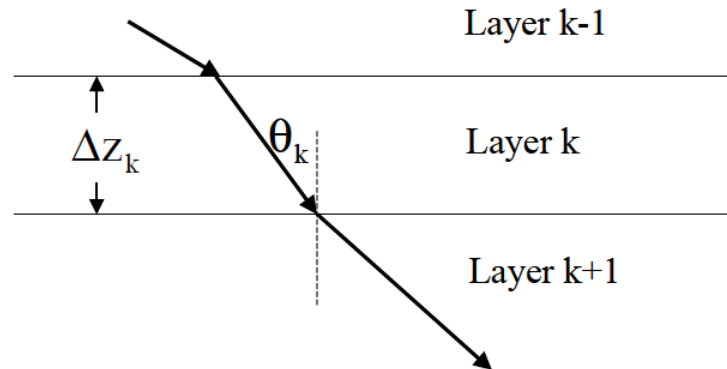


**Figure IV.2.** A ray is traced across a set of horizontal layers

The procedure just described is known as ray shooting. Because the starting point and direction of the ray are specified but the final position is not known until the calculation is completed. Often, it is desired to trace rays between two specific points such as a source and receiver, perhaps via a reflection at a specific depth. For general  $v(z)$ , there is no known solution technique that solves this two-point raytracing problem in one step. Instead, an iterative procedure must be used. Suppose it is desired to trace a fan of rays from some fixed point  $x_1$ , at the top of layer 1 to a point  $x_2$  at the bottom of layer N. The *shootray* procedure can be used to shoot a fan of M rays from  $x_1$  that is estimated to bracket the point  $x_2$ . Assuming that  $x_2 > x_1$ , the fan can have extremal p values of  $p_1=0$  and  $p_M=v_{max}^{-1}$  that, if it is indeed possible to trace a ray to  $x_2$ , will bracket  $x_2$ . Suppose it is found that rays  $p_k$  and  $p_{k+1}$  (of the fan of M rays,  $k \in \{1, 2, \dots, M-1\}$ ) bracket the point  $x_2$ , then a new fan of M rays can be shot with  $p_k$  and  $p_{k+1}$  as the extremal ray parameters. This procedure can then be repeated as often as desired until a ray is found that comes within an arbitrary “capture radius” of  $x_2$ . Thus the two-point problem of shooting a ray across of stack of layers can be solved to any desired precision. However, a solution is not guaranteed because there can be “shadow zones” where classical rays cannot penetrate [34].

Matlab function *traceray\_pp* uses the procedure just described to trace a reflection from a source at  $x_1$  via a reflector at an arbitrary depth  $z_r$  to a receiver at  $x_2$ . The reflector depth need not be a layer boundary. Rather than trace a ray down to the bottom of a stack of N layers and then back up, an equivalent problem using 2N layers and one-way raytracing is formulated and solved (Figure IV.3). If the reflector depth occurs within layer N, then that layer is reshaped to terminate at  $z_r$ . A stack of 2N layers is then formed by reversing the order of layers  $1 \rightarrow N$  and placing them beneath layer N. That is, the new

stack has the layer sequence numbers: 1, 2, . . . N-1, N, N, N-1, . . . 2, 1. Then, the two-point procedure described in the preceding paragraph is performed to trace a ray from  $x_1$  at the top of layer 1 to  $x_2$  at the bottom of layer 2N. This ray will have the same traveltimes and ray parameter as that which solves the original problem.

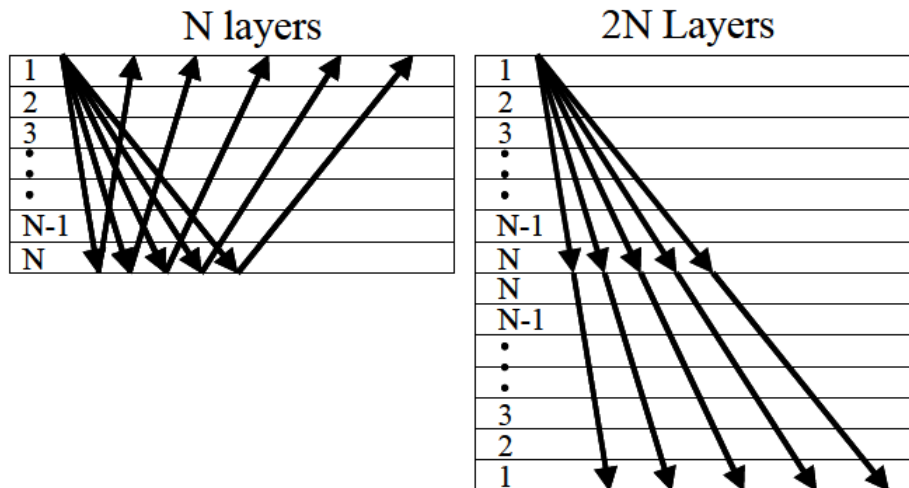


**Figure IV.3** The two-point problem of tracing a fan of rays down to a reflector and back up to receivers through N layers (left) is equivalent to tracing the rays directly through a stack of 2N layers (right) [34]

Function *traceray\_ps* does a similar process to solve the problem of tracing a P-S reflection. The only difference is that the second (inverted) stack of N layers in the 2N layer stack is assigned S-wave velocities. Thus two velocity models must be supplied, for P and S waves, and they may have completely different layer boundaries. Once the 2N layer stack is built, solving the two-point problem across it solves the desired P-S reflection problem. The same function can also trace an S-P reflection by simply reversing the meaning of P and S wave velocities.

Both functions *traceray\_pp* and *traceray\_ps* can accommodate sources and receivers at different depths by simply altering the layer stack to only include those layers actually traversed on the down and up legs.

Function *traceray* uses this process to trace a general multimode through a layered medium. The multimode is described by a raycode that is a list of ordered pairs,  $(z_m, i_m)$ , where  $z_m$  the depth at the start of a ray segment and  $i_m$  is either 1 (for a P-wave) or 2 (for an S-wave). For example, the raycode [0, 1; 1000, 2; 500, 2; 1000, 1; 0, 1] indicates a P-S-S-P mode. It is a P-wave from 0 to 1000 m, an S-wave from 1000 to 500 m, and S-wave from 500 to 1000 m, and finally a P-wave from 1000 to 0 m. (Note that

the final value of  $i_m$  is meaningless.) This problem is solved with the same stratagem as before by building an equivalent stack of layers and tracing rays through it one-way. In this way, a completely arbitrary multimode can be traced through a  $v(z)$  medium.

### Examples

In this section we will describe a number of examples for the  $v(z)$  raytrace facility. These are all taken directly from the m-file *raytrace\_demo* that is included with the CREWES software distribution. Thus, any of them can be recreated by simply running that demo.

For the velocity model shown in Figure IV.4, consider the task of tracing P-P and P-S reflections from a target at  $z_s=3000$  m depth. This velocity model includes a 200m thick water layer at the top so OBC geometry is adopted. Let the source be at  $z_{src}=50$  m and the receivers on the ocean bottom at  $z_{rec}=200$  m. Also let the receivers are at offsets  $xoff= [1000, 1100, 1200, \dots, 3000]$  for a total of 21 receivers. Then Figure IV.5 shows the Matlab code required to trace the P-P reflection and produce Figure IV.6. The code example is a bit involved because it was decided to show all of the code required to produce the fully annotated plot. The actual raytracing is done on the third line. Of the inputs to *tracelay\_pp*, the first two are the P-wave velocity and layer depths, the next four specify the recording geometry, and the next six numeric values are respectively: the capture radius (10 meters), a flag indicating that the initial ray fan is to be determined automatically, the number of iterations to attempt before nonconvergence is assumed (10), a flag indicating that the final times are to be improved by linear interpolation between the captured ray and the next closest ray, a flag requesting that information about failed rays be printed on the screen, and a flag requesting a plot of the raypaths in the current figure window. (To see a complete description of these parameters, run Matlab and type “*help tracelay\_pp*” at the command line.) The returned variables from *tracelay\_pp* are a vector of traveltimes ( $t$ ) and a vector of ray parameters ( $p$ ). The traveltimes are plotted versus offset on line 12 of this example [34].

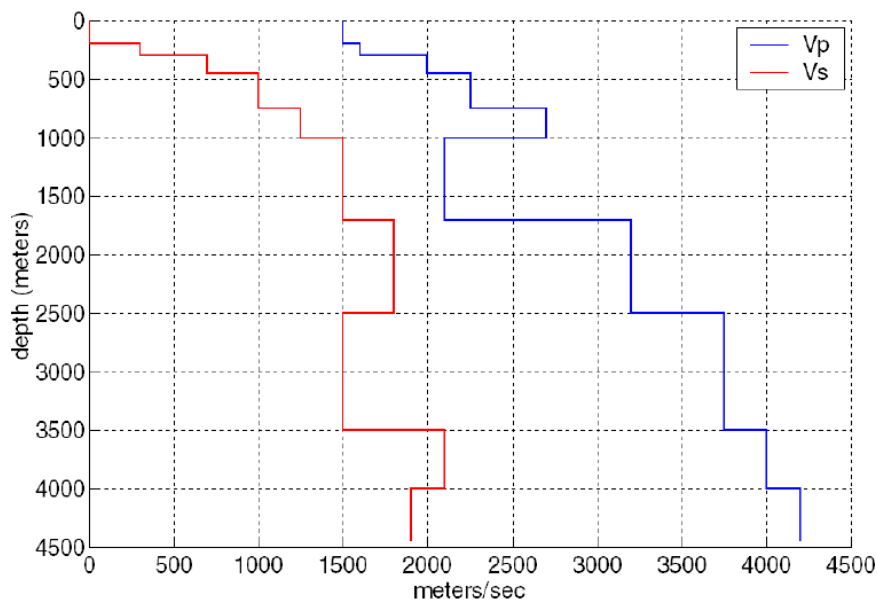


**Figure IV.4.** A simple layered medium is shown as characterized by its P-wave velocity curve (right) and its S-wave velocity curve (left). Note the 200 m water layer at the top [34]

```

1 - figure;subplot(2,1,1);flipy
2 - %Trace P-P rays and plot in upper subplot
3 - [t,p]=tracelay_pp(vp,zp,zsrc,zrec,zd,xoff,10,-1,10,1,1,2);
4 - %put source and receiver markers
5 - line(xoff,zrec*ones(size(xoff)),'color','b','linestyle','none','marker','v')
6 - line(0,zsrc,'color','r','linestyle','none','marker','*')
7 - %annotate plot
8 - title('OBC simulation, P-P mode, water depth 200 meters')
9 - xlabel('meters');ylabel('meters');grid
10 - %plot traveltme versus offset in lower subplot
11 - subplot(2,1,2);flipy;
12 - plot(xoff,t);grid;xlabel('meters');ylabel('seconds')
13 - xlim([0 3000])

```

**Figure IV.5.** This sequence of Matlab code uses the velocity model of Figure IV.4 to trace P-P rays and create Figure IV.6



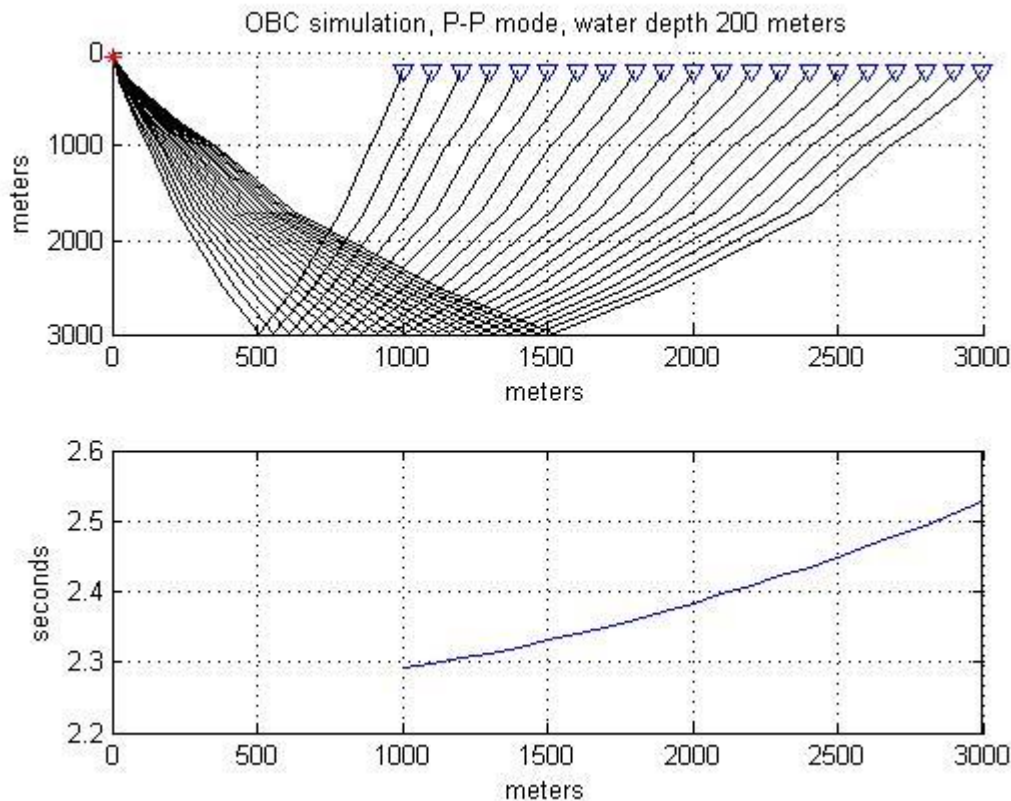


**Figure IV.6.** Running the code of figure IV.5 creates this figure using the velocity model of figure IV.4. In the top frame are the actual raypaths as plotted by `tracera_y_pp` in line 3. In the bottom frame, the traveltimes are plotted versus offset

The code snippet of Figure IV.7 demonstrates the use of `tracera_y_ps` to model the P-S reflection corresponding to the P-P reflection just discussed. As before, the rays are both traced and plotted in the upper half of Figure IV.8 by line 3. The syntax to invoke `tracera_y_ps` is almost identical to `tracera_y_pp` except that there are two additional input parameters in the third and fourth position to describe the S-wave velocity structure.

```

1 - figure;subplot(2,1,1);flipy
2 - %Trace P-S rays and plot in upper subplot
3 - [t,p]=tracera_y_ps(vp,zp,vs,zs,zsrc,zrec,zd,xoff,10,-1,10,1,1,2);
4 - %put source and receiver markers
5 - line(xoff,zrec*ones(size(xoff)),'color','b','linestyle','none','marker','v')
6 - line(0,zsrc,'color','r','linestyle','none','marker','*')
7 - %annotate plot
8 - title('OBC simulation, P-S mode, water depth 200 meters')
9 - grid;xlabel('meters');ylabel('meters');
10 - %plot traveltme versus offset in lower subplot
11 - subplot(2,1,2);flipy;
12 - plot(xoff,t);grid;xlabel('meters');ylabel('seconds')
13 - xlim([0 3000])

```

**Figure IV.7.** This sequence of Matlab code uses the velocity model of Figure IV.4 to trace P-S rays and create Figure IV.8



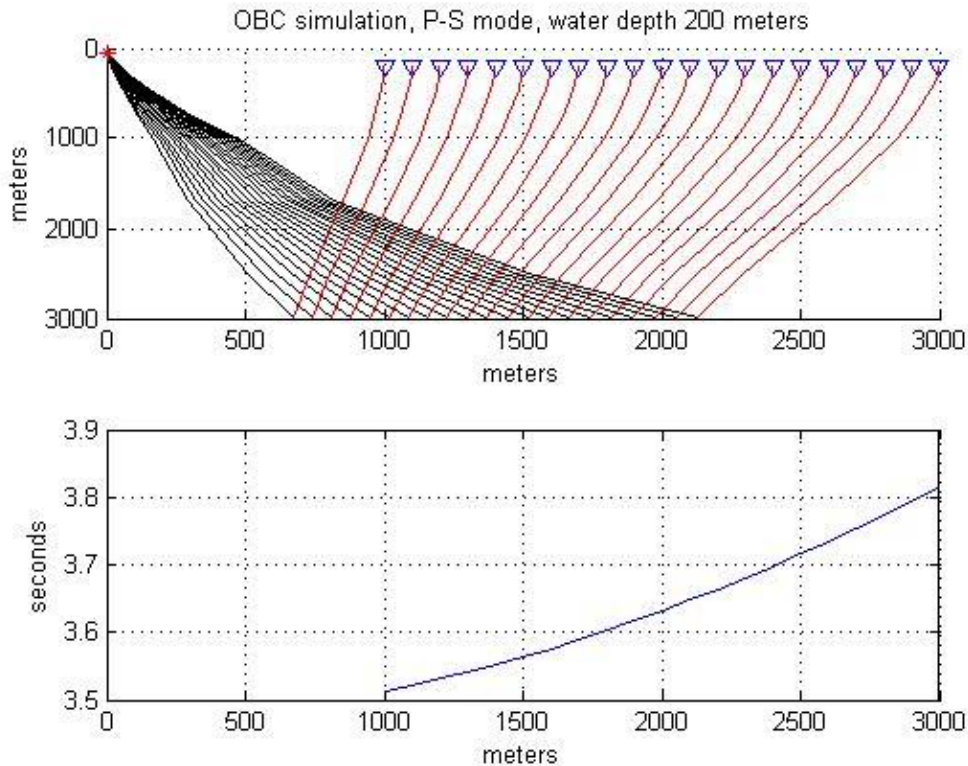


**Figure IV.8.** Running the code of Figure IV.7 creates this figure using the velocity model of Figure IV.4. In the top frame are the actual raypaths as plotted by *traceray\_ps* in line 3. In the bottom frame, the traveltimes are plotted versus offset

Next, consider the task of calculating P-P and P-S reflections for an offset VSP. Let the source be at the surface and offset 1500 m from the well. The receivers are in the well from 500 to 2500 m at 100 m intervals. Let the P-wave velocity structure be given by  $v_p(z) = 1800 + .6z$  with  $v_p/v_s = 2$ . The code to model a P-P arrival from a reflection at  $z_d = 3000$  m is shown in Figure IV.9 and the resulting plot is in Figure IV.10. Line 2 creates the velocity model for both P and S and line 5 preallocates a vector to hold the traveltimes. Lines 7-9 loop over receiver depth and call *traceray\_pp* for each receiver. As before, *traceray\_pp* draws the raypaths in the upper part of Figure IV.10 while the traveltimes are plotted in the lower part of the same Figure by the command on line 18.

The P-S reflection for the VSP geometry is drawn by the code in Figure IV.11. The strategy is identical to the P-P case with the only difference being that *traceray\_ps* is called in the loop instead of *traceray\_pp*.

Most recording geometries can be accommodated by writing a suitable loop. For example, a VSP with a non-vertical borehole simply requires that the both receiver coordinates ( $x, z$ ) be changed with each iteration. Crosswell experiments could be done by changing both source and receiver depths at each iteration.

```

1  %build the velocity model
2  - zp=0:10:4000;vp=1800+.6*zp;vs=.5*vp;zs=zp;
3  %P-P offset VSP
4  - figure;subplot(2,1,1);flipy
5  - t=zeros(size(zrec)); %preallocate t
6  %loop over receiver depth
7  - for kk=1:length(zrec);
8  -     [t(kk),p]=traceray_pp(vp,zp,zsrc,zrec(kk),zd,xoff,10,-2,30,1,1,2);
9  - end
10 %draw source and receiver symbols
11 - line(xoff,zrec,'color','b','linestyle','none','marker','v')
12 - line(0,zsrc,'color','r','linestyle','none','marker','*')
13 %annotation
14 - title([' VSP Vertical gradient simulation, P-P mode '])
15 - grid;xlabel('meters');ylabel('meters');
16 %plot traveltimes versus depth
17 - subplot(2,1,2);
18 - plot(t,zrec);xlabel('seconds');ylabel('depth (meters)')
19 - grid;flipy;ylim([0 3000])

```

Figure IV.9. This code models a P-P reflection for offset VSP geometry

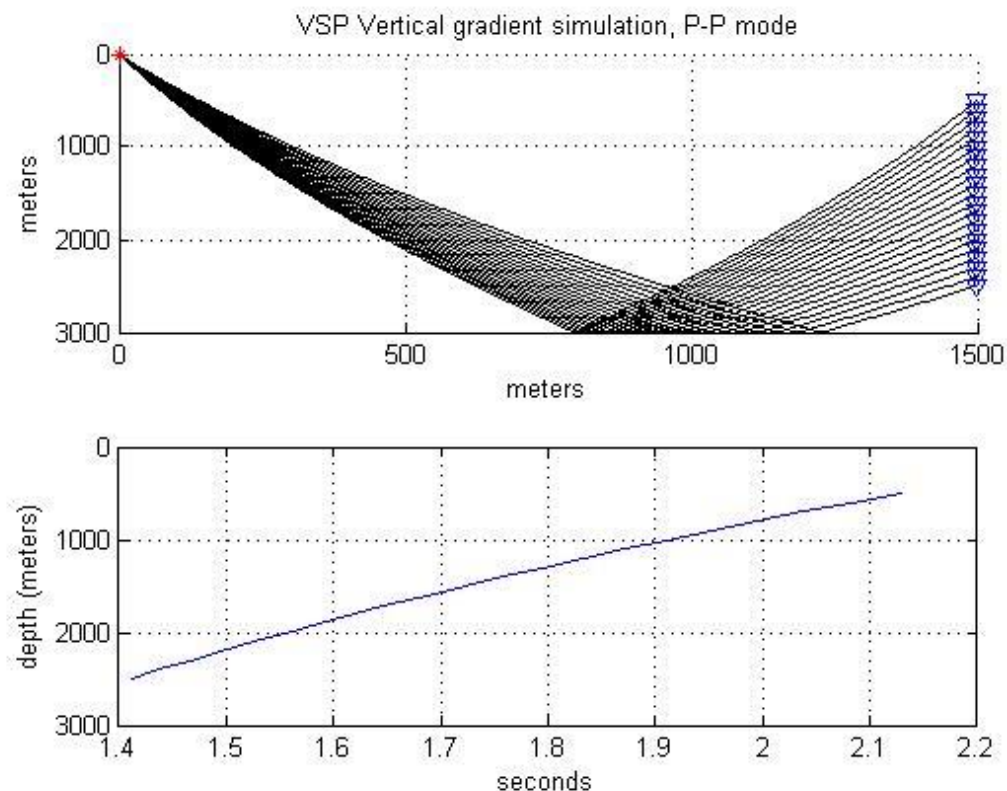


Figure IV.10. A P-P reflection for an offset VSP recording is shown. The raypaths (top) and traveltimes (bottom) were computed by the code in Figure IV.9

```

1   %P-S offset VSP
2   figure;subplot(2,1,1);flipy;
3   t=zeros(size(zrec)); %preallocate t
4   for kk=1:length(zrec);
5       [t(kk),p]=tracelay_ps(vp,zp,vs,zs,zsrc,zrec(kk),zd,xoff,10,-2,30,1,1,2);
6   end
7   %draw source and receiver symbols
8   line(xoff,zrec,'color','b','linestyle','none','marker','v')
9   line(0,zsrc,'color','r','linestyle','none','marker','*')
10  %annotation
11  title([' VSP Vertical gradient simulation, P-S mode '])
12  grid;xlabel('meters');ylabel('meters');
13  %plot travelttime versus depth
14  subplot(2,1,2);
15  plot(t,zrec);xlabel('seconds');ylabel('depth (meters)')
16  grid;flipy;ylim([0 3000])

```

Figure IV.11. This code models a P-S reflection for an offset VSP

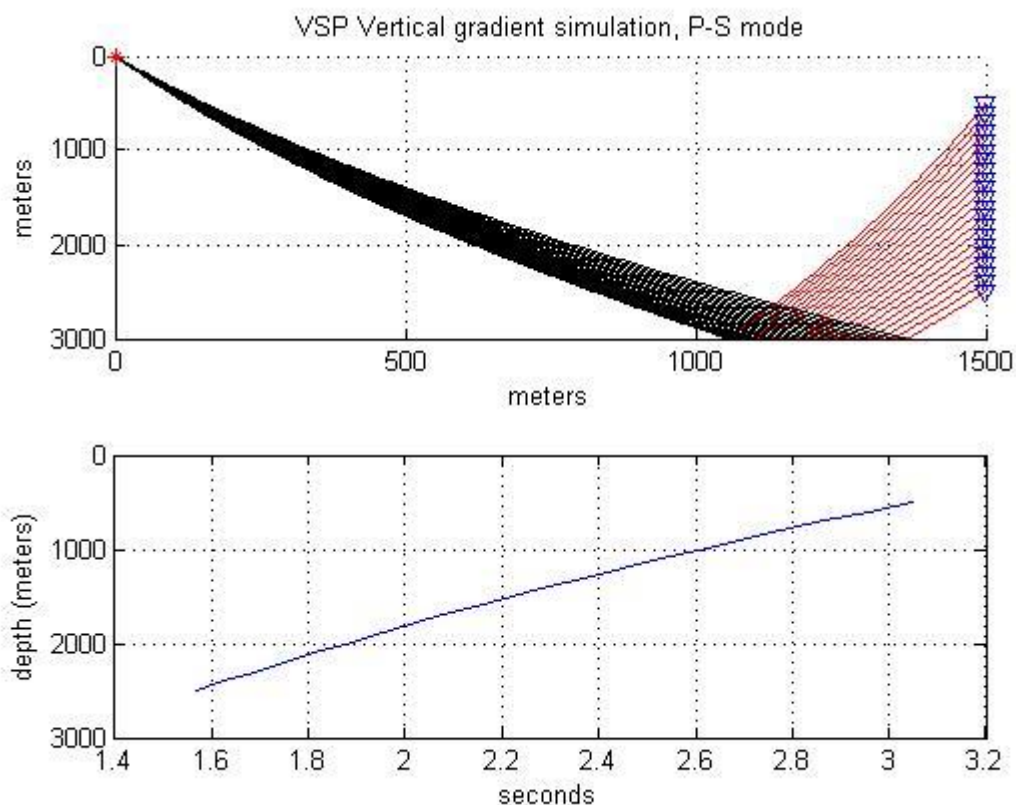


Figure IV.12. A P-S reflection for an offset VSP is shown. This was created by the code in Figure IV.11

As a final example, consider the task of tracing a complex multimode. That is, let the ray bounce up and down between various depths and change back and forth between P and S. This is possible with the function `traceray_pp`, the most general of the three “`trace_ray`” functions. All use the algorithm described previously that makes an equivalent stack of layers and traces the ray through it in a single direction. The functions `traceray_pp` and `traceray_ps` are optimized to trace primary (single bounce) reflections from a single source to an array of receivers. Function `traceray` is far more general and can trace a ray that undergoes any number of bounces and mode conversions. The ray is described through a ray code as described previously. For an M-bounce multiple, the raycode is a matrix with M+2 rows and 2 columns. The extra two rows are for the start and end depths. The first column is a list of depths that the ray is to visit and the second is a list of flags indicating P or S mode. The list of depths corresponds either to points of reflection or mode-conversion or both. These depth values need have no connection to layers in the velocity models. Figure IV.13 shows the raycode (lines 2-3) for a complicated multi-bounce P-wave that starts at depth zero and ends at depth 300 m. The raycode is simply typed in as a list of number pairs separated by a semi-colon (Matlab.s row separator). On line 7, `traceray_pp` is invoked with a list of receiver offsets from 1000 to 3000 m. The creation of the P and S-wave velocity models is not shown but is the same lineargradient medium as for the VSP example of Figure IV.9. Most of the parameters in `trace_ray` are analogous to those in `traceray_ps` and have already been discussed. However, there are no specifications of source and receiver depth because those are part of the raycode.

```

1  %define the ray code for a pure P multiple
2  raycode=[0 1;1500 1;1300 1;2000 1;1800 1;3000 1;2000 1;2300 1;1000 1;1500 1; 300 1];
3  figure;subplot(2,1,1);flipy
4  %trace the rays
5  xoff=1000:100:3000;
6  [t,p]=traceray(vp,zp,vs,zs,raycode,xoff,10,-1,10,1,1,2);
7  %Source and receiver symbols
8  line(xoff,raycode(end,1)*ones(size(xoff)),'color','b','linestyle','none','marker','v')
9  line(0,raycode(1,1),'color','r','linestyle','none','marker','*')
10 %annotate
11 title('A P-P-P-P-P-P-P-P-P mode in vertical gradient media');grid
12 %Plot traveltimes
13 subplot(2,1,2);flipy
14 plot(xoff,t);grid;xlabel('offset');ylabel('time')
15 xlim([0 3000])

```

**Figure IV.13.** This code example illustrates the use of `traceray_pp` to create a complicated multiple that remains a P-wave at every bounce

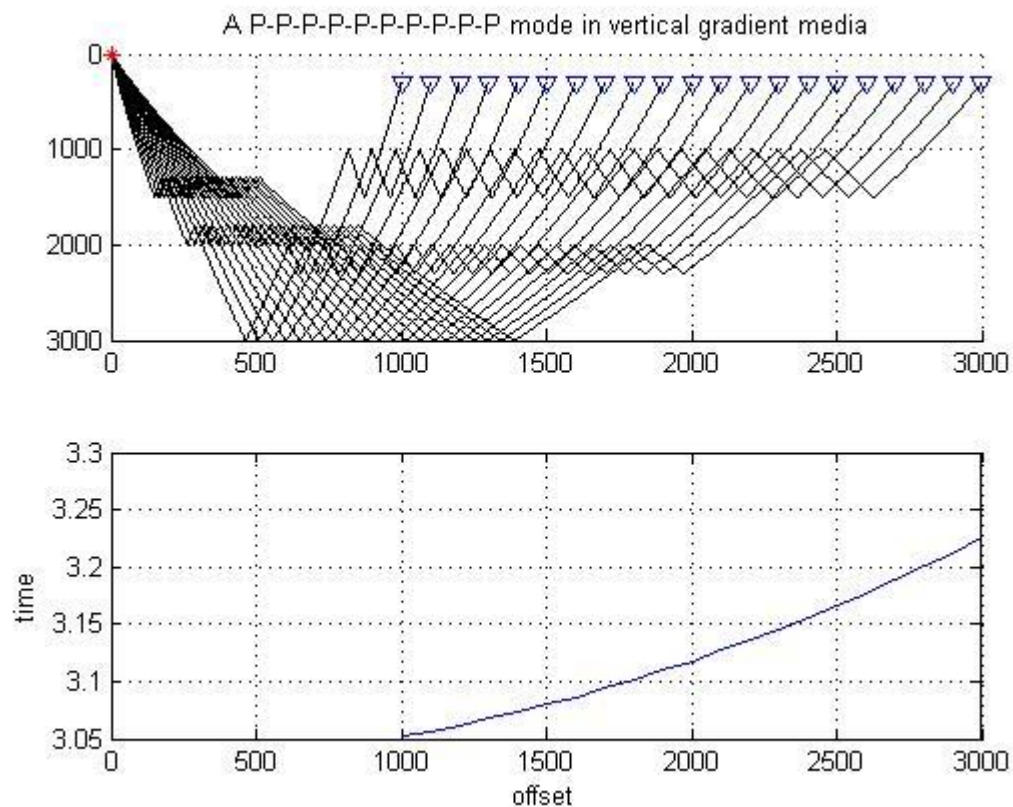


Figure IV.14. The raypath of a complicated multiple is shown (top) that remains a P-wave at every bounce

```

1  %define the ray code for a P-S multimode
2  - raycode=[0 1;1500 2;1300 2;2000 2;1800 2;3000 1;2000 1;2300 1;1000 1;1500 2; 300 1];
3  - figure;subplot(2,1,1);flipy
4  %trace the rays
5  - xoff=1000:100:3000;
6  - [t,p]=tracelay(vp,zp,vs,zs,raycode,xoff,10,-1,10,1,1,2);
7  %Source and receiver symbols
8  - line(xoff,raycode(end,1)*ones(size(xoff)),'color','b','linestyle','none','marker','v')
9  - line(0,raycode(1,1),'color','r','linestyle','none','marker','*')
10 %annotate
11 - title('A P-S-S-S-P-P-P-P-S mode in vertical gradient media');grid
12 %Plot traveltimes
13 - subplot(2,1,2);flipy
14 - plot(xoff,t);grid;xlabel('offset');ylabel('time')
15 - xlim([0 3000])

```

Figure IV.15. This code creates a multimode similar to that of Figure IV.14 except that the raycode requests a P-S conversion at 1300 m, an S-P conversion at 3000 m, and another P-S conversion at 1500 m (on the up leg)



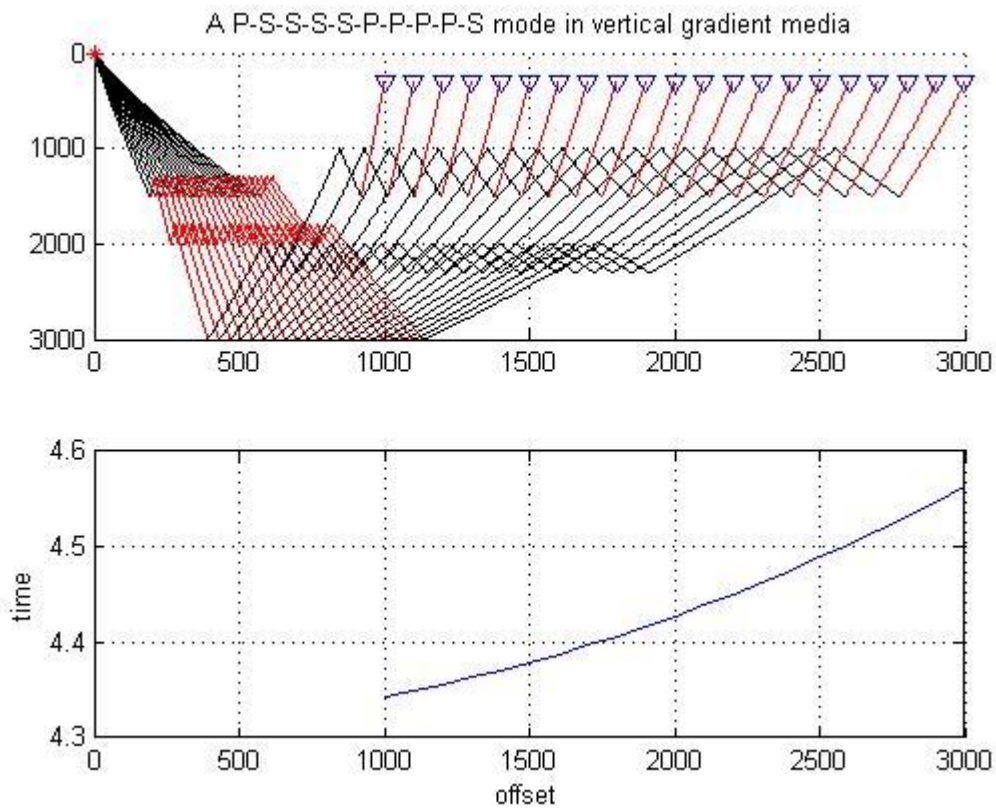


Figure IV.16. The raypath for a complicated P-S multimode is shown (top) as produced by the code snippet in Figure IV.15

## IV.4. GemPy toolbox

GemPy is an open-source Python package that provides a framework for 3D geological modeling. It is designed to help geologists and other earth scientists create geological models that can be used to study the subsurface structure of the Earth. The package is built on top of popular scientific libraries such as NumPy, SciPy, and Matplotlib [35].

GemPy uses a combination of mathematical algorithms and geological principles to model the geological features of a given area. The software allows users to create geological models by defining the shape, orientation, and properties of different geological units, such as layers of rock, faults, and other geological structures.

One of the key features of GemPy is its ability to create complex, multi-layered geological models. The software can handle multiple layers of rock with varying properties, as well as faults and other geological structures that can cut across these layers.

GemPy also provides a range of visualization tools that allow users to view and manipulate their models in 3D. This includes the ability to view cross-sections, generate isosurfaces, and create realistic geological maps.

### IV.4.1. Basics of geological modeling with GemPy

#### Importing GemPy

```
import gempy as gp

# Importing auxiliary libraries
import numpy as np
import pandas as pd
import matplotlib.pyplot as plt
import os

# Setting options
np.random.seed(1515)
pd.set_option('precision', 2)
```

#### Importing and creating a set of input data

Python objects are used to hold the data that GemPy uses to build models. The primary data categories are:

- Surface\_points
- Orientations
- Grid
- Surfaces
- Series
- Additional data
- Faults

The majority of data can also be created using raw data that is presented as CSV files (comma-separated values). These files can be created with spreadsheet programs like Microsoft Excel or LibreOffice Calc or by simply exporting model data from another tool like GeoModeller.

In this example, importing such CSV files creates all of the input data. These sample files can be found in the GemPy root folder's *input\_data* folder. All surface points' x, y, and z positional values as well as orientation measurements are included in the data. Poles, azimuth, and polarity are also covered in the latter. Furthermore, a formation is given to surface points. This could be a structural element like a "Main Fault" or a lithological unit like "Sandstone". It is crucial to keep in mind that interface position points in GemPy indicate the bottom of a layer. In order to make such locations resemble the top of a formation (for example, while simulating an intrusion), an appropriate inverted orientation measurement must be defined.

We must specify our model's actual extent in x, y, and z as well as the required resolution for each axis as we build our Data from CSV-files. The quantity of voxels used in the modeling process will be determined by this resolution. In this case, we use a medium resolution of 50x50x50, or 125,000 voxels. The model's scope should be selected so that it includes all pertinent data in a representative area. The resolution may differ from the extent since the voxels in our model are prisms rather than cubes. Given that higher resolutions will require more computing power, we don't advise going much higher than 100 cells in each direction (1,000,000 voxels).

```
geo_model = gp.create_model('Simple_Example')

data_path = 'https://raw.githubusercontent.com/cgre-aachen/gempy_data/master/'
# Importing the data from CSV-files and setting extent and resolution
gp.init_data(geo_model, [0, 2000., 0, 2000., 0, 750.], [50, 50, 50],
             path_o=data_path + "/data/input_data/getting_started/"
                 "simple_fault_model_orientations.csv",
             path_i=data_path + "/data/input_data/getting_started/"
```



```
"simple_fault_model_points.csv",
default_values=True)
```

Out:

```
Active grids: ['regular']
```

```
Simple_Exemple 2023-05-02 16:26
```

[geo\\_model\\_surfaces](#)

	surface	series	order_surfaces	color	id
0	Shale	Default series	1	#015482	1
1	Sandstone_1	Default series	2	#9f0052	2
2	Siltstone	Default series	3	#ffbe00	3
3	Sandstone_2	Default series	4	#728f02	4
4	Main_Fault	Default series	5	#443988	5
5	basement	Basement	1	#ff3f20	6

The input data can then be listed using the command `gp.get_data`. Note that the order of formations and respective allocation to series is still completely arbitrary. We will fix this in the following.

```
gp.get_data(geo_model, 'surface_points').head()
```

	X	Y	Z	smooth	surface
0	1000	50	450.00	2.00e-06	Shale
1	1000	150	433.33	2.00e-06	Shale
2	1000	300	433.33	2.00e-06	Shale
3	1000	500	466.67	2.00e-06	Shale
4	1000	1000	533.33	2.00e-06	Shale

```
gp.get_data(geo_model, 'orientations').head()
```

	X	Y	Z	G_x	G_y	G_z	smooth	surface
0	1000	1000	300	0.32	1.00e-12	0.95	0.01	Shale
1	400	1000	420	0.32	1.00e-12	0.95	0.01	Sandstone_2
2	500	1000	300	-0.95	1.00e-12	0.32	0.01	Main_Fault

### Declaring the sequential order of geological formations

We want the arrangement of our geological units to match their ages. For instance, a depositional sequence of stratigraphy, unconformities caused by erosion or other lithological genesis processes like igneous intrusions may provide such order. The flaws in our model are to be declared in a similar age-related sequence. By using a declaration in a Python dictionary, the GemPy method `set_series` can be used to assign formations to various sequential series.

Our example model comprises four main layers (plus an underlying basement that is automatically generated by GemPy) and one main normal fault displacing those layers. Assuming a simple stratigraphy where each younger unit was deposited onto the underlying older one, we can assign these layer formations to one series called “*Strat\_Series*”. For the fault, we declare a respective “*Fault\_Series*” as the first key entry in the `set_series` dictionary. We could give any other names to these series, the formations however have to be referred to as named in the input data.

```
geo_model.surfaces
```

	surface	series	order_surfaces	color	id
0	Shale	Default series	1	#015482	1
1	Sandstone_1	Default series	2	#9f0052	2
2	Siltstone	Default series	3	#ffbe00	3
3	Sandstone_2	Default series	4	#728f02	4
4	Main_Fault	Default series	5	#443988	5
5	basement	Basement	1	#ff3f20	6

```
gp.map_stack_to_surfaces(geo_model,
    {"Fault_Series": 'Main_Fault',
     "Strat_Series": ('Sandstone_2', 'Siltstone',
                     'Shale', 'Sandstone_1', 'basement')},
    remove_unused_series=True)
```

	surface	series	order_surfaces	color	id
4	Main_Fault	Fault_Series	1	#443988	1
0	Shale	Strat_Series	1	#015482	2
1	Sandstone_1	Strat_Series	2	#9f0052	3
2	Siltstone	Strat_Series	3	#ffbe00	4
3	Sandstone_2	Strat_Series	4	#728f02	5
5	basement	Strat_Series	5	#ff3f20	6

```
geo model.surfaces
```

	surface	series	order_surfaces	color	id
4	Main_Fault	Fault_Series	1	#443988	1
0	Shale	Strat_Series	1	#015482	2
1	Sandstone_1	Strat_Series	2	#9f0052	3
2	Siltstone	Strat_Series	3	#ffbe00	4
3	Sandstone_2	Strat_Series	4	#728f02	5
5	basement	Strat_Series	5	#ff3f20	6

```
geo model.stack
```

	order_series	BottomRelation	isActive	isFault	isFinite
<b>Fault_Series</b>	1	Erosion	True	False	False
<b>Strat_Series</b>	2	Erosion	True	False	False

```
geo model.set is fault(['Fault_Series'])
```

Out:

Fault colors changed. If you do not like this behavior, set change\_color to False.

	order_series	BottomRelation	isActive	isFault	isFinite
<b>Fault_Series</b>	1	Fault	True	True	False
<b>Strat_Series</b>	2	Erosion	True	False	False

```
geo_model.faults.faults relations df
```

	Fault_Series	Strat_Series
Fault_Series	False	True
Strat_Series	False	False

```
geo_model.faults
```

	order_series	BottomRelation	isActive	isFault	isFinite
Fault_Series	1	Fault	True	True	False
Strat_Series	2	Erosion	True	False	False

```
geo_model.faults.faults relations df
```

	Fault_Series	Strat_Series
Fault_Series	False	True
Strat_Series	False	False

### Returning information from our input data

Our model input data, referred to as "*geo\_model*" above, has all the details necessary for building our model. By using *gp.get\_data* or just by using the APIs, we may get many types of data.

For instance, we may use the following to retrieve the coordinates of our modeling grid:

```
geo_model.grid
```

Out:

```
Grid Object. Values:
array([[ 20. ,  20. ,   7.5],
       [ 20. ,  20. ,  22.5],
       [ 20. ,  20. ,  37.5],
       ...,
       [1980. , 1980. ,  712.5],
       [1980. , 1980. ,  727.5],
       [1980. , 1980. ,  742.5]])
```

As mentioned before, GemPy's core algorithm is based on interpolation of two types of data: - surface\_points and - orientation measurements

We introduced the function `get_data` above. You can also specify which kind of data you want to call, by declaring the string attribute “*dtype*” to be either 'surface\_points' (interfaces) or 'orientations'.

### Interfaces Dataframe

```
gp.get_data(geo_model, 'surface_points').head()
```

	X	Y	Z	smooth	surface
52	700	1000	300.0	2.00e-06	Main_Fault
53	600	1000	200.0	2.00e-06	Main_Fault
54	500	1000	100.0	2.00e-06	Main_Fault
55	1000	1000	600.0	2.00e-06	Main_Fault
56	1100	1000	700.0	2.00e-06	Main_Fault

### Orientations Dataframe

```
gp.get_data(geo_model, 'orientations')
```

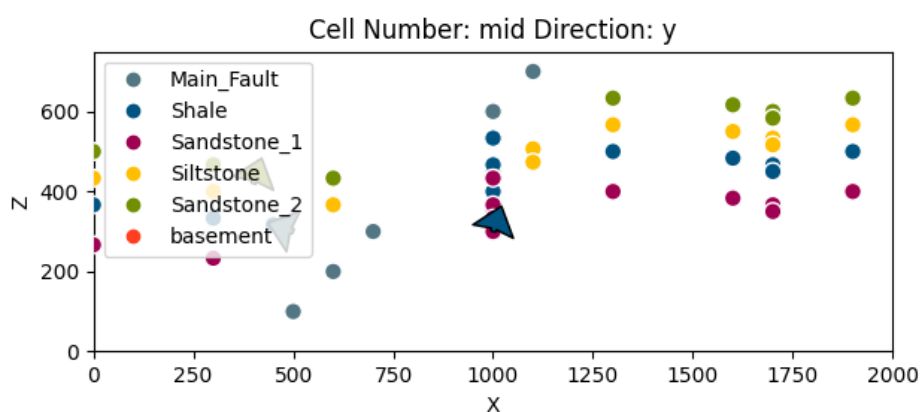
X	Y	Z	G_x	G_y	G_z	smooth	surface
2	500	1000	300	-0.95	1.00e-12	0.32	Main_Fault
0	1000	1000	300	0.32	1.00e-12	0.95	Shale
1	400	1000	420	0.32	1.00e-12	0.95	Sandstone_2

We notice that now all surfaces have been assigned to a series and are displayed in the correct order (from young to old).

### Visualizing input data

Our input data can be seen as well. This could be beneficial, for instance, to verify that all measurements and points are defined as desired. The function `plot_data` allows us to project our data points in two dimensions onto a plane in the direction of our choice (x, y, or z).

```
plot = gp.plot_2d(geo_model, show_lith=False, show_boundaries=False)
plt.show()
```

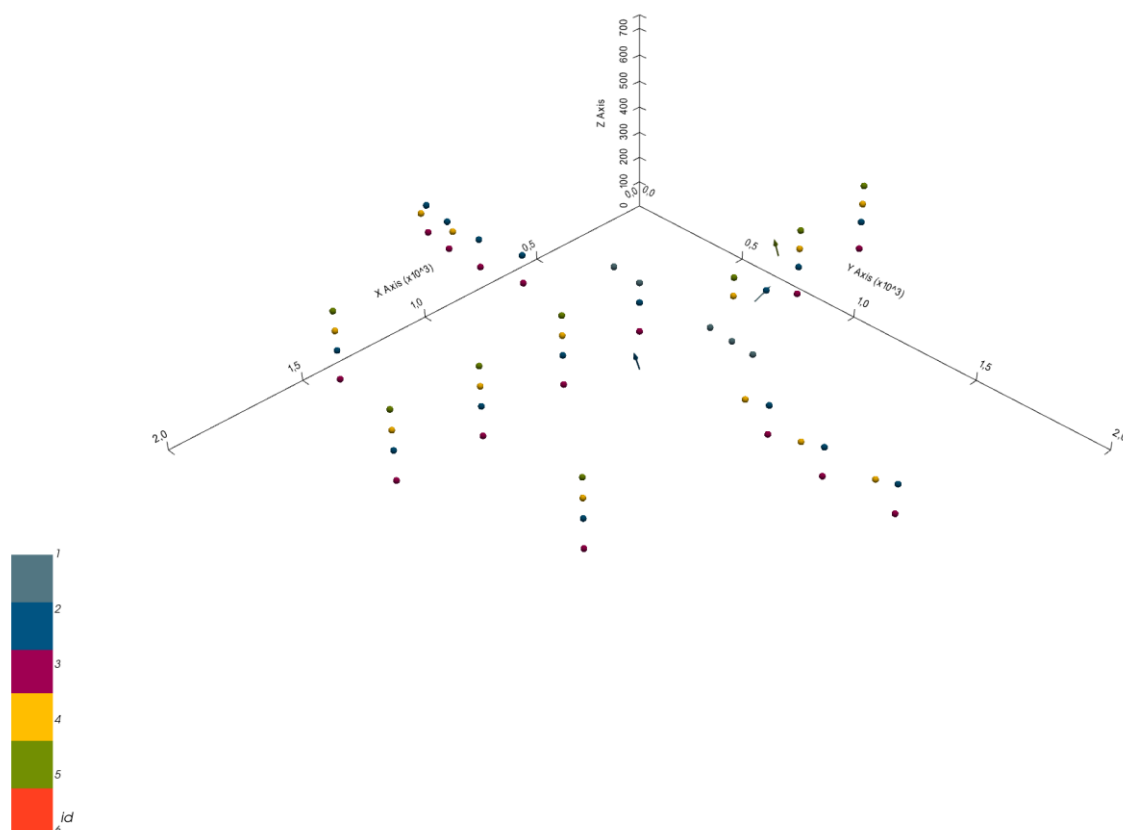


We may also see this data in three dimensions by using `plot_data_3D`. The Visualization Toolkit (VTK) must be installed for direct 3D visualization in GemPy.

GemPy's 3D charts are all interactive. This enables us to drag and drop any measurement or data point. To move points only on a specified 2D plane, VTK's perpendicular axis views are especially helpful. Any modifications will then be saved in the "InputData" dataframe permanently. Then, we must reload our initial input data if we want to reset our data points.

By executing the cell below, a new window containing a 3D interactive plot of our data will be displayed.

```
gpv = gpv.plot_3d(geo_model, image=False, plotter_type='basic')
```



## Model generation



Once we have ensured that all of our primary data has been defined as desired in our object `DataManagement`. We can move on to the following phase of developing our geological model: preparing the input data for interpolation. `InputData` (called *geo\_data* in our example).

This is accomplished by creating an `InterpolatorData` object from our `InputData` object using the following function:

```
gp.set_interpolator(geo_model,
                    compile_theano=True,
                    theano_optimizer='fast_compile',
                    )
```

Out:

```
Setting kriging parameters to their default values.
Compiling theano function...
Level of Optimization: fast_compile
Device: cpu
Precision: float64
Number of faults: 1
Compilation Done!
Kriging values:
                values
range           2926.17
$C_o$          203869.05
drift equations [3, 3]

<gempy.core.interpolator.InterpolatorModel object at 0x7fcb8ab2c5e0>
```

This function rescales the extent and coordinates of the original data (and store it in the attribute *geo\_data\_res* which behaves as a usual `InputData` object) and adds mathematical parameters that are needed for conducting the interpolation. The computation of this step may take a while, as it also compiles a theano function which is required for the model computation. However, should this not be needed, we can skip it by declaring *compile\_theano = False* in the function.

We currently have everything we require to compute our whole model using `compute_model`. This will typically yield two distinct solutions as arrays. The first provides details on the lithological formations, and the second on the model's fault network. Each of these arrays has two subarrays as entries:

1. Lithology block model solution:

- Entry [0]: This array shows what kind of lithological formation is found in each voxel, as indicated by a respective formation\_number.
- Entry [1]: Potential field array that represents the orientation of lithological units and layers in the block model.

## 2. Fault network block model solution:

- Entry [0]: Array in which all fault-separated areas of the model are represented by a distinct number contained in each voxel.
- Entry [1]: Potential field array related to the fault network in the block model.

Below, we illustrate these different model solutions and how they can be used.

```
sol = gp.compute_model(geo_model)
```

```
sol
```

Out:

```
Lithology ids
[6. 6. 6. ... 2. 2. 2.]
```

```
geo_model.solutions
```

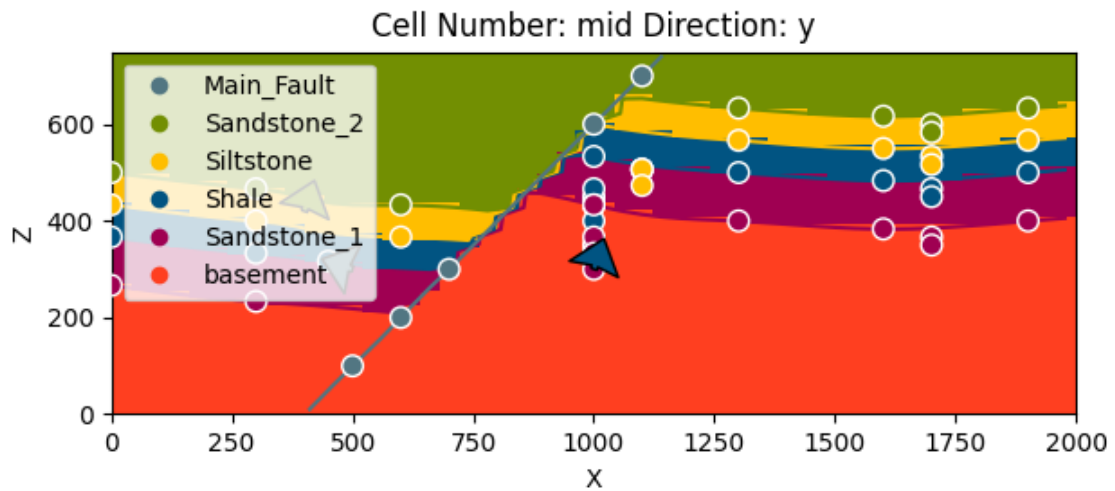
Out:

```
Lithology ids
[6. 6. 6. ... 2. 2. 2.]
```

## Direct model visualization in GemPy

In GemPy directly, model solutions can be quickly viewed in 2D sections. Now let's examine our lithology block:

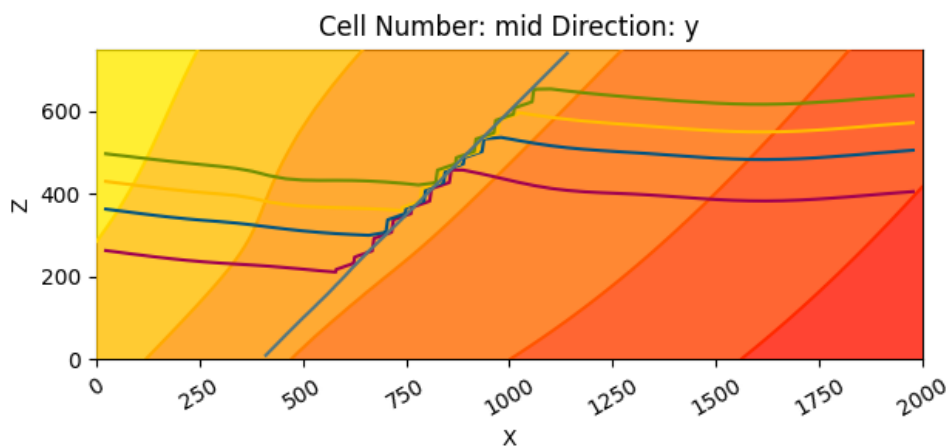
```
gp.plot_2d(geo_model, show_data=True)
plt.show()
```



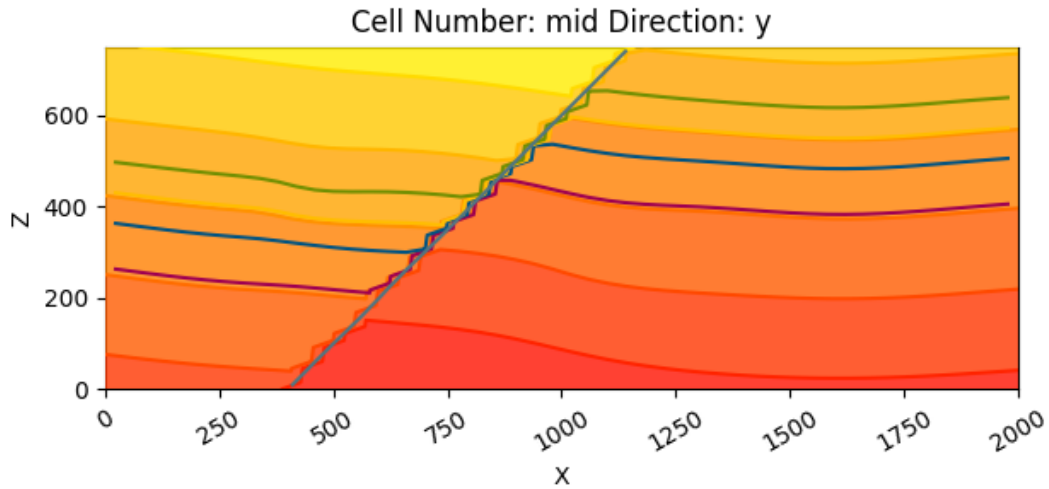
With `cell_number=25` and remembering that we defined our resolution to be 50 cells in each direction, we have chosen a section going through the middle of our block. We have moved 25 cells in direction='y', the plot thus depicts a plane parallel to the x and y axes. Setting `plot_data=True`, we could plot original data together with the results. Changing the values for `cell_number` and `direction`, we can move through our 3D block model and explore it by looking at different 2D planes.

We can do the same without lithological scalar-field solution:

```
gp.plot_2d(geo_model, show_data=False, show_scalar=True, show_lith=False)
plt.show()
```



```
gp.plot_2d(geo_model, series_n=1, show_data=False, show_scalar=True, show_lith=False)
plt.show()
```



This is a good example of how the stratigraphy has been deformed by folds and how the fault has affected the layers.

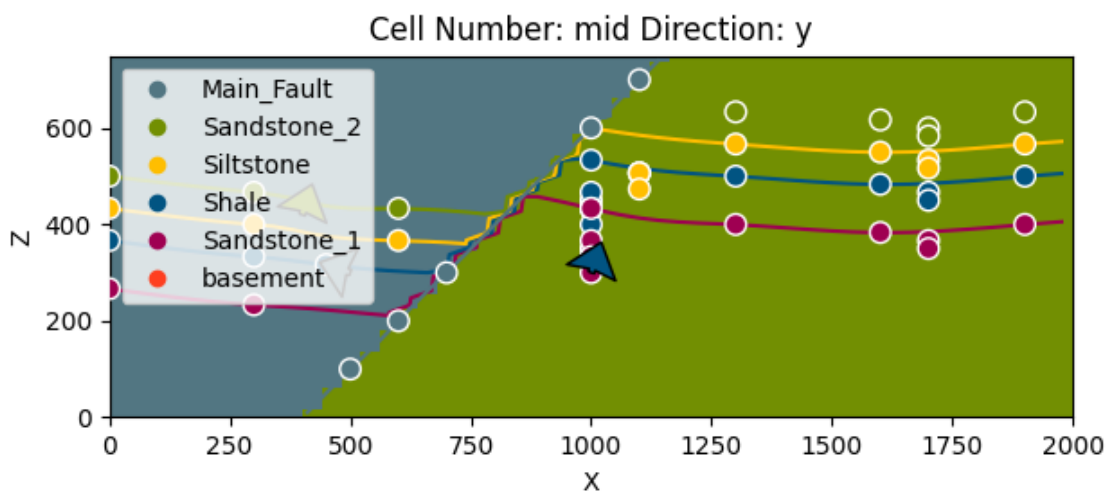
The fault network modeling solutions can be visualized in the same way:

```
geo_model.solutions.scalar_field_at_surface_points
```

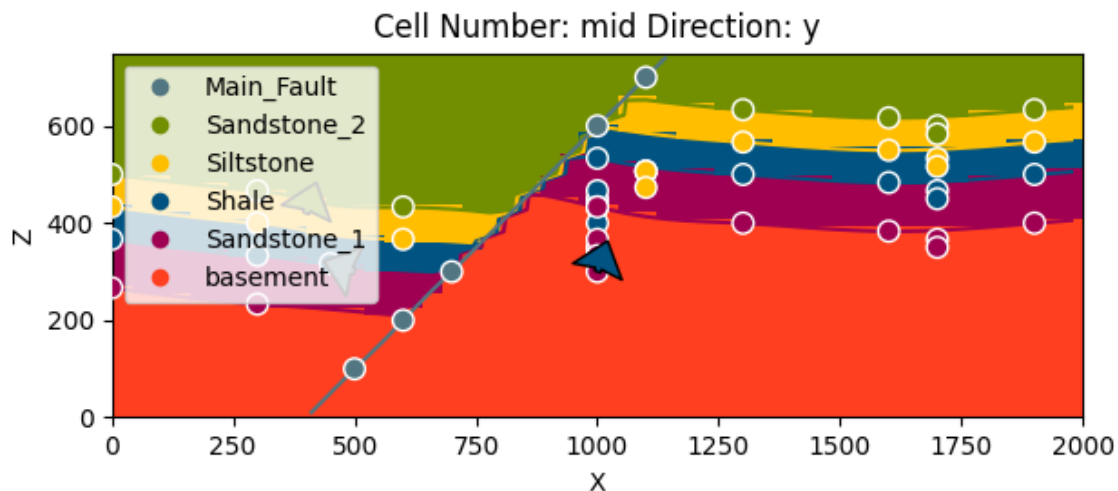
Out:

```
array([[0.03075848, 0.          , 0.          , 0.          , 0.          ],
       [0.          , 0.77174354, 0.72471042, 0.80357372, 0.83598092]])
```

```
gp.plot_2d(geo_model, show_block=True, show_lith=False)
plt.show()
```



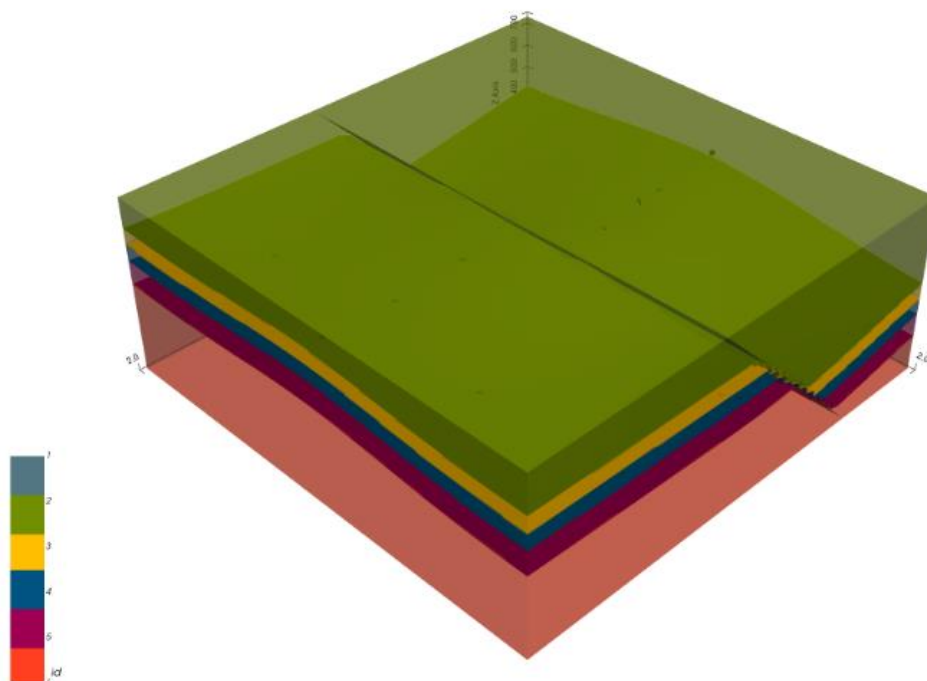
```
gp.plot_2d(geo_model, series_n=1, show_block=True, show_lith=False)
plt.show()
```



### Marching cubes and vtk visualization

We can extract surfaces in addition to 2D sections for 3D rendering. In VTK, surfaces can be seen as 3D triangle complexes. We must take the appropriate vertices and simplices from the potential fields of lithologies and faults in order to form these triangles. With the help of the `get_surface` function in GemPy, this procedure is automated.

```
ver, sim = gp.get_surfaces(geo_model)
gpv = gp.plot_3d(geo_model, image=False, plotter_type='basic')
```



We can now run our 3D VTK visualization in an interactive mode using the rescaled interpolation data, enabling us to modify and update our model in real-time. The adjustments are permanently recorded (in the `InterpolationInput.dataframe` object), just like the interactive 3D representation of our input data. The ensuing modifications to the geological models are also updated in real-time.

### Adding topography

```
geo_model.set_topography(d_z=(350, 750))
```

Out:

```
Active grids: ['regular' 'topography']
```

Grid Object. Values:

```
array([[ 20.         ,  20.         ,  7.5         ],
       [ 20.         ,  20.         ,  22.5        ],
       [ 20.         ,  20.         ,  37.5        ],
       ...,
       [2000.        , 1918.36734694,  423.48951452],
       [2000.        , 1959.18367347,  430.25455308],
       [2000.        , 2000.         ,  431.07163663]])
```

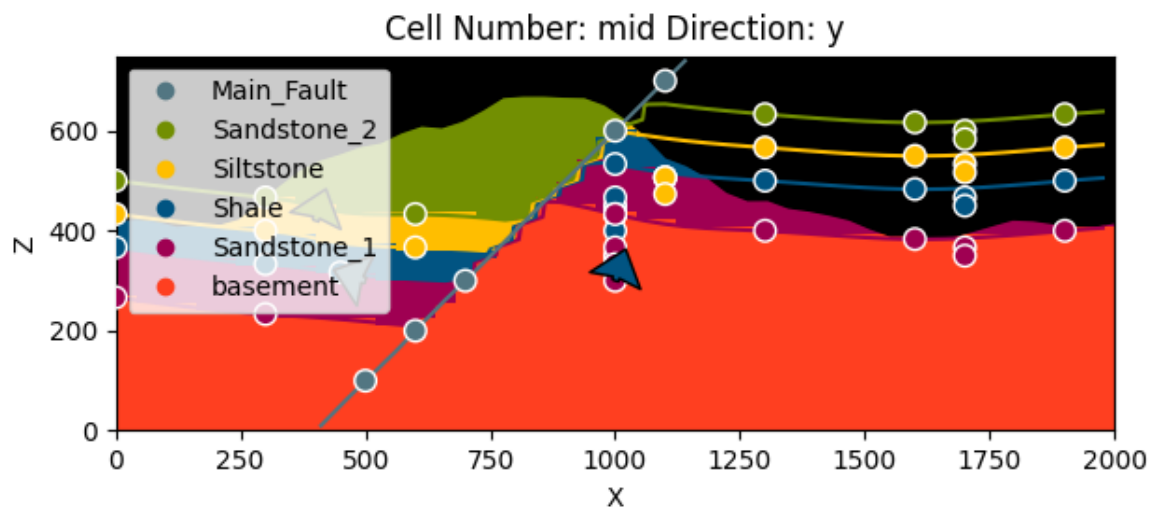
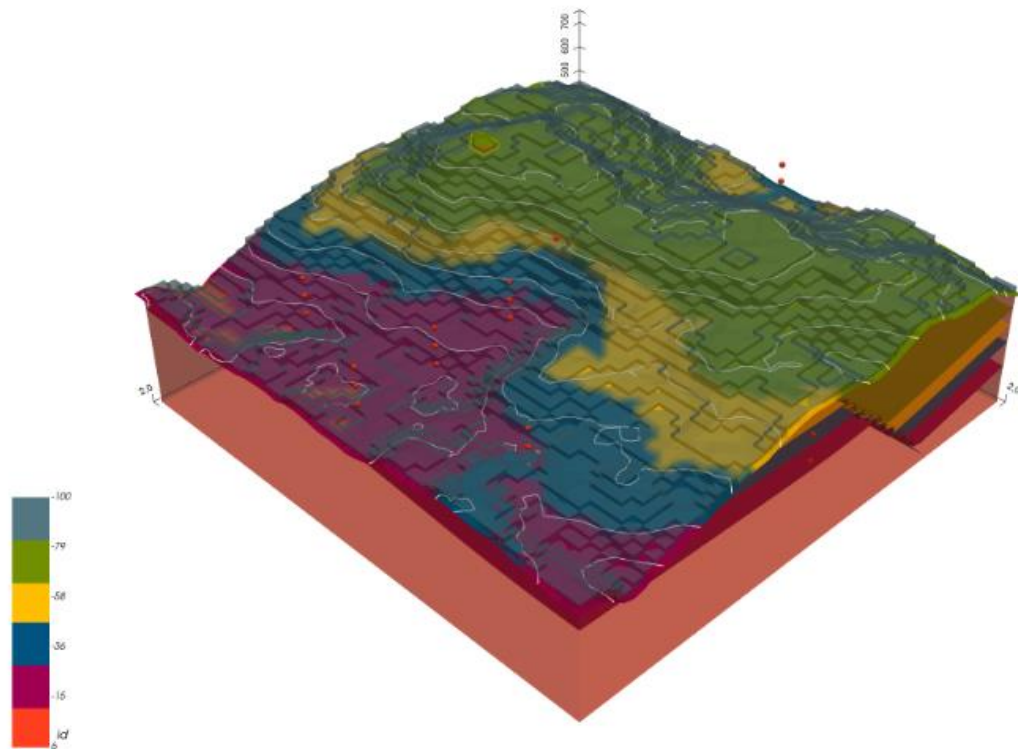
```
gp.compute_model(geo_model)
```

```
gp.plot_2d(geo_model, show_topography=True)
```

```
plt.show()
```

```
# sphinx_gallery_thumbnail_number = 9
```

```
gpv = gp.plot_3d(geo_model, plotter_type='basic', show_topography=True,
                show_surfaces=True,
                show_lith=True,
                image=False)
```



Out:

/WorkSSD/PythonProjects/gempy/gempy/core/solution.py:173: VisibleDeprecationWarning: Creating an ndarray from ragged nested sequences (which is a list-or-tuple of lists-

or-tuples-or ndarrays with different lengths or shapes) is deprecated. If you meant to do this, you must specify 'dtype=object' when creating the ndarray.

```
self.geological_map = np.array(
```

### Compute at a given location

This is done by modifying the grid to a custom grid and recomputing. Notice that the results are given as *grid* + *surfaces\_points\_ref* + *surface\_points\_rest* locations

```
x_i = np.array([[3, 5, 6]])
sol = gp.compute_model(geo_model, at=x_i)
```

Out:

```
Active grids: ['custom']
```

```
/WorkSSD/PythonProjects/gemPy/gemPy/core/solution.py:168: VisibleDeprecationWarning:
Creating an ndarray from ragged nested sequences (which is a list-or-tuple of lists-
or-tuples-or ndarrays with different lengths or shapes) is deprecated. If you meant to
do this, you must specify 'dtype=object' when creating the ndarray.
```

```
self.custom = np.array(
```

Therefore if we just want the value at **x\_i**:

```
sol.custom
```

Out:

```
array([array([[6.]]), array([[0.18630133],
                                [0.63163565]])], dtype=object)
```

This gives each series' id and scalar field values.

### Save the model

GemPy uses Python [pickle] for fast storing temporary objects (<https://docs.python.org/3/library/pickle.html>). However, module version consistency is required. For loading a pickle into GemPy, you have to make sure that you are using the same version of pickle and dependent modules (e.g.: Pandas, NumPy) as were used when the data was originally stored.

For long term-safer storage we can export the pandas.DataFrames to csv by using:

```
gp.save_model(geo_model)
```

Out:

```
True
```



### IV.5. Numerical example and simulation

To study the stick-slip characteristics of the drill string system during the movement with torsional vibration, the numerical example analysis is performed according to the dynamics equations in chapter 3 and the related parameter in Table IV.1

Table IV.1. Related example parameters

Variable	Values
Moment of inertia of top drive $J_r$	930 kg.m <sup>2</sup>
Moment of inertia of drill pipes $J_p$	2782.25 kg.m <sup>2</sup>
Moment of inertia of drill collars $J_c$	700 kg.m <sup>2</sup>
Moment of inertia of drill tool $J_t$	1.2978 kg.m <sup>2</sup>
Moment of inertia of drill Bit $J_b$	471 kg.m <sup>2</sup>
Stiffness between top drive and drill pipes $K_{rp}$	1200 Nm/rad
Stiffness between drill pipes and drill collars $K_{pc}$	1180 Nm/rad
Stiffness between drill collars and drill tool $K_{ct}$	951 Nm/rad
Stiffness between drill tool and drill bit $K_{tb}$	824 Nm/rad
Damping between top drive and drill pipes $C_{rp}$	139.6 Nms/rad
Damping between drill pipes and drill collars $C_{pc}$	190 Nms/rad
Damping between drill collar and drill tool $C_{ct}$	181.5 Nms/rad
Damping between drill tool and drill bit $C_{tb}$	230.15 Nms/rad
Viscous damping coefficient of top drive $C_r$	425 Nms/rad
Viscous damping coefficient of drill bit $C_b$	50 Nms/rad
WOB	97 KN
Radius of drill bit $R_b$	155 mm
Outer diameter of drill tool	178 mm
Dynamic friction factor factor $\mu_{sb}$	0.8
Coulomb friction factor factor $\mu_{cb}$	0.5
Conversion factor factor $\gamma_b$	0.5

### IV.5.1. Simulation results

The motion of the top drive and drill bit is simulated using the established dynamic model of the drill string given in Chapter 3 when the top drive follows a constant speed of 7.33 rad/s.

The torque and angular velocity of the top drive and drill bit are shown in Figure 3. We can note that the drill bit has a stick-slip vibration phenomenon: The torque of the drill bit is at a constant value at the initial moment and then it suddenly decreases and increases, the initial moment of the angular velocity of the drill bit is 0, then suddenly accelerates, and then rapidly decreases to 0.

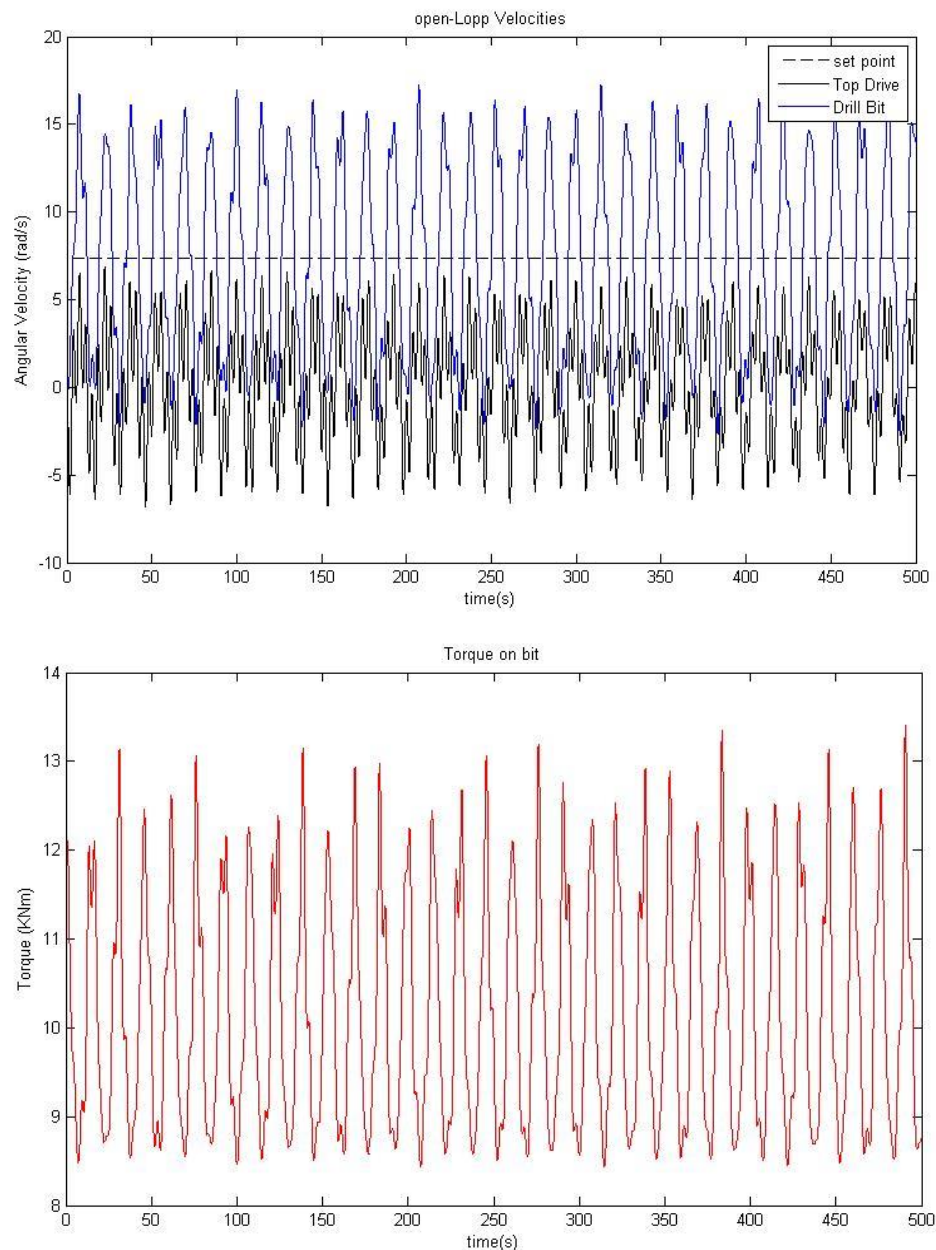


Figure IV.17. Torque and angular velocity of top drive and drill bit with torsional vibration

### IV.5.2. Different rotation rotational speeds results

The angular velocity of the drill bit is obtained individually for various rotational speeds of the top drive. As demonstrated in Fig IV.18.19.20, the lower the rotational speed of the top drive, the longer the stick-slip vibration period of the drill bit and the greater the fluctuation of the angular velocity will be. 1 rad/s, 10 rad/s, and 50 rad/s are the respective values. As illustrated in Fig IV.18.19.20, when the top drive's rotating speed is 1 rad/s, the stick-slip vibration time is the longest, and the drill bit almost always becomes stuck; when the rotational speed is 50 rad/s, the stick-slip vibrations are brief.

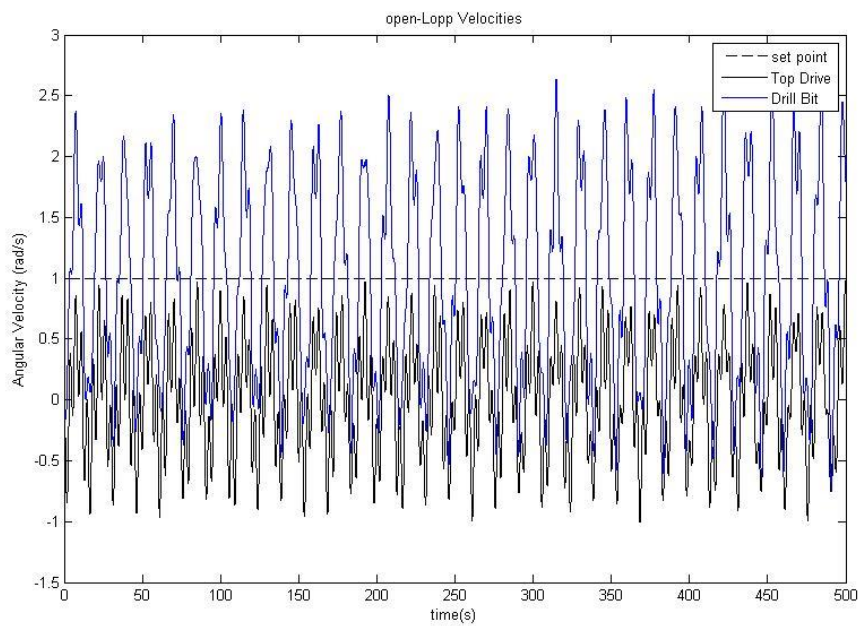


Figure IV.18. Angular velocity at 1 rad/s

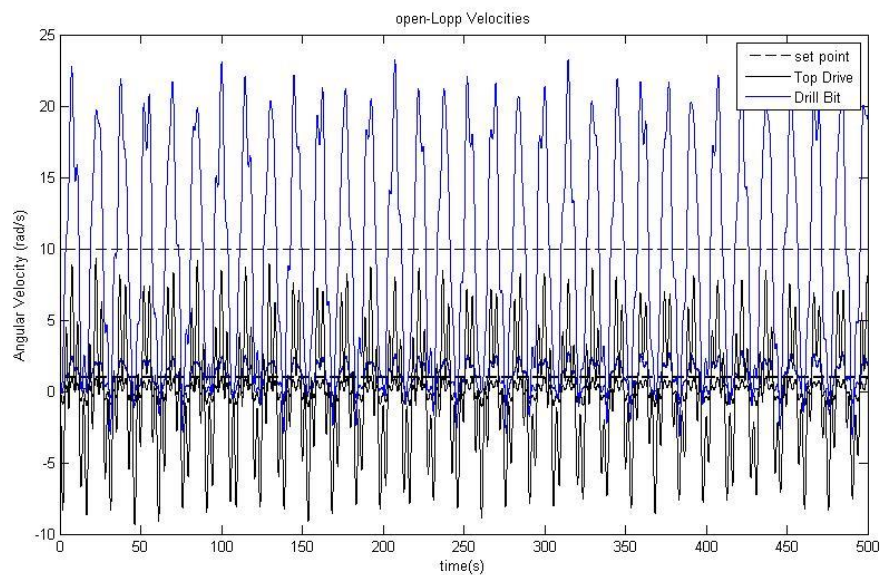


Figure IV.19. Angular velocity at 5 rad/s

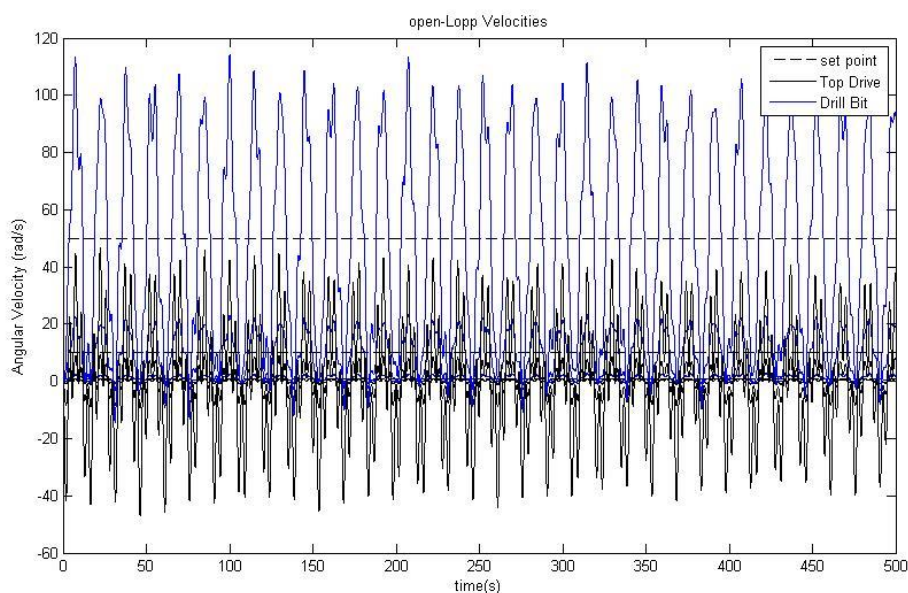


Figure IV.20. Angular velocity at 50 rad/s

### IV.5.3. Different WOBs results

The angular velocity of the drill bit is simulated at various WOBs when the top drive runs at a constant speed of 7.33rad/s. Figure IV.21 shows that the drill bit exhibits obvious stick-slip vibrations at the chosen WOB. As the WOB increases, the stick-slip vibrations period of the drill bit is longer, and the fluctuation range of the angular velocity is larger. The friction torque rises with increasing WOB, which causes an unstable stick-slip behavior. If the WOB keeps rising, the drill bit will certainly be trapped.

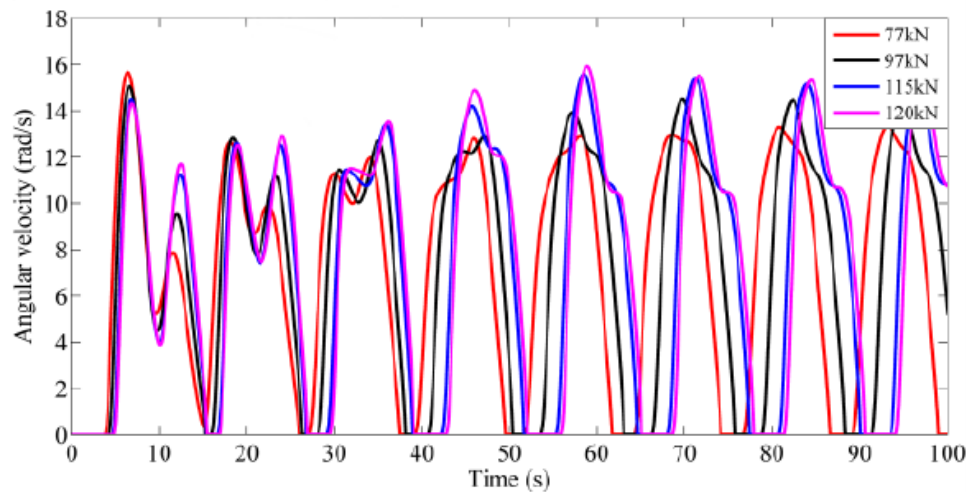


Figure IV.21. Angular velocity of the drill bit at different WOBs [38]

The study's findings suggest that stick-slip vibrations will be somewhat reduced by the top drive's faster rotation and smaller WOB. The actual field conditions are combined with the nonlinear dynamic model and computation method developed in this section [38].

## IV.6. Conclusion and recommendation

Based on the simulation and analysis of seismic while drilling using drill bit stick-slip vibration as a source, we can conclude that this technique has the potential to significantly improve the accuracy and resolution of subsurface imaging during drilling operations for Algerian oil field.

The stick-slip vibration model used in SWD has been shown to be superior to other methods in terms of providing a higher quality seismic signal, which can lead to better identification of hydrocarbon reservoirs and reduce drilling risks.

However, there are some limitations to consider. The effectiveness of SWD depends on several factors, including the type of rock formation, the depth of the well, and the drilling conditions. In some cases, the stick-slip vibration may not be strong enough to generate the desired seismic signal, or it may interfere with other drilling operations.

Therefore, it is recommended that further research and experimentation be conducted to fully understand the capabilities and limitations of SWD using drill bit stick-slip vibration as a source in the Algerian oil field. Additionally, continued development of advanced processing techniques for analyzing and interpreting the acquired data can help to further improve the accuracy and resolution of subsurface imaging.

In the end, SWD with drill bit stick-slip vibration as a source shows potential as a real-time subsurface imaging technology during drilling operations in the Algerian oil field. To ensure the technique's effectiveness and practicality, however, certain drilling conditions and geological formations must be carefully considered.

## **General conclusion**

Our research conducted in this thesis focused on the simulation of Seismic While Drilling (SWD) processes based on the stick-slip vibration model in the Algerian petroleum field. The study aimed to explore the potential of SWD as a real-time subsurface imaging technique during drilling operations.

The initial chapters highlighted the significance of borehole seismic surveys and their advantages, such as high resolution, cost-effectiveness, and improved characterization of alteration and structurally compromised zones. The need for advancements in reservoir monitoring techniques led to the proposal of SWD as a promising solution.

Throughout our research, different SWD techniques were examined, with a particular focus on the stick-slip vibration model. The advantages of this technique, such as its ability to provide a high-quality seismic signal for accurate reservoir identification and reduced drilling risks, were emphasized. However, the limitations and challenges associated with SWD, including geological variations and potential interference with drilling operations, were also acknowledged.

Our simulations conducted in the thesis provided valuable insights into the feasibility and effectiveness of SWD using stick-slip vibration in the Algerian oil field. The results indicated that this technique has the potential to significantly enhance subsurface imaging accuracy and resolution during drilling operations. Nonetheless, the research emphasizes the importance of considering specific drilling conditions and geological formations when implementing SWD.

To fully exploit the capabilities of SWD using drill bit stick-slip vibration as a source in the Algerian oil field, further research and experimentation are recommended. This will help to better understand the technique's limitations and potential applications. Additionally, the continuous development of advanced processing techniques for data analysis and interpretation can contribute to improving the accuracy and resolution of subsurface imaging.

In the end and based on the research conducted and the findings presented in this thesis, we highly recommend the implementation of this technique in the Algerian petroleum industry. The numerous positives associated with this method clearly outweigh its negatives, making it a promising approach for real-time subsurface imaging during drilling operations. While certain limitations and challenges were acknowledged, such as geological variations and potential interference with drilling operations, the overall benefits of SWD outweigh these concerns. The potential of SWD to revolutionize reservoir



monitoring and enhance exploration and production performance cannot be overlooked. By embracing SWD, the Algerian petroleum industry can benefit from enhanced subsurface imaging during drilling operations, leading to more informed decision-making, optimized reservoir characterization, and ultimately, improved exploration and production performance.



## Bibliography

- [1] John Blackburn, John Daniels, Scott Dingwall, Geoffrey Hampden-Smith, Scott Leaney, Joël Le Calvez Les Nutt Henry Menkiti, Adrian Sanchez, Marco Schinelli, Borehole Seismic Surveys: Beyond the Vertical Profile, September 2007
- [2] S Stunes, Methods of Pore Pressure Detection from Real-time Drilling Data, 2012, Norwegian University of science and technology. P.10
- [3] Solano, G.E, zero offset VSP data processing and estimates in the oil sands.2004, university of alberta p.110
- [4] Bolmer R.T, Bnffer, H, Hoskins, R.A, Stephen, and Suift, S.A. vertical seismic profile at site 765 and seismic reflectors in the argo albyssal plain 1 in ocean drilling program.1992
- [5] Arroyo, J.L., Brenton, P., Dijkerman, H., Dingwall, S., Guerra, R., Hope, R., Williams, H.B.M., Jimenez, R.R., Tulett, L.J., Leaney, S., Lim, T.k., Menkiti, H.,Tcherkashnev, P.S., Burg, T.T., Veliac, M., Superior Seismic Data from the Borehole. 2003.
- [6] David Eaton, Matt Salisbury , David Forsyth, Bernd Milkereit, Sean Guest, Doug Schmitt, Dean Grick, Borhole seismic imaging of near-vertical structures: a case history
- [7] Enwenode Onajite, in Seismic Data Analysis Techniques in Hydrocarbon Exploration, 2014
- [8] Rector, J.W.; Mangriotis, M.D. (2011). "Vertical Seismic Profile". In Gupta, Harsh K. (ed.). Encyclopedia of Solid Earth Geophysics. Encyclopedia of Earth Sciences Series. Dordrecht: Springer Netherlands
- [9] James W. Rector, Bruce P. Marion; The use of drill-bit energy as a downhole seismic source. Geophysics 1991;; 56 (5): 628–634. doi: <https://doi.org/10.1190/1.1443079>
- [10] Borehole seismic survey using multimode optical fibers in a hybrid wireline, Measurement, Volume 125, 2018, Pages 694-703, ISSN 0263-2241, <https://doi.org/10.1016/j.measurement.2018.04.058>
- [11] Kumar, Rajeev, and Pierre Bettinelli. "Borehole Seismic: Essential Contributions Over the Oilfield Lifecycle." Paper presented at the SPE Middle East Oil & Gas Show and Conference, event canceled, November 2021. doi: <https://doi.org/10.2118/204889-MS>
- [12] Jean Auriol, Nasser Kazemi, Kristopher Innanen, Roman Shor. Combining Formation Seismic Velocities while Drilling and a PDE-ODE observer to improve the Drill-String Dynamics Estimation. ACC 2020 - American Control Conference, Jul 2020, Denver, United States. fahal-02524281f
- [13] Kristoffer Evensen, Surface Seismic While Drilling (A new method for relief well drilling), June 2013
- [14] Toshiyuki Yokota, Kyosuke Onishi, Tetsuji Ohno, Akinori Ota, Tsutomu Kaneko, Hirokazu Ksawa, Seismic while drilling: Basic experiments using a percussion drill as an energy source Exploration Geophysics (2004) 35, 255-259,
- [15] G. BERNASCONI , P- and S-wave migration of while drilling data, Department of Electronics and Information, Politecnico di Milano, Italy (Received: March 28, 2007; accepted: November 21, 2007).
- [16] Mads Herring Jensen, Introduction to the Elastic Waves, Time Explicit Interface, COMSOL Blog May 28, 2020
- [17] Anchliya, A. "A Review of Seismic-While-Drilling (SWD) Techniques: A Journey From 1986 to 2005." Paper presented at the SPE Europec/EAGE Annual Conference and Exhibition, Vienna, Austria, June 2006. doi: <https://doi.org/10.2118/100352-MS>
- [18] F. Poletto and F. Miranda, Seismic while drilling, fundamentals of Drill-bit seismic for exaplorations, handbook of Geophysical explorations, Elsevier 2004.
- [19] Andrey Bakulin, Ali Aldawood, Ilya Silvestrov, Emad Hemyari, Flavio Poletto; Seismic-while-drilling applications from the first DrillCAM trial with wireless geophones and instrumented top drive. The Leading Edge 2020;; 39 (6): 422–429. doi: <https://doi.org/10.1190/tle39060422.1>
- [20] E.B. Raknes , T.J. Moser , B. Arntsen , S.Johansen , S. Sangesland "Surface Seismic While Drilling - Imaging of Well Bores in Seismic Context", June 2017
- [21] Hokstad, Ketil, Sollie, Roger, and Inge M. Carlsen. "VSP While Drilling For Geosteering Applications." Paper presented at the 2001 SEG Annual Meeting, San Antonio, Texas, September 2001
- [22] Eric Zimmermann, Joseph Wyble, Jim Troutman Seismic Sources in Marine and Land Reflection Seismology Surveys

- [23] Stssensors (STS) Mud Pulse Telemetry: MWD Data Transmission with Pressure Sensors Wednesday, 1 July, 2020
- [24] Schlumberger site: <https://www.slb.com/-/media/files/fe/brochure/swings-br.ashx> logged in 2/2/2023
- [25] Dethloff, Morten H., and Steen Agerlin Petersen. "Seismic-While-Drilling Operation and Applications." Paper presented at the SPE Annual Technical Conference and Exhibition, Anaheim, California, U.S.A., November 2007. doi: <https://doi.org/10.2118/109893-MS>
- [26] Kristoffer Evensen, Sigbjørn Sangesland, Ståle Emil Johansen, Espen Birger Raknes, Børge Arntsen, Norwegian University of Science and Technology (NTNU), Relief Well Drilling Using Surface Seismic While Drilling (SSWD), 4–6 March 2014
- [27] Kolle, J. J., and K. Theimer. "Seismic-While-Drilling Using a Swept Impulse Source." Paper presented at the SPE/IADC Drilling Conference, Amsterdam, Netherlands, February 2005. doi: <https://doi.org/10.2118/92114-MS>
- [28] F. Poletto, F. Miranda, Seismic While Drilling. Fundamentals of Drill Bit Seismic for Exploration, Elsevier, Amsterdam, 2004.
- [29] jardine,S,Malone,D,and Sheppard,M."putting a damper on drilling's bad vibration," oilfield review (january 1994).
- [30] Idir Kessai, Samir Benammar, Mohamed Zinelabidine Doghmane and Kong Fah Tee- Drill Bit Deformations in Rotary Drilling Systems under Large-Amplitude Stick-Slip Vibrations 18 September 2020
- [31] Riane, R.; Kidouche, M.; Illoul, R.; Doghmane, M.Z. Unknown Resistive Torque Estimation of a Rotary Drilling System Based on Kalman Filter. IETE J. Res. 2020.
- [32] Smith, J. (2021). Simulating Complex Processes: MATLAB and Python Functions for Seismic Data Analysis. (Unpublished doctoral thesis). University of XYZ.
- [33] SeisLab Documentation.
- [34] Gary F. Margrave, New seismic modelling facilities in Matlab.
- [35] GemPy Documentation. GemPy: An Open-Source Python Package for 3D Geological Modeling. Retrieved from <https://www.gempy.org/documentation>
- [36] Rami Riane, Mohamed Zinelabidine Doghmane, Madjid Kidouche, Kong Fah Tee, and Sofiane Djezzar, Stick-Slip Vibration Suppression in Drill String Using Observer-Based LQG Controller.
- [37] Madjid Kidouche, Mohamed Zinelabidine Doghmane, Samir Benammar, Kong Fah Tee, Rock-bit interaction effects on high-frequency stick-slip vibration severity in rotary drilling systems, 10 August 2021
- [38] Jialin Tian, Genyin Li,Liming Dai,Lin Yang, Hongzhi He, Shuhui Hu1, Torsional Vibration and Nonlinear Dynamic Characteristics of Drill String s and Stick-Slip Reduction Mechanism

**[Annex]** In order to measure the pulses of mud, the sensors to accurately measure even the slightest pressure variations must meet high standards. The sensors must be able to endure pressures of up to 1,000 bar. In very deep drill holes, the drill head needs to be powered by extremely high pressures which also affect the pressure transmitters used for mud pulse telemetry on the surface [23].